

APPLICATIONS OF DITHIENO[3,2-*b*:2',3'-*d*]PYRROLES AND ITS
ANALOGUES TO CONJUGATED MATERIALS

A Thesis
Submitted to the Graduate Faculty
of the
North Dakota State University
of Agriculture and Applied Science

By

Casey Brian McCausland

In Partial Fulfillment of the Requirements
for the Degree of
MASTER OF SCIENCE

Major Department:
Chemistry and Biochemistry

June 2014

Fargo, North Dakota

North Dakota State University
Graduate School

Title

Applications of Dithieno[3,2-*b*:2',3'-*d*]pyrroles and its Analogues to
Conjugated Materials

By

Casey Brian McCausland

The Supervisory Committee certifies that this *disquisition* complies with North Dakota State University's regulations and meets the accepted standards for the degree of

MASTER OF SCIENCE

SUPERVISORY COMMITTEE:

Seth C. Rasmussen

Chair

Andrew Croll

Erika Offerdahl

Pinjing Zhao

Approved:

6/20/2014

Date

Gregory R. Cook

Department Chair

ABSTRACT

The promise of semiconducting materials with tunable electronic and optical properties that share the same mechanical flexibility, low production costs and ease of processing displayed by traditional polymers fuels the intense interest seen in developing devices employing conjugated polymers (CPs). Many examples of π -conjugated systems have been studied and reported in the literature, of which Rasmussen and coworkers have advanced the field with their work involving *N*-alkyl, *N*-aryl, and *N*-acyl-dithieno[3,2-*b*:2',3'-*d*]pyrroles (DTPs). Using DTP as a template current investigations are targeting two analogues: pyrrolo[3,2-*d*:4,5-*d'*]bisthiazole (PBTz) and difuro[3,2-*b*:2',3'-*d*]pyrroles (DFP). In comparison to polymers of DTP, the electron-deficient nature of thiazoles is known to stabilize HOMO levels of PBTz-based polymers. Furan-based oligomers exhibit many of the properties displayed by DTPs and it is a reasonable assumption that the properties of DFPs would be comparable to DTPs. The synthesis and characterization of PBTz and DFPs and a comparison to DTP-based materials will be presented.

ACKNOWLEDGEMENTS

First and foremost I would like to acknowledge my wife, Gwen. She was my foundation during my tenure as a graduate student. Her love, encouragement, and support made it all possible. Secondly, I would like to mention my son Liam. His laugh, smile, and overabundance of energy were a welcomed distraction from the daily grind. I would be negligent if I did not mention my extended family and all they did to support Gwen, Liam, and I during our stay in Fargo. My sisters-in-laws, Laura Peterson and Dr. Maggie Peterson, respectively gave us a place to live and chiropractic care. My in-laws, Dr. Andrew and Myrene Peterson, supplied us with an abundance of farmed-raised meat in addition to veterinary care for our cats, Pete and Oscar. Finally, thanks to everyone who rearranged their busy schedules, often at a moment's notice, to help us look after or care for a sick little boy so Gwen and I wouldn't miss work or class.

During my time at NDSU, I was fortunate to be surrounded by a very supportive group of individuals in the Chemistry and Biochemistry Department. They helped me navigate the many challenges one faces as a graduate student. I would first like to acknowledge both current and former members of the Rasmussen Research Group, listed here in no particular order: Dr. Sean Evenson, Dr. Mike Mulholland, Dr. Ryan Schwiderski, Cole Larsen, Rylan Wolfe and Eric Uzelac. Additionally, thanks must be given to both Dr. Anthony Ostlund and Dr. Narayanaganesh Balasubramian. I cannot stress how helpful the above listed-individuals were in assisting me with my research and course work. They unfailingly took the time to listen to my questions providing me with helpful tips, constructive advice, and always with an abundance of patience and a smile.

DEDICATION

This body of work is dedicated to my mother Teri Marie McCausland (7/26/1947 – 11/28/2013), who left us at too young an age. She was so very proud of all her children, grandchildren, and their accomplishments. Mom, you were loved by us all and your absence is felt every day.

TABLE OF CONTENTS

ABSTRACT.....	iii
ACKNOWLEDGEMENTS.....	iv
DEDICATION.....	v
LIST OF TABLES.....	x
LIST OF FIGURES.....	xi
LIST OF ABBREVIATIONS.....	xiv
CHAPTER 1. INTRODUCTION.....	1
1.1. Conjugated polymers.....	1
1.2. Measuring optical and electrical properties.....	3
1.3. Tuning of band gap.....	5
1.4. Research goals.....	11
1.5. References.....	12
CHAPTER 2. 2,4-DIBROMO-1,3-THIAZOLES AS BUILDING BLOCKS FOR SYNTHESIS OF PYRROLO[3,2- <i>d</i> : 4,5- <i>d'</i>]BISTHAZOLES.....	19
2.1. Introduction.....	19
2.2. Reactivity of thiazoles.....	21
2.3. Generation of 4,4'-dibromo-2,2'-bis(triisopropylsilyl)-5,5'-bithiazole.....	22
2.4. Results and discussions.....	27
2.5. Conclusion.....	35
2.6. Experimental.....	35
2.6.1. Synthesis of 2,4-dibromothiazole using PBr ₅ as brominating agent.....	36
2.6.2. Synthesis of 2,4-dibromothiazole with P ₂ O ₅ , Bu ₄ NBr and toluene.....	36
2.6.3. Synthesis of 2,4,5-tribromothiazole.....	37

2.6.4. Synthesis of 4-bromo-2-(triisopropylsilyl)thiazole.....	37
2.6.5. Synthesis of 2,2',4,4'-tetrabromo-5,5'bithiazole - route two.....	38
2.6.6. Synthesis of 2,2',4,4'-tetrabromo-5,5'bithiazole - route three.....	39
2.6.7. Synthesis of 4,4'-dibromo-2,2'-bis(triisopropylsilyl)-5,5'-bithiazole.....	39
2.7. References.....	40
CHAPTER 3. SYNTHESIS AND CHARACTERIZATION OF FUNCTIONALIZED, FUSED-RING PYRROLO[3,2- <i>d</i> :4,5- <i>d'</i>]BISTHIAZOLES AND COMPARISON TO THE <i>N</i> -ALKYL- AND <i>N</i> -ACYL-DITHIENO[3,2- <i>b</i> :2',3'- <i>d</i>]PYRROLES.....	42
3.1. Introduction.....	42
3.2. Reported synthesis of thiazole analogues of DTP.....	47
3.3. Results and discussion.....	49
3.3.1. Generation of <i>N</i> -alkylPBTz.....	49
3.3.2. Generation of <i>N</i> -acylPBTz.....	51
3.3.3. Electrochemistry of monomeric PBTz units.....	52
3.3.4. Electrtopolymerized homopolymers of PBTz.....	53
3.3.5. UV-vis spectroscopy of PBTz monomers.....	54
3.3.6. UV-vis spectroscopy of PBTz homopolymers.....	55
3.3.7. Spectroelectrochemistry.....	57
3.4. Conclusion.....	57
3.5. Experimental.....	59
3.5.1. Synthesis of 2,6-bis(triisopropylsilyl)-4-octyl-4 <i>H</i> -pyrrolo[2,3- <i>d</i> :5,4' <i>d'</i>] bisthiazole.....	59
3.5.2. Synthesis of 4-octyl-4 <i>H</i> -pyrrolo[2,3- <i>d</i> :5,4']bisthiazole.....	60
3.5.3. Electrochemistry and electropolymerizations.....	60

3.5.4. UV-vis-NIR spectroscopy.....	61
3.5. References.....	61
CHAPTER 4. SYNTHESIS AND CHARACTERIZATION OF N-FUNCTIONALIZED FUSED-RING DIFURO[3,2-<i>b</i>:2',3'-<i>d</i>]PYRROLES AND COMPARISON TO THE <i>N</i>-ALKYL- AND <i>N</i>-ACYL-DITHIENO[3,2-<i>b</i>:2',3'-<i>d</i>]PYRROLES.....	
4.1. Introduction.....	64
4.2. Results and discussion.....	67
4.2.1. Synthesis of 3,3'-dibromo-2,2'-bifuran.....	67
4.2.2. Synthesis of <i>N</i> -alkylDFPs.....	68
4.2.3. Synthesis of <i>N</i> -acylDFPs.....	70
4.3. Conclusions.....	71
4.4. Experimental.....	72
4.4.1. Synthesis of 3,3'-dibromo-2,2'-bifuran.....	73
4.4.2. Attempted synthesis of <i>N</i> -octyldifuro[3,2- <i>b</i> :2',3'- <i>d</i>]pyrroles.....	73
4.4.3. Attempted synthesis of <i>N</i> -octanoyldifuro[3,2- <i>b</i> :2',3'- <i>d</i>]pyrroles.....	74
4.5. References.....	74
CHAPTER 5. SYNTHESIS OF <i>N</i>-(4-OCTYLBENZOYL)DITHIENO[3,2-<i>b</i>:2',3'-<i>d</i>] PYRROLE AND POLY(<i>N</i>-OCTYLDITHIENO[3,2-<i>b</i>:2',3'-<i>d</i>]PYRROLE- <i>CO</i>-<i>N</i>-OCTANOYLDITHIENO[3,2-<i>b</i>:2',3'-<i>d</i>]PYRROLE.....	
5.1. Introduction.....	76
5.2. Results and discussion.....	78
5.2.1. Synthesis of <i>N</i> -(4-octylbenzoyl)DTP.....	78
5.2.2. Synthesis of copolymer of 1 st and 2 nd generation DTP.....	81
5.2.3. Electrochemistry of poly(<i>N</i> -octylDTP- <i>co</i> - <i>N</i> -octanoylDTP.....	83
5.2.4. UV-vis spectroscopy of poly(<i>N</i> -octylDTP- <i>co</i> - <i>N</i> -octanoylDTP).....	84

5.3. Conclusion.....	84
5.4. Experimental.....	86
5.4.1. Synthesis of 4-octylbenzamide method A.....	87
5.4.2. Synthesis of 4-octylbenzamide method B.....	87
5.4.3. Prefer method for synthesis of 4-octylbenzamide.....	88
5.4.4. <i>N</i> -(4-Octylbenzoyl)dithieno[3,2- <i>b</i> :2',3'- <i>d</i>]pyrrole.....	88
5.4.5. Poly(<i>N</i> -octyldithieno[3,2- <i>b</i> :2'3'- <i>d</i>]pyrrole- <i>co</i> - <i>N</i> -octanoyldithieno[3,2- <i>b</i> :2',3' <i>d</i>]pyrrole).....	89
5.5. References.....	89
CHAPTER 6. SUMMARY AND FUTURE DIRECTIONS.....	91
6.1. Summary.....	91
6.2. Future directions.....	93
6.3. References.....	95

LIST OF TABLES

<u>Table</u>	<u>Page</u>
2.1. A sampling of thiazoles found in nature and materials.....	21
2.2. Optimization of PBr ₅ reaction conditions.....	29
2.3. Further optimization of PBr ₅ reaction conditions.....	30
3.1. A comparison of thiazole and thiophene annulated conjugated polymers.....	47
3.2. Summary of reaction conditions for generation of <i>N</i> -acylPBTz.....	51
3.3. Electrochemical properties and cyclic voltammograms of <i>N</i> -octylPBTz, <i>N</i> - octylDTP and <i>N</i> -acylDTP.....	52
3.4. Oxidation potentials and cyclic voltammograms of electropolymerized films of poly(<i>N</i> -octylPBTz), poly(<i>N</i> -decylDTP) and poly(<i>N</i> -acylDTP).....	54
3.5. The absorption spectra and properties for <i>N</i> -octylPBTz, <i>N</i> -octylDTP and <i>N</i> -acylDTP....	55
3.6. Solid state absorption spectra of electropolymerized films of poly(<i>N</i> -octylPBTz), poly(<i>N</i> -octylDTP) and poly(<i>N</i> -octanoylDTP).....	56
4.1. Attempted monoamination of 3-bromofuran.....	69
4.2. Attempted generation of <i>N</i> -acylDFPs.....	71
5.1. Summary of optical data for <i>N</i> -(4-octylbenzoyl)DTP with a comparison to <i>N</i> -benzoylDTP.....	81
5.2. Cyclic voltammograms of films of poly(<i>N</i> -octylDTP- <i>co</i> - <i>N</i> -octanoylDTP),poly(<i>N</i> -octylDTP) and poly(<i>N</i> -octanoylDTP).....	83
5.3. Solid state absorption spectra of films poly(<i>N</i> -octylDTP- <i>co</i> - <i>N</i> -octanoylDTP),poly(<i>N</i> -octylDTP) and poly(<i>N</i> -octanoylDTP).....	84

LIST OF FIGURES

<u>Figure</u>	<u>Page</u>
1.1. Formation of bands in π -conjugated materials.....	1
1.2. Stereoisomers of polyacetylene.....	2
1.3. Optical band gaps: A) Extrapolation of transition B) Plot of eV vs $(A \times hv)^2$	4
1.4. Electrochemical determination of band gap.....	5
1.5. Degenerate resonance forms of <i>trans</i> -polyacetylene.....	5
1.6. Non-degenerate resonance forms of polyaromatic systems.....	6
1.7. Non-degenerate resonance forms of isothianaphthene (PITN).....	6
1.8. Band gaps of common conjugated polymers.....	7
1.9. Relative aromaticity of monomeric units.....	7
1.10. Electron affinities of heteroatoms.....	8
1.11. A) β -hydrogen interactions B) Chain-chain and chain-backbone interactions resulting in torsional strain.....	9
1.12. Heteroalkyl side chains on polythiophenes.....	9
1.13. Annulation of bithiophene.....	10
1.14. Examples of commonly used donor and acceptors.....	10
1.15. MO mixing for donor-acceptor model.....	11
1.16. Synthesis of DTP analogues.....	12
2.1. Fused-ring analogue of thiophene based polymer.....	20
2.2. Synthesis of 1 st and 2 nd generation DTPs.....	20
2.3. Observed reactivity of thiazoles.....	22
2.4. Reported generation of PBTz.....	23

2.5.	Conversion of 2,5-dibromothiophene into 3,5-dibromothiophene-2-lithiothiophene via the halogen dance.....	24
2.6.	An unexpected rearrangement.....	25
2.7.	Use of (TMP) ₂ Zn•2MgCl ₂ •LiCl in generation of 4,4'-dibromo-2,2-bis(triisopropylsilyl)-5,5'-bithiazole.....	26
2.8.	Use of POBr ₃ for the generation of 2,4-dibromothiazole.....	28
2.9.	Equilibrium shift of PBr ₅ and use of brominating agent.....	28
2.10.	Preferred synthetic route to the production of 2,4-dibromothiazole.....	31
2.11.	Synthetic routes for generation of 4,4'-dibromo-2,2'bis(triisopropylsilyl)5,5' bithiazole.....	32
3.1.	Pervious synthetic route to N-functionalized DTPs.....	43
3.2.	Tertiary bis(3-thienyl)amine route to N-functionalized DTPs.....	43
3.3.	Improved method for synthesis of N-functionalized DTPs.....	44
3.4.	Alternative routes to the generation of 3,3'-dibromo-2,2'-bithiophene.....	44
3.5.	Preferred method for the generation of 3,3'-dibromo-2,2'-bithiophene.....	45
3.6.	Generation and comparisons of first and second generation DTPs.....	46
3.7.	First reported synthesis <i>N</i> -alkyl functionalized PBTz.....	47
3.8.	Alternative synthesis of PBTz and related analogues.....	48
3.9.	Removal of the TIPS protecting group and addition of bromines.....	49
3.10.	Proposed synthetic scheme for generation of thiazole analogues of first and second generation of DTP molecules.....	49
3.11.	Generation of <i>N</i> -alkylPBTz.....	50
3.12.	Removal of TIPS protecting group.....	50
3.13.	Cycling of the CV to show polymerization of poly(<i>N</i> -octylPBTz).....	53
3.14.	Spectroelectrochemisrty of poly(<i>N</i> -octylPBTz).....	57

4.1.	Heximeric furan- and thiophene- based oligomers.....	64
4.2.	Steric interactions between heteroatoms and beta-hydrogens.....	65
4.3.	Proposed synthetic scheme for generation of difuro[3,2- <i>b</i> :2',3'- <i>d</i>]pyrroles (DFPs).....	67
4.4.	Generation of 3,3'-dibromo-2,2'-bifuran.....	68
4.5.	Attempted synthesis of <i>N</i> -octylDFP.....	68
4.6.	Proposed catalytic cycle for Buchwald-Hartwig amination.....	69
5.1.	Comparison of band gaps of fused ring N-functionalized DTP to parent polythiophene.....	77
5.2.	Synthetic route for <i>N</i> -acyl-phenylDTPs.....	78
5.3.	Early synthetic route to 4-octylbenzamide (Method A and B).....	79
5.4.	Preferred method for generation of 4-octylbenzamide.....	80
5.5.	Generation of: A) distannane of <i>N</i> -octylDTP B) and dibromide of <i>N</i> -octanoylDTP.....	82
5.6.	Stille cross-coupling of 1st and 2nd generation DTPs.....	83
6.1.	Proposed synthetic route to <i>N</i> -aryl functionalized PBTz.....	94
6.2.	Proposed synthetic route to <i>N</i> -acylDFP.....	94

LIST OF ABBREVIATIONS

Abs.....	Absorbance
BINAP.....	2,2'-bis(diphenylphosphino)-1,1'-binaphthyl
BuLi.....	Butyllithium
^t BuLi.....	<i>tert</i> -butyllithium
C-C.....	Carbon-carbon bond
C-N.....	Carbon-nitrogen bond
C=N.....	Carbon-nitrogen double bond
C-O.....	Carbon-oxygen bond
C=O.....	Carbonyl bond
cm.....	Centimeters
CP.....	Conjugated polymers
CT.....	Charge-transfer
CV.....	Cyclic voltammetry
D-A.....	Donor-acceptor
dba.....	Dibenzylideneacetone
DCM.....	Dichloromethane
DFPs.....	Difuro[3,2- <i>b</i> :2',3'- <i>d</i>]pyrroles
DMEDA.....	Dimethylethylenediamine
DMF.....	Dimethylformamide
DTP.....	Dithieno[3,2- <i>b</i> :2',3'- <i>d</i>]pyrrole
DTT.....	Dithieno[3,2- <i>b</i> :2',3'- <i>d</i>]thiophene
E _g	Band gap
E _{HOMO}	Energy of highest occupied molecular orbital

E_{LUMO}	Energy of lowest unoccupied molecular orbital
E_{onset}	Electrochemical peak onset
E_{pa}	Anodic peak potential
E_{pc}	Cathodic peak potential
$E_{1/2}$	Cathodic peak potential
eV	Electron volt
GC-MS	Gas chromatography-mass spectrometry
HD	Halogen dance
HOMO	Highest occupied molecular orbital
HRMS	High resolution mass spectrometry
ICT	Intramolecular charge transfer
LDA	Lithium diisopropylamine
LUMO	Lowest unoccupied molecular orbital
MeCN	Acetonitrile
MeOH	Methanol
MO	Molecular orbital
mp	Melting point
MS	Mass spectrometry
mV	Millivolt
NBS	<i>N</i> -bromosuccinimide
NMR	Nuclear magnetic resonance
OFET	Organic field effect transistor
OLED	Organic light emitting diode
OPV	Organic photovoltaic
PBTz	Pyrrrolo[3,2- <i>d</i> :4,5- <i>d'</i>]bisthiazole

PEDOT.....	Poly(3,4-ethylenedioxythiophene)
Ph.....	Phenyl
PITN.....	Poly(isothianaphthene)
<i>p</i> Ka.....	Acid dissociation constant
RT.....	Room temperature
S.....	Siemens
TBAF.....	Tetrabutylammonium fluoride
TBAPF ₆	Tetrabutylammoniumhexa-fluorophosphate
TEA.....	Triethylamine
THF.....	Tetrahydrofuran
TIPS.....	Triisopropylsilyl
TIPSCI.....	Triisopropylsilyl chloride
TLC.....	Thin layer chromatography
TMS.....	Trimethylsilyl
TMSCI.....	Trimethylsilyl chloride
TMEDA.....	Tetramethylethylenediamine
UV-vis.....	Ultraviolet-visible
V.....	Volts

CHAPTER 1. INTRODUCTION

1.1. Conjugated polymers

Conjugated polymers (CPs) or ‘synthetic metals’ are a class of organic polymers that exhibit electrical properties similar to those observed for inorganic semiconductors. The movement of electrical charges can occur in CPs due to the overlapping of p-orbitals which results in a delocalization of the π -electrons throughout the polymer’s spine.¹ As the extent of conjugation along the polymer’s backbone increases so does the number of molecular orbitals (MOs). In the bulk solid state additional π - π stacking between adjacent chains of polymers further enhances the electron delocalization. The net effect of both of these interactions is the formation of multiple MOs into bands all with indistinguishable energetics and is shown in Figure 1.1. The lower energy band, or valence band, contains the delocalized π electrons MOs whilst the higher energy band, or conduction band, is populated by the empty band of π^* MOs. The energetic difference between the filled valence band and empty conduction band of a material in the solid state is defined as the band gap and is measured in electron volts (eV).

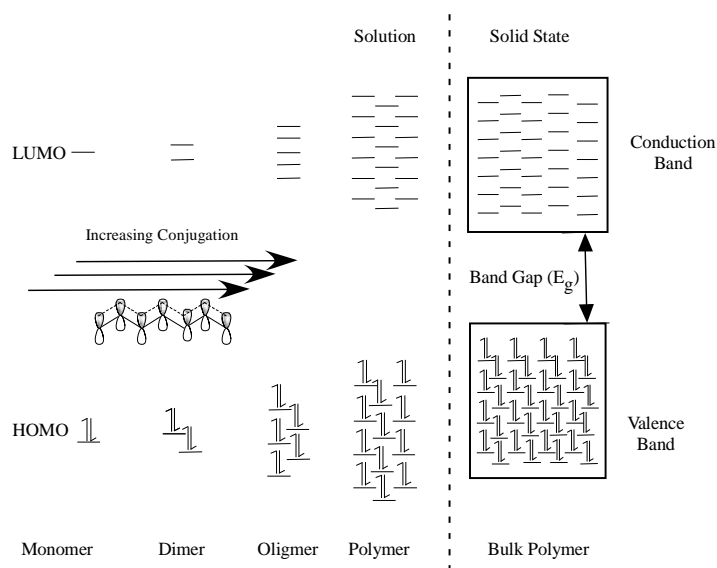


Figure 1.1. Formation of bands in π -conjugated materials

Alan MacDiarmid took notice of the polyacetylene film and its unusual properties. At the time, MacDiarmid and Alan Heeger were collaborating on a conductivity study of an inorganic analogue poly(sulfur nitride).³⁴ It was known that exposure of poly(sulfur nitride) to bromine vapor increased the film's conductivity and in 1976 the three men teamed up together to investigate the conductivity of the newly discovered polyacetylene films.³⁴ Experimentally it was determined that doping the polymer with bromine vapors caused a four-fold increase in conductivity but prolonging the exposure caused a decrease in conductivity. Additional studies using *trans*-polyacetylene films doped with iodine vapor showed a seven magnitude increase in conductivity. In 1977, when the results were reported, it held the record for the highest conductivity for a conjugated polymer at room temperature.³⁵ The combined efforts of MacDiarmid, Heeger and Shirakawa were rewarded in 2000 with the three of them sharing a Nobel Prize in Chemistry for their ground-breaking research.³⁶

1.2. Measuring optical and electrical properties

Absorption spectroscopy is a common tool used to measure the energetic difference between a material's HOMO and LUMO energy levels. Often it is employed for both solutions and films of conjugated polymers but the term band gap is only applicable for measurements taken of the films due to the formation of the conduction and valence bands in the bulk solid state. Additionally, CPs in solution tends to have larger energetic differences between their HOMO and LUMO energy levels, when compared to films, due to limited inter-chain coupling and diminished electron delocalization. The difference between the HOMO and LUMO energy level is measured by finding the steepest slope of the lowest energy transition and then extrapolating to the baseline of the spectrum, illustrated in Figure 1.3A. The wavelength is then converted into an energy which corresponds to the optical band gap of films of CPs. This is a

quick and relatively easy method for determination of a band gap but due to the inherent inconsistencies in visually determining the slope it suffers from diminished accuracy. The formally accepted method for determination of band gap requires the creation of an absorption profile where $h\nu$ vs. $(A \times h\nu)^2$ are plotted on a graph, where $h\nu$ is the photon energy and A is absorbance and is illustrated in Figure 1.3.³⁷

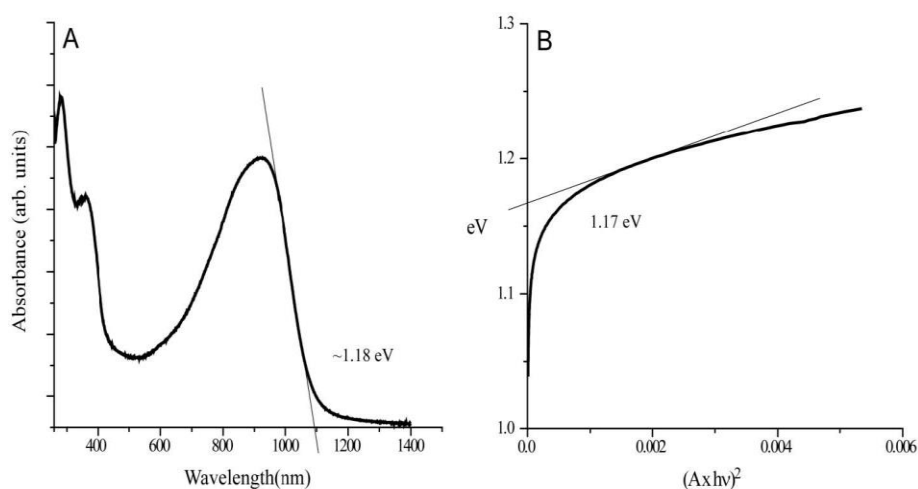


Figure 1.3. Optical band gaps: A) Extrapolation of transition
B) Plot of eV vs $(A \times h\nu)^2$

The electrochemical technique cyclic voltammetry (CV) can be used to determine the HOMO and LUMO energies, in addition to the band gap. A representative cyclic voltammogram is shown in Figure 1.4.³⁷ The HOMO and LUMO can be calculated by extrapolation of the onset of potential of oxidation and the reduction potential respectively, and then converting these energy values vs. vacuum. The band gap is simply the difference between the two calculated values. Since CVs are taken in a solvent this method can pose certain limitations. Specifically the oxidation and reduction potentials of the material being tested must fall inside the solvent window and for larger band gaps this could be an issue.

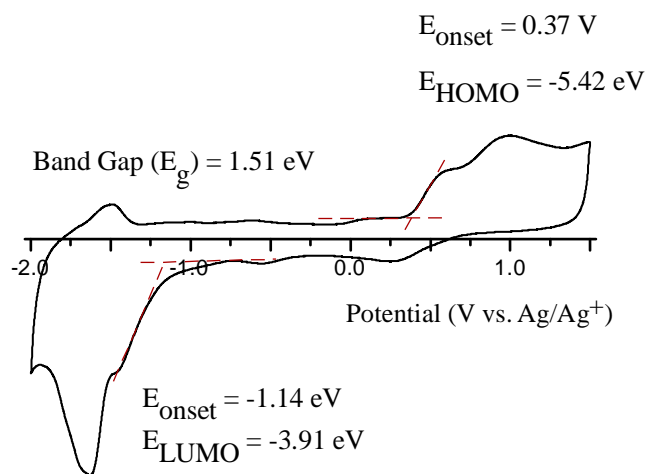


Figure 1.4.³⁸ Electrochemical determination of band gap

1.3. Tuning of band gap

One of the promising features of conjugated polymers is the ability to adjust their optical and electronic properties via structural modifications at the molecular level. A great deal of time and effort has thus far been expended into understanding the factors that affect the HOMO, LUMO, and band gap of the resulting materials and the ways in which they can be manipulated. In systems with degenerate resonance states, such as polyacetylene, bond length alternation plays a key role (Figure 1.5). A decrease in the band gap is observed when there is a greater uniformity between the lengths of the bonds along the backbone of the polymer.³⁹⁻⁴²

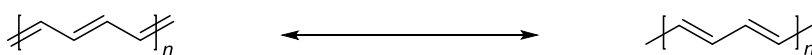


Figure 1.5. Degenerate resonance forms of *trans*-polyacetylene

Polyaromatic systems are different in that they exhibit non-degenerate resonance forms: a quinoidal and aromatic form (Figure 1.6). The aromatic form is the most stable and is

representative of the ground state.^{39,40,43} It is possible to modify the band gap of a material by enhancing either the aromatic or quinoidal nature of the polymer.

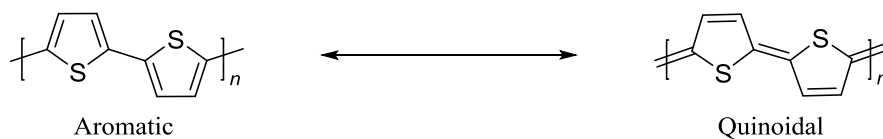


Figure 1.6. Non-degenerate resonance forms of polyaromatic systems

Polyisothianaphthene (PITN) is a fused-ring, thiophene-based polymer and has a low band gap (Figure 1.7). The fused nature of the monomer allows only the benzene or thiophene to be in the aromatic state in any given resonance form.⁴⁴ Benzene, with the higher resonance energy, favors the aromatic form giving the thiophene ring more quinoidal character, resulting in an enhanced quinoidal nature along the polymer's backbone with greater electron delocalization decreasing the material's band gap.



Figure 1.7. Non-degenerate resonance forms of isothianaphthene (PITN)

To clarify, the term low band gap has been used rather loosely in the literature when referring to the optical properties of a material. Pomerantz, in 1988, noted that many of the studied parent conjugated polymers were not commonly considered low band gap materials (Figure 1.8). In fact many of the band gaps were in excess of 2.0 eV with polyacetylene having the lowest E_g of 1.5 eV. Thus Pomerantz defined *low band gap* as those materials with an E_g less than 1.5 eV.⁴⁵ Rasmussen and coworkers, in an attempt at standardization, have proposed using the term *reduced band gap* when referring to polymers with E_g values between 1.5 eV and 2.0 eV, while retaining Pomerantz definition for low band gap materials.⁴⁶

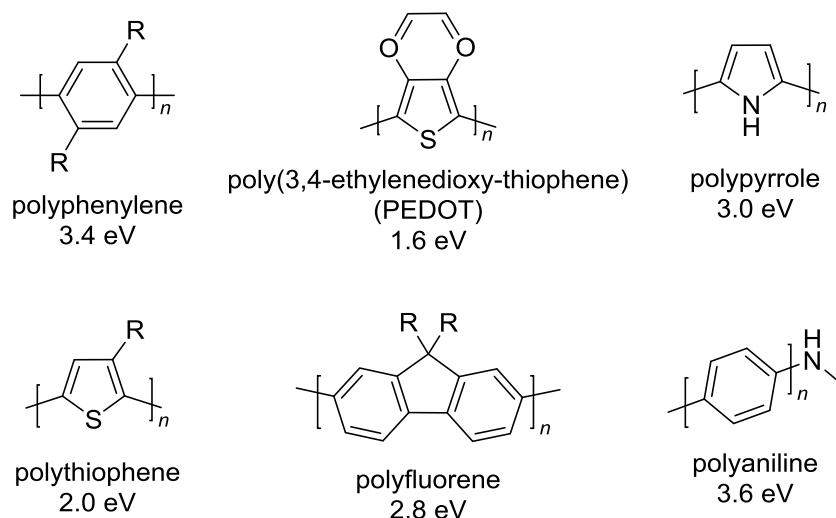


Figure 1.8. Band gaps of common conjugated polymers⁴⁷

The aromaticity of the monomeric unit of the polymer determines the confinement potential of the π -electrons. This directly affects the amount of electron delocalization along the polymer's backbone. Increasing the relative aromaticity of a system decreases electron delocalization, corresponding to an increase in the polymer's band gap (Figure 1.9).⁴⁸

Increased Aromaticity = Increased Band Gap

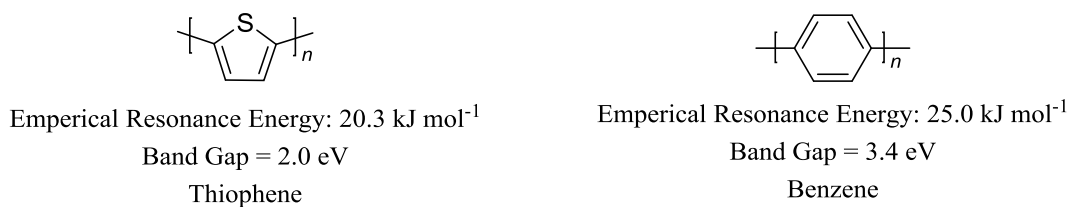


Figure 1.9. Relative aromaticity of monomeric units⁴⁷

Additionally the electron affinity of the heteroatom found in a heterocyclic system will affect the electronic properties of the resulting polymer. An inverse relationship exists between band gap and electron affinity. A reduction in band gap, due to increased electron delocalization along the polymer's backbone, is seen when heteroatoms of greater electron affinities are employed (Figure 1.10).⁴⁹

Increased Electron Affinities = Decreased Band Gap

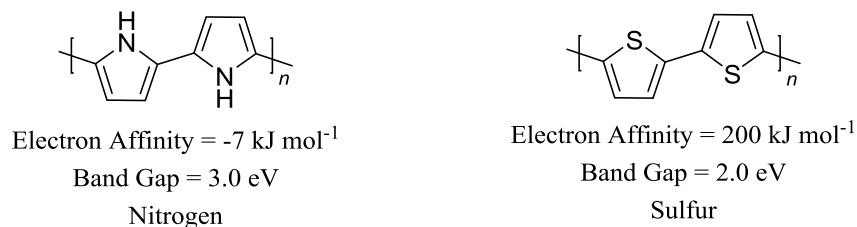


Figure 1.10. Electron affinities of heteroatoms⁴⁷

Additionally, torsional strain also affects the ability of neighboring p orbitals to overlap. This can be caused by β -hydrogen interactions between adjacent units (Figure 1.11A) or incorporation of side chains, usually long alkyl chains, to enhance the material's solubility (Figure 1.11B). A typical example of side chains used to solubilize a conjugated polymer is on the thiophene molecule. The asymmetric nature of 3-alkylthiophenes results in three possible couplings between two thiophene molecules at the alpha positions: 2,2'-coupling or head to head (HH), 5,5'-coupling or tail-tail (TT), and 2,5'-coupling or head-tail (HT). The regioregularity, or the coupling of these asymmetric units, affects the band gap of the resulting polymers. Minimizing interactions amongst the substituents increases the polymer's planarity, which increases conjugation length and results in a decrease in band gap. HT-HT coupling causes the least amount of twisting along the polymer's backbone, whilst the most torsional strain is encountered with HH-HT coupling causing the greatest deviation from planarity. The hydrogens found on the α -methylene of the side chain will also interact with the lone pair of electrons on the neighboring sulfur atom, thus diminishing the planarity of the polymer.⁵⁰

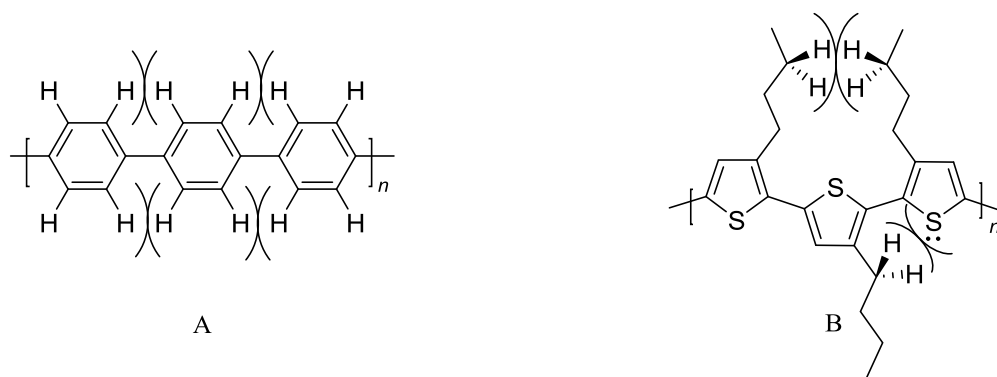


Figure 1.11. A) β -hydrogen interactions B) Chain-chain and chain-backbone interactions resulting in torsional strain

The substitution of heteroalkyl side chains can reduce the Van der Waals radius of the moiety found in the α -position of the side chain, thus lower steric interactions (Figure 1.12). Heteroalkyl side chains also alter the polymer's electronic properties through inductive effects.⁵¹ Polyalkoxythiophenes see a destabilization of the HOMO due to electron donation from the oxygen lowering the potential for oxidation as well as the band gap. Unfortunately, the reduced steric strain of the polyalkoxythiophenes leads to materials with limited solubility. A compromise is the use of alkylamino side chains. They are of an intermediate size between the alkoxide and methylene groups. In addition, the nitrogen has comparable electron-donating abilities to oxygen. The resulting poly(alkylaminothiophene)s have better solubility than the polyalkoxythiophenes but their conjugation is not as ample.⁴³

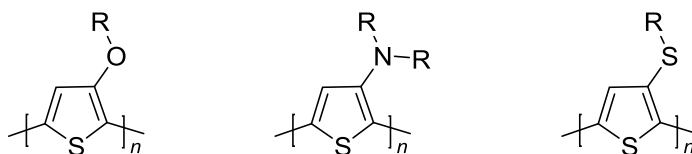


Figure 1.12. Heteroalkyl side chains on polythiophenes

As previously stated, the valence and conduction bands are formed in the bulk solid state. They occur via π -stacking between polymer chains (i.e. interchain coupling). The inclusion of side chains to enhance solubility can have a negative effect on the packing in the solid state of

the polymer by increasing the distance between polymer chains reducing the interchain coupling.⁵² Annulation of aromatic repeat units is one synthetic technique used to enhance interchain coupling. When a bridging unit is inserted between the adjacent thiophenes, such as in a molecule of 2,2'-bithiophene (Figure 1.13), this decreases interannular bond rotation resulting in a rigid system which increases the planarity of the repeat units causing a more efficient delocalization of electrons along the polymer backbone. Additionally these fused-ring systems can be functionalized at the bridging unit allowing the molecule to remain symmetrical, thus reducing potential problems with regioirregularity in the polymeric materials. Dithieno[3,2-*b*:2',3'-*d*]pyrroles (DTPs) are an example of a nitrogen-functionalized fused-ring system.⁵³⁻⁵⁷

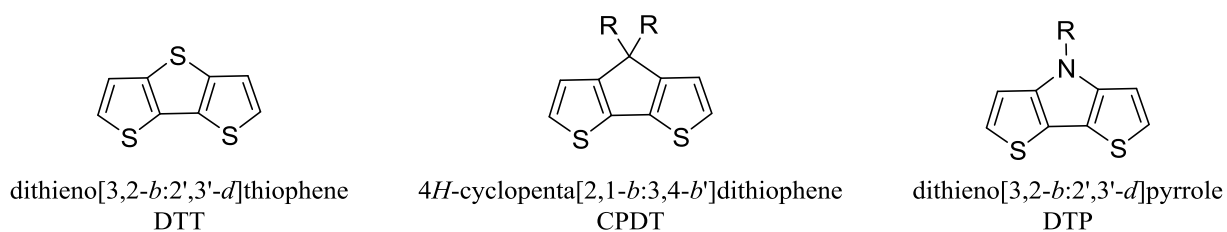


Figure 1.13. Annulation of bithiophene

Another popular synthetic technique used to tune band gaps is called the donor-acceptor method (Figure 1.14).

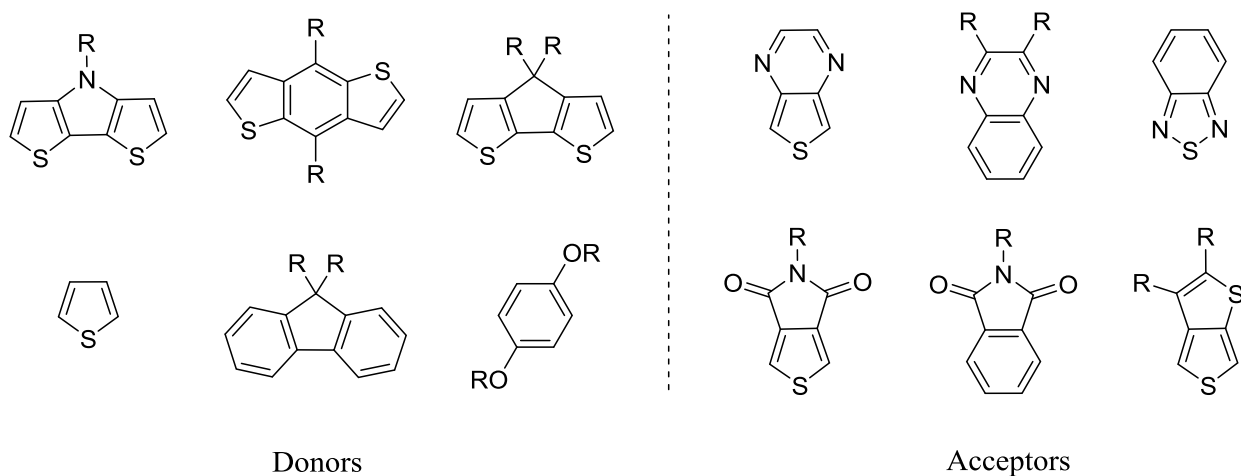


Figure 1.14. Examples of commonly used donor and acceptors⁴⁷

This is based on the ideal of creating a copolymer of alternating electron-rich aromatic units (donor) and electron-poor aromatic units (acceptor).^{1,58} A few examples of common donors and acceptors are shown in Figure 1.14.

One school of thought attributes the band gap of the resulting copolymer to the hybridization of the HOMO and LUMO of the donor and acceptor units. The donor unit contributes to the resulting HOMO whilst the acceptor unit corresponds to the LUMO (Figure 1.15).

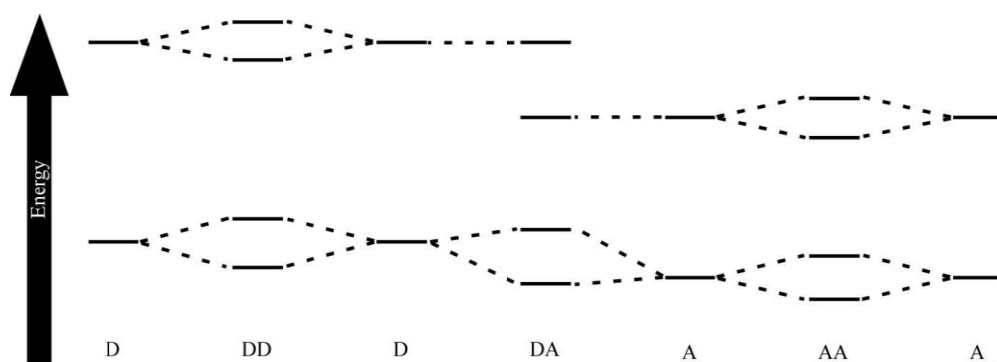


Figure 1.15. MO mixing for donor-acceptor model⁴⁷

That being said conjugated polymers created using this method can exhibit qualities of low, reduced or higher band gaps depending on the nature of the donor and accepting units. Low band gap materials are typically seen with copolymers of good donors and strong acceptors.⁵⁹⁻⁶³

1.4. Research goals

The promise of semiconducting materials with tunable electronic and optical properties that share the same mechanical flexibility, low production costs and ease of processing displayed by traditional polymers fuels the intense interest seen in developing devices employing conjugated polymers. Many examples of π -conjugated systems have been studied and reported in the literature, of which Rasmussen and coworkers have advanced the field with their work

involving *N*-alkyl, *N*-aryl, and *N*-acylDTPs.^{53,54,55,64,65} Using their efforts as a template, the goal of this research is to create related compounds to probe the relationship between their structure and the corresponding electronic and optical properties.

Two such analogues of interest are pyrrolo[3,2-*d*:4,5-*d'*]bisthiazole (PBTz) and difuro[3,2-*b*:2',3'-*d*]pyrroles (DFPs). The increased electron-deficient nature of the thiazole ring has been shown to stabilize the HOMO level and to reduce the band gap of PBTz-based polymers in comparison to DTP materials.^{66,67} The ability to synthesize furans from biomass feedstock and the fact they have comparable aromaticity with thiophenes makes them an attractive option as building blocks for conjugated polymers.⁶⁸ Additionally one would expect to see an increase in fluorescence with furan-based conjugated materials due to reduction of the heavy atom effect. Methods to generate PBTz and DFP along with their characterization and material applications in relation to DTP-based materials will be presented.

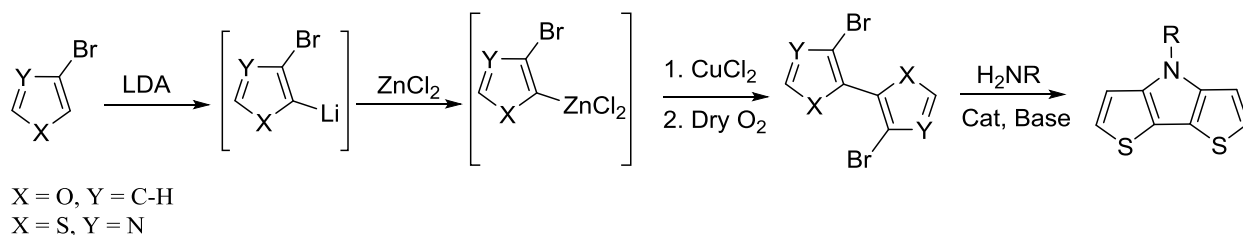


Figure 1.16. Synthesis of DTP analogues

1.5. References

1. Nyugen, T. P.; Destruel, P. Electroluminescent Devices Based on Organic Materials and Conjugated Polymers. In *Handbook of Luminescence, Display Materials, and Devices*, Inouye, H. S.; Rohwer, L. S., Eds; Organic, American Scientific Publishers, Severson Ranch, CA, 2003; Vol 1; p 5.
2. Roncali, J. *Chem. Rev.* **1992**, 92, 711-738.

3. Roncali, J. *Chem. Rev.* **1997**, *97*, 173-205.
4. Friend, R. H.; Greenham, N. C. Electroluminescence in Conjugated Polymers. In *Handbook of Conducting Polymers*, 2nd Ed.; Skotheim, T. A., Elsenbaumer, R. L., Reynolds, J. R., Eds.; Marcel Dekker, Inc: New York, 1998; pp 823-880.
5. Cui, T.; Liu, Y. In *Organic Electronics and Photonics: Electronic Materials and Devices*, Nalwa, H. H., Ed.; American Scientific: Stevenson Ranch, 2008; Vol. 1, pp 263-303.
6. Christian-Pandya, H.; Vaidyanathan, S.; Galvin, M. In *Handbook of Conducting Polymers*, 3rd ed.; Skotheim, T. A., Reynolds, J. R., Eds.; CRC Press: Boca Raton, FL, 2007; Chapter 5.
7. Grimsdale, A. C.; Chan, K. L.; Martin, R. E.; Jokiš, P. G.; Holmes, A. B. *Chem. Rev.* **2009**, *109*, 897-1091.
8. Epstein, A. J.; Wang, Y. Z. In *Semiconducting Polymer: Applications, Properties, and Synthesis*, Hsieh, B. R., Wei, Y., Eds.; American Chemical Society: Washington, DC, 1999; pp 160-173.
9. Murray, M. M.; Holmes, A. B. In *Semiconducting Polymers: Chemistry, Physics, and Engineering*; Hadziioannou, G., van Hutten, P. F., Eds.; Wiley-VCH: Weinheim, 2000; pp 1-35.
10. Campbell, I. H.; Smith, D. L. In *Semiconducting Polymer: Chemistry, Physics, and Engineering*; Hadziioannou, G., van Hutten, P. F., Eds.; Wiley-VCH: Weinheim, 2000; pp 333-364.
11. Scott, J. C.; Malliaras, G. G. In *Semiconducting Polymers: Chemistry, Physics, and Engineering*; Hadziioannou, G., van Hutten, P. F., Eds.; Wiley-VCH: Weinheim, 2000; pp 411-462.

12. Mozer, A. J.; Sariciftci, N. S. In *Handbook of Conducting Polymers: Processing and Applications*, 3rd ed.; Skotheim, T. A., Reynolds, R., Eds.; CRC Press: Boca Raton, FL, 2007; pp 10-1-10-37.
13. Brabec, C. J.; Sariciftci, N. S. In *Semiconducting Polymers: Chemistry, Physics, and Engineering*; Hadziioannou, G., van Hutten, P. F., Eds.; Wiley-VCH: Weinheim, 2000; pp 515-560.
14. Barbella, G.; Melucci, M. In *Handbook of Thiophene-Based Materials: Applications in Organic Electronics and Photonics*; Perepichka, I. F., Perepichka, D. F., Eds.; Wiley: West Sussex, U. K., 2009; Vol. 1, pp 255-292.
15. Katz, H. E.; Dadabalapur, A.; Bao, Z. *Oligo- and Polythiophenes*; Fichous, D., Eds; Wiley-VCH, Germany, 1999; pp 490-495.
16. Tessler, N.; Veres, J.; Globerman, O.; Rappaport, N.; Preezant, Y.; Roichman, Y.; Solomesch, O.; Talk, S.; Gershman, E.; Alder, M.; Zolotarev, V.; Gorelik, V.; Eichen, Y. In *Handbook of Conducting Polymers: Processing and Applications*, 3rd Ed.; Skotheim, T. A., Reynolds, J. R., Eds., CRC Press: Boca Raton, FL, 2007; pp 7-1-7-42.
17. Bao, Z. In *Semiconducting Polymers: Applications, Properties, and Synthesis*; Hsieh, B. R., Wei, Y., Eds.; American Chemical Society: Washington, DC, 1999; pp 244-257.
18. Horowitz, G. In *Semiconducting Polymers: Chemistry, Physics and Engineering*; Hadziioannou, G.; van Hutten, P. F., Eds.; Wiley-VCH: Weinheim, 2000; pp 463-514.
19. Otsubo, T.; Takimiya, K. In *Handbook of Thiophene-Based Materials: Applications in Organic Electronics and Photonics*; Perepichka, I. F., Perepichka, D. F., Eds.; Wiley: West Sussex, U. K., 2009; Vol. 1, pp 321-340.

20. Hotta, S. In *Handbook of Thiophene-Based Materials*; Perepichka, I. F., Perepichka, D. F., Eds.; Wiley: West Sussex, U. K., 2009; Vol. 1, pp 477-496.
21. Fachetti, A. In *Handbook of Thiophene-Based Materials*; Perepichka, I. F., Perepichka, D. F., Eds.; Wiley: West Sussex, U. K., 2009; Vol. 1, pp 595-646.
22. McCulloch, I.; Heeney, M. In *Handbook Thiophene-Based Materials*; Perepichka, I. F., Perepichka, D. F., Eds.; Wiley: West Sussex, U. K., 2009; Vol. 1, pp 647-672.
23. Thomas, C. A.; Reynolds, J. R. In *Semiconducting Polymers: Applications, Properties, and Synthesis*; Hsieh, B. R., Wei, Y., Eds.; American Chemical Society: Washington, DC, 1999; pp 367-373.
24. Meng, X. S.; Desjardins, P.; Wang, Z. Y. In *Semiconducting Polymers: Applications, Properties, and Synthesis*; Hsieh, B. R., Wei, Y., Eds.; American Chemical Society: Washington, DC, 1999; pp 61-75.
25. Invernale, M. A.; Acik, M.; Sotzing, G. A. In *Handbook of Thiophene-Based Materials: Applications in Organic Electronics and Photonics*; Perepichka, I. F., Perepichka, D. F., Eds.; Wiley: West Sussex, U. K., 2009; Vol. 1, pp 757-782.
26. Beaujuge, P. M.; Reynolds, R. *Chem Rev.* **2010**, *110*, 268-320.
27. Beaujuge, P. M.; Amb, C. M.; Reynolds, J. R. *Acc. Chem. Res.* **2010**, *43*, 1396-1407.
28. McNeil, R.; Siudak, R.; Wardlaw, J. H.; Weiss, D. E. *Aust. J. Chem.* **1963**, *16*, 1056-1075.
29. Bolto, B. A.; Weiss, D. E. *Aust. J. Chem.* **1963**, *16*, 1076-1089.
30. Bolto, B. A.; McNeill, R.; Weiss, D. E. *Aust. J. Chem.* **1963**, *16*, 1090-1103.
31. De Surville, R.; Jozefowicz, M.; Yu, L. T.; Perichon, J.; Buvet, R. *Elect. Chim. Acta.* **1968**, *13*, 1451-1458.

32. Doriomedoff, M.; Hautiere-Cristofini, F.; De Durville, R.; Jozefowicz, M.; Yu, L.-T.; Buvet, R. *J. Chim. Phys. Phys.-Chim.Biol.* **1971**, *68*, 1055-1069.
33. Shirakawa, H. *Angew. Chem. Int. Ed.* **2001**, *40*, 2574-2580.
34. Heeger, A. J. *Angew. Chem. Int. Ed.* **2001**, *40*, 2591-2611.
35. Shirakawa, H.; Louis, E. J.; MacDiarmid, A. G.; Chiang, C. K.; Heeger, A. J. *Chem. Commun.* **1977**, 578-580.
36. Norden, B.; Krutmeijer, E., *The Royal Swedish Academy of Sciences* **2000**. 1-16
37. Cardona, C. M.; Li, W.; Kaifer, A. E.; Stockdale, D.; Bazan, G. C. *Adv. Mater.* **2011**, *23*, 2367
38. Schwiderski, L. R. Ph.D. Dissertation, North Dakota State University: Fargo, ND, 2014
39. Brédas, J.-L. *J. Chem. Phys.* **1985**, *82*, 3808-3811.
40. Brédas, J.-L. In *Electronic Properties of Polymers and Related Compounds*; Kuzmany, H., Mehring, M. S., Roth, S. Eds.; Springer-Verlang: Berlin, 1985.
41. Dkhissi, A.; Louwet, F.; Groenendaal, L.; Beljonne, D.; LAzzaroni, r.; Brédas, J. L. *Chem. Phys. Lett.* **2002**, *359*, 466-472.
42. Brédas, J. L.; Street, G. B.; Thémans, B.; André, J. M. *J. Chem. Phys.* **1985**, *83*, 13231329.
43. Rasmussen S. C.; Ogawa, K.; Rothstein, S. D. In *Handbook of Organic Electronics and Photonics: Electronic Materials and Devices*; Nalwa, H. S. Ed.; American Scientific Publishers; Stevenson Ranch, CA, 2008; Vol. 1, pp 1-50.
44. Cary, F. A.; Sunberg, R. J. *Advanced Organic Chemistry part A: Structure and Mechanisms*, 4th Ed.; Kluwer Academic/Plenum Publisher, New York, 2000; pp 541-542.
45. Pomerantz, M. In *Handbook of conducting Polymers*, 2nd Ed.; Skotheim, T. A., Elsenbaumer, R. L., Reynolds, J. R., Eds.; Marcel Dekker Inc.: New York, 1998; pp 277310.

46. Rasmussen, S. C.; Schwiderski, L.; Mulholland, M. E. *Chem. Commun.* **2011**, *47*, 11394-11410.
47. Rasmussen, S. C. Low Bandgap Polymers. SpringerReference [Online], July 25, 2013. <http://www.springerreference.com/docs/html/chapterdbid/358935.html> (accessed July 7, 2014).
48. Hernandez, V.;Castiglioni, C.; Del Zoppo, M.; Zerbi, G. *Phys. Rev. B* **1994**, *50*, 9815
49. Hutchinson, G. R.; Zhao, Y. J.; Delley, B.; Freeman, A.J.; Ratner, M.A.; Marks, T.J. *Phys. Rev. B* **2003**, *68*, 35204
50. Loewe, R. S.; Khersonksy, S. M.; McCullough, R. D. *Adv. Mater.* **1999**, *11*, 250-253.
51. Daoust, G.; Leclerc, M. *Macromolecules* **1991**, *24*, 455-459.
52. Kondo, T.; Ishii, A.; Manabe, H.; Munekata, H. *Appl. Phys. Lett.* **2001**, *78*, 1352-1354.
53. Ogawa, K.; Rasmussen, S. C. *J. Org. Chem.* **2003**, *68*, 2921-2928
54. Ogawa, K.; Rasmussen, S. C. *Macromolecules* **2006**, *39*, 1771-1778.
55. Evenson, S. J.; Mumm, M.; Konstantin, P. I.; Rasmussen, S. C. *Macromolecules* **2011**, *44*, 835-841.
56. Liu, J.; Zhang, R.; Sauv , G.; Kowalewski, T.; McCullough, R. D. *J. Am. Chem. Soc.* **2008**, *130*, 13167-13176
57. Evanson, S.J.; Rasmussen S.C. *Prog. Polym. Sci.* **2013**, *12*, 1773-1804
58. Kirchmeyer, S.; Reuter, K.; Simpson, J. C. In *Handbook of Conducting Polymers: Theory, Synthesis, Properties, and Characterization*, 3rd ed.; Skotheim, T. A., Reynolds,
59. Amb, C. M.; Chen, S.; Graham, K. R.; Subbiah, J.; Small, C. E.; So, F.; Reynolds, J. R. *J. Am. Chem. Soc.* **2011**, *133*, 10062-10065.

60. Helgesen, M.; Krebs, F. C. *Macromolecules* **2010**, *43*, 1253-1260.
61. Steckler, T. T.; Zhang, X.; Hwang, J.; Honeyager, R.; Ohira, S.; Zhang, X.-H.; Grant, A.; Ellinger, S.; Odom, S. A.; Sweat, D.; Tanner, D. B.; Rinzler, A. G.; Barlow, S.; Brédas, J.-L.; Kippelen, B.; Marder, S. R.; Reynolds, J. R. *J. Am. Chem. Soc.* **2008**, *131*, 2824-2826.
62. Zhang, X.; Steckler, T. T.; Dasari, R. R.; Ohira, S.; Potscavage, W. J.; Tiwari, S. P.; Coppée, S.; Ellinger, S.; Barlow, S.; Brédas, J.-L.; Kippelen, B.; Reynolds, J. R.; Marder, S. R. *J. Mater. Chem.* **2010**, *20*, 123-134.
63. Zhang, X.; Shim, J. W.; Tiwari, S. P.; Zhang, Q.; Norton, J. E.; Wu, P.; Barlow, S.; Jenekhe, S. A.; Kippelen, B.; Brédas, J.-L.; Marder, S. R. *J. Mater. Chem.* **2011**, *21*, 4971-4982.
64. Ogawa, K.; Radke, K. R.; Rothstein, S. D.; Rasmussen, S. C. *J. Org. Chem.* **2001**, *66*, 9067-9070.
65. Evenson, S. J.; Rasmussen, S. C. *Org. Letters* **2010**, *18*, 4054-4057
66. Al-Hashimi, M.; Labram, J.G.; Watkins, S.; Motevalli, M.; Anthopoulos, T.D.; Heeney, M. *Org. Lett.* **2010**, *23*, 5478-5481
67. Getmanenko, Y. A.; Risko, C.; Tongwa, P.; Kim, E.G.; Li, H.; Sandhu, B.; Timofeeva, T.; Brédas, J. L.; Marder, S. R. *J. Org. Chem.* **2011**, *76*, 2660-2671
68. Sonar, P.; Foong, T. R. B.; Singh, S. P.; Li, Y.; Dodabalapur, A. *Chem. Commun.* **2012**, *48*, 8383-8385

CHAPTER 2. 2,4-DIBROMO-1,3-THIAZOLES AS BUILDING BLOCKS FOR SYNTHESIS OF PYRROLO[3,2-*d*:4,5-*d'*]BISTHAZOLES

2.1. Introduction

Since the discovery of conjugated polymers (CPs), interest in their synthesis, device fabrication and improving their performance has steadily grown. In no small part, this has been fueled by their unique properties: low production costs, mechanical flexibility and the ease of processing which is also displayed by conventional polymers. Additionally the ability to tune the electrical and optical properties of CPs at the molecular level makes them an attractive option for many types of applications.¹⁻³

One synthetic method used to control the band gap of conjugated polymers is to create fused-ring analogues of the traditional polymer systems. Figure 2.1. illustrates how a bridging unit inserted between adjacent thiophenes decreases interannular bond rotation, resulting in a more rigid system. Increasing the planarity causes a more efficient delocalization of electrons along the polymer backbone. Additionally these fused-ring systems can be functionalized at the bridging unit giving them a convenient handle to add solubilizing side chains. This allows the molecule to remain symmetrical, thus reducing potential problems with regioirregularity in the polymeric materials. Examples of such nitrogen-functionalized units found in the literature are *N*-alkyl-, *N*-acyl-, and *N*-aryl-dithieno[3,2-*b*:2',3'-*d*]pyrroles (DTPs).⁴ Polymers of these thiophene-based units show enhanced optical properties, lowered band gaps, and improved charge carrier mobilities in addition to improved solid state and solution fluorescence.⁵

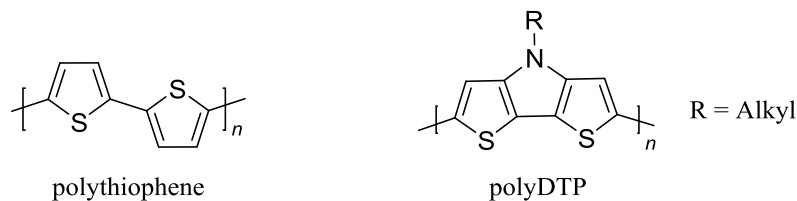


Figure 2.1. Fused-ring analogue of thiophene based polymer

The current method for the synthesis of DTPs is shown in Figure 2.2 and uses the cost-effective 3-bromothiophene (**2.1**) as the starting material. Lithium diisopropylamide (LDA) is used to selectively deprotonate at the two-position of the thiophene ring, generating a lithiated intermediate. Next a sequential transmetalation step occurs, by first adding ZnCl_2 and then CuCl_2 . The oxidative homo-coupling is then assisted by the use of dry O_2 to produce 3,3'-dibromo-2,2'-bithiophene (**2.2**) in yields of 85-90%. The N-functionalized DTP monomeric unit is then made through either a Pd- or Cu-catalyzed reaction involving an amine or amide.⁶

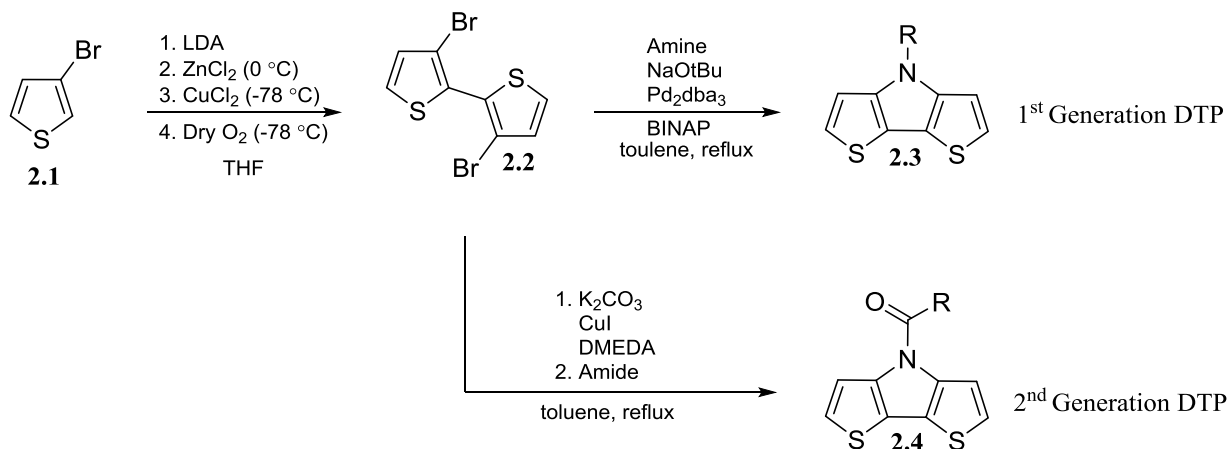


Figure 2.2. Synthesis of 1st and 2nd generation DTPs

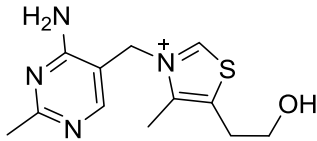
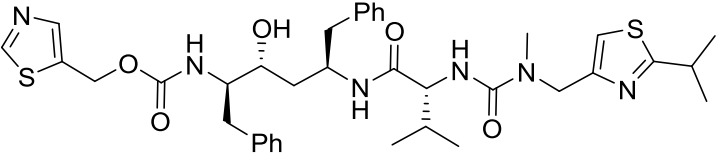
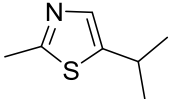
However DTP-based materials suffer from poor oxidative stability due to the high energy level of the materials HOMO. One attempt at stabilizing the HOMO and LUMO of DTP-based materials has focused on replacing the alkyl chain on the pyrrole ring with an electron-

withdrawing acyl group.⁵ Another avenue is to replace the thiophene units with a more electron deficient heterocycle, such as thiazole.^{7,8}

2.2. Reactivity of thiazoles

Thiazoles are five-membered aromatic rings that contain two heteroatoms, sulfur and nitrogen, which are found in a variety of natural products and materials (Table 2.1). One prominent example of a natural product containing thiazole is thiamin, vitamin B1, which is essential for proper neural function and metabolism. Additionally they are found in pharmaceutical compounds such as Ritonavir, an HIV1 protease inhibitor.⁹ In the food industry, they are commonly used as agents to produce meaty and roasted flavors.¹⁰ Because of their optical and electronic properties they are also of interest to material scientists for use as liquid crystals or in OPVs and OLEDs.^{7,11}

Table 2.1. A sampling of thiazoles found in nature and materials

Ritovar	
HIV1 protest inhibitor	
Thiamin	
Essential for proper neural and metabolism	
5-methyl-2-isopropyl thiazole	
Mouldy, fruity, vegetable flavor	

The two heteroatoms found on a thiazole ring create a variety of electronic conditions which offer different degrees of reactivity towards lithiation, S_NAr reactions, and electrophilic aromatic substitution (Figure 2.3).^{11,12} The 2-position is the most electron-deficient on the ring due to the flanking heteroatoms. This position is not easily susceptible to electrophilic aromatic

substitution but will undergo nucleophile-based reactions such as S_NAr chemistry. This electron-poor position also is the most acidic ($pK_a = 29.6$) allowing for selective lithiation.¹³ The 5-position is the most electron rich in the ring and will easily undergo electrophilic aromatic substitution. The 4-position is moderately electron rich and will only succumb to an electrophilic aromatic substitution if the 5-position is blocked.^{11,12}

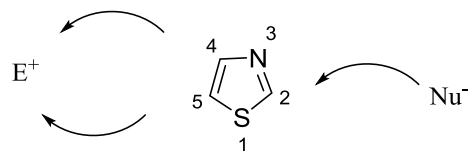


Figure 2.3. Observed reactivity of thiazoles

2.3. Generation of 4,4'-dibromo-2,2'-bis(triisopropylsilyl)-5,5'-bithiazole

One of the aims of this research was to create an analogue of DTP in which the flanking thiophenes are replaced with thiazoles units. A review of the literature showed that only a few groups have reported on the synthesis and characterization of pyrrol[3,2-*d*:4,5-*d'*]bisthiazoles (PBTz) and related bridged 5,5'-bithiazoles.⁷ The reaction schemes used by both groups varied in the number of steps and reagents used, but both started with the costly 2-bromothiazole (**2.5**) and used the precursor 4,4'-dibromo-2,2'-bis(triisopropylsilyl)-5,5'-bithiazole (**2.10**) to generation their tricyclic thiazole-based monomeric units. These combined factors led to a desire to find a new synthetic route which decreased both the cost of the reagents and number of steps required to generate **2.10**.

In 2010, Marder and co-workers reported the synthesis and characterization of a tricyclic molecule that included flanking thiazoles with mono (**2.12a**) and dicarbonyl (**2.12b**) bridges (Figure 2.4).¹⁴ The same group, in 2014, published another scheme in which they described the synthesis and characterization of two *N*-alkylPBTz molecules, analogues of DTP (Figure 2.4).⁸

Both papers used the same approach in the generation of **2.10**, the precursor to the thiazole-based monomeric repeat units. Each starts with **2.5** which undergoes a lithium-bromine exchange initiated by using BuLi at $-78\text{ }^{\circ}\text{C}$ followed by the addition of triisopropylsilyl chloride (TIPSCl) to afford 2-triisopropylsilyl thiazole (**2.6**). The second step requires a bromination at the 5-position of the thiazole by first using BuLi and then adding bromine, again at a temperature of $-78\text{ }^{\circ}\text{C}$.¹² With the 5-bromo-2-(triisopropylsilyl)thiazole (**2.7**) in hand, **2.10** is made through an efficient rearrangement of atoms on the thiazole ring. Compound **2.7** is deprotonated using LDA and the lithiated species undergoes a lithium-halogen exchange between the 4- and 5-position producing the desired intermediate (**2.9**) which then undergoes a copper-promoted oxidative coupling to produce **2.10**.^{7,8,14}

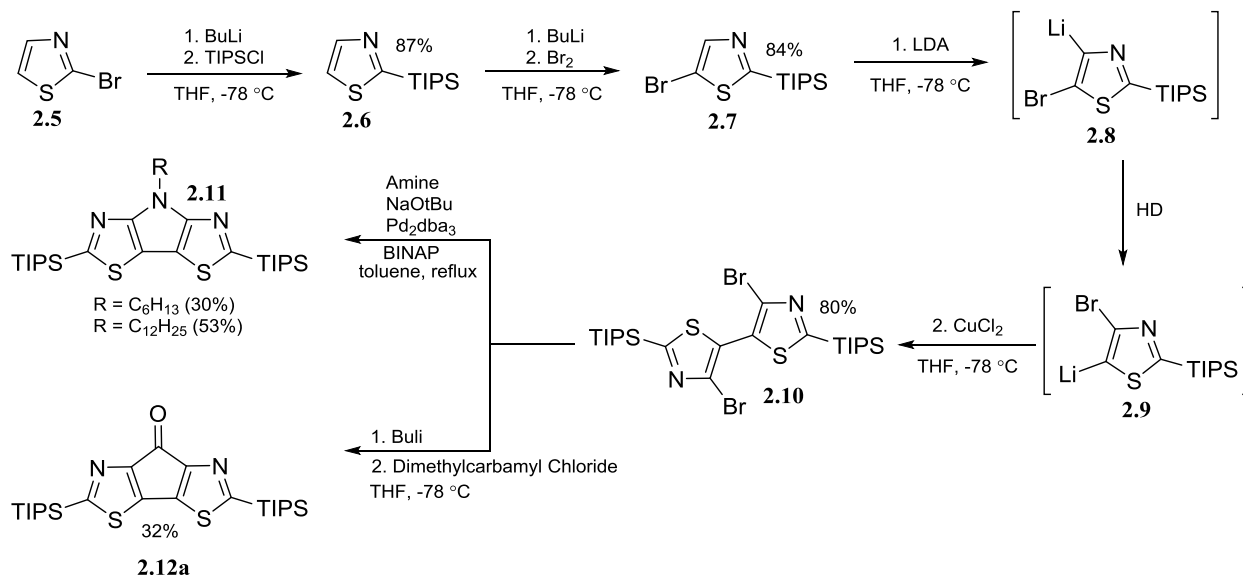


Figure 2.4. Reported generation of PBTz

The rearrangement of the bromine from the 5- to 4-position is commonly referred to as the halogen dance (HD). This reaction starts with the formation of an organolithium aromatic species followed by an intermolecular exchange of the lithium with a halogen from an adjacent

molecule. Driving the transposition of these moieties is the formation of a more stable organolithium intermediate.¹⁶

Figure 2.5 outlines the mechanism for the conversion of 2,5-dibromothiophene into a 3,5-dibromothiophene species via the halogen dance.¹⁶ For both thiophenes and thiazoles the formation of the most thermodynamically stable intermediate causes the observed reorganization of the moieties. Since variations of pKa's exist on the both rings, the highly reactive carbon-lithium bond prefers the location with the greatest acidity. On thiazoles, the 2-position is the most acidic closely followed by the 5-position and the 4-position is the least.¹⁵

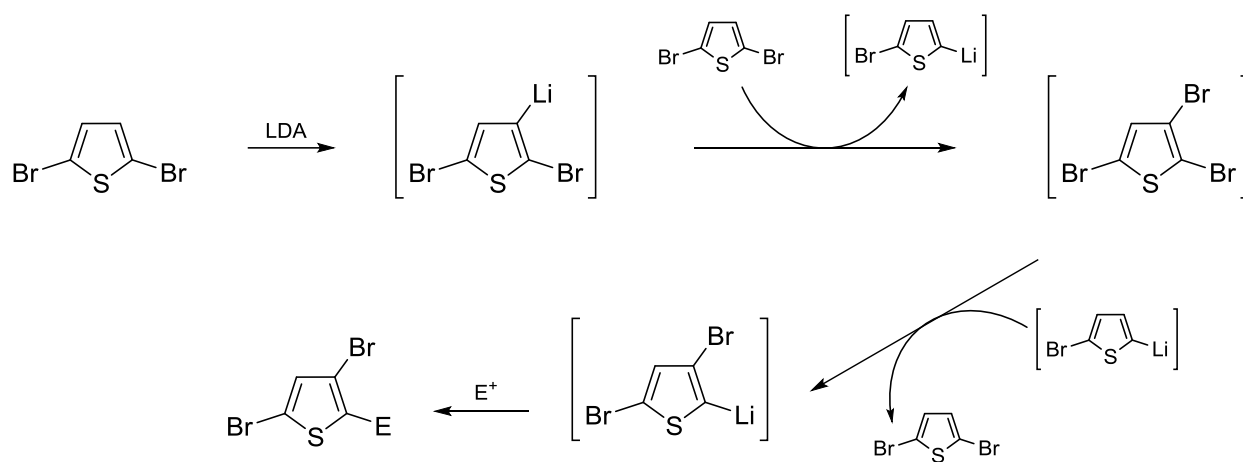


Figure 2.5. Conversion of 2,5-dibromothiophene into 3,5-dibromothiophene-2-lithiothiophene via the halogen dance

For the HD to occur both the metalated and unmetalated species must be present in the reaction mixture at the same time. This simple fact allows chemists to manipulate the extent of the rearrangement that occurs through careful control of the reaction conditions. At lower temperatures the rate of metalation is retarded, relative to rates seen at elevated temperatures, and thus allows for the coexistence of both species encouraging the halogen dance. The choice of ‘fast’ reacting electrophiles (TMSCl, MeOH) versus that of ‘slow’ reacting electrophiles (DMF)

has been shown to suppress the halogen dance.¹⁶ Trapping of the lithiated species occurs at a greater rate when a ‘fast’ electrophile is used preventing the concurrent presence of both the lithated and unlithated species. Also the order in which the reactants are added to each other will affect the outcome. If the base is slowly added to the halide substrate this allows for unreacted starting material and the lithiated starting material to coexist encouraging the halogen dance.¹⁷

It is this behavior seen in thiazoles that necessitates the placement of a protecting group at the 2-position on the ring. Formation of **2.10** in Figure 2.4 requires an oxidative coupling which is initiated by the creation of an organolithium intermediated which is then transmetalated by copper. If the protecting group was absent at the 2-position the lithio intermediate would undergo the HD and coupling would occur there instead of the desired 5-position. Also the choice of protecting group is important. When trimethylsilyl and trimethylstannyl are placed in the 2-position a rearrangement is observed akin to the mechanism seen in the HD (Figure 2.6).^{18,19} Marder and co-workers were able to halt this rearrangement through the use of the bulkier TIPS as the protecting group.¹⁴

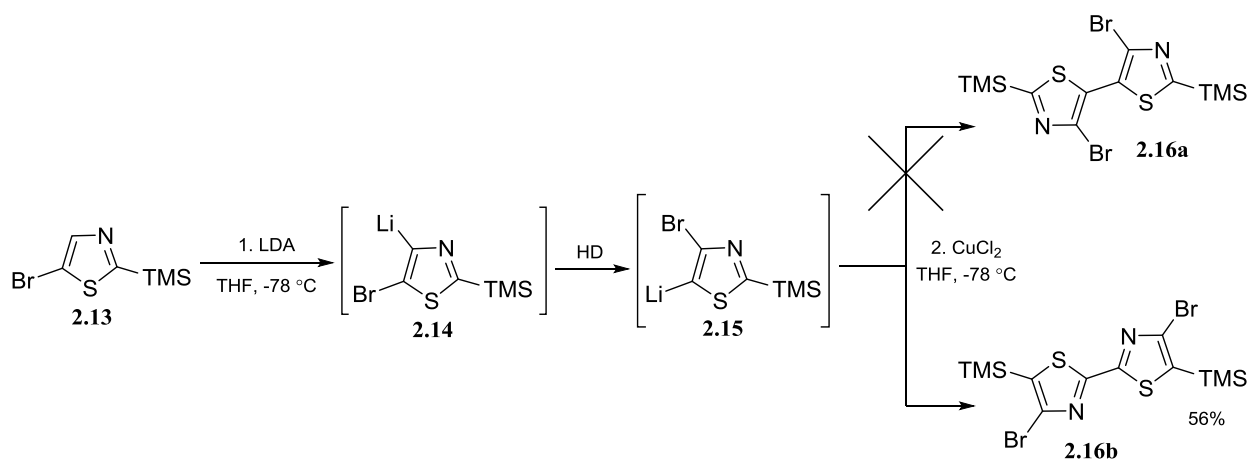


Figure 2.6. An unexpected rearrangement

As previously mentioned, Heeney and co-workers also reported on the synthesis of PBTz in 2010 (Figure 2.6). Their original synthetic scheme followed a similar path to Marder's group in that they attempted to protect the 2-position before performing the copper-assisted oxidative coupling. Starting with commercially available 2-(trimethylsilyl)-5-bromothiazole (**2.13**) cooled to $-78\text{ }^{\circ}\text{C}$ they lithiated the 4-position with LDA assuming the HD would allow for the smooth rearrangement between the moieties on the 4- and 5-positions. Instead of the desired product 4,4'-dibromo-2,2'-bis(trimethylsilyl)-5,5'-bithiazole (**2.16a**) they unexpectedly formed 5,5'-dibromo-4,4'-bis(trimethylsilyl)-2,2'-bithiazole (**2.16b**) which they explained through the swapping of the lithio moiety at the 4-position with the TMS group at the 2-position.

Due to this unexpected rearrangement a retooling of their synthetic approach was conducted based largely on the work of Knochel and coworkers. In 2007 they published a series of papers in which they reported the use of $(\text{TMP})_2\text{Zn}\cdot 2\text{MgCl}_2\cdot \text{LiCl}$ (TMP = 2,2,6,6-tetramethylpiperidine) as a selective base for the direct transmetalation of arenes and heterocycles (Figure 2.7).²⁰

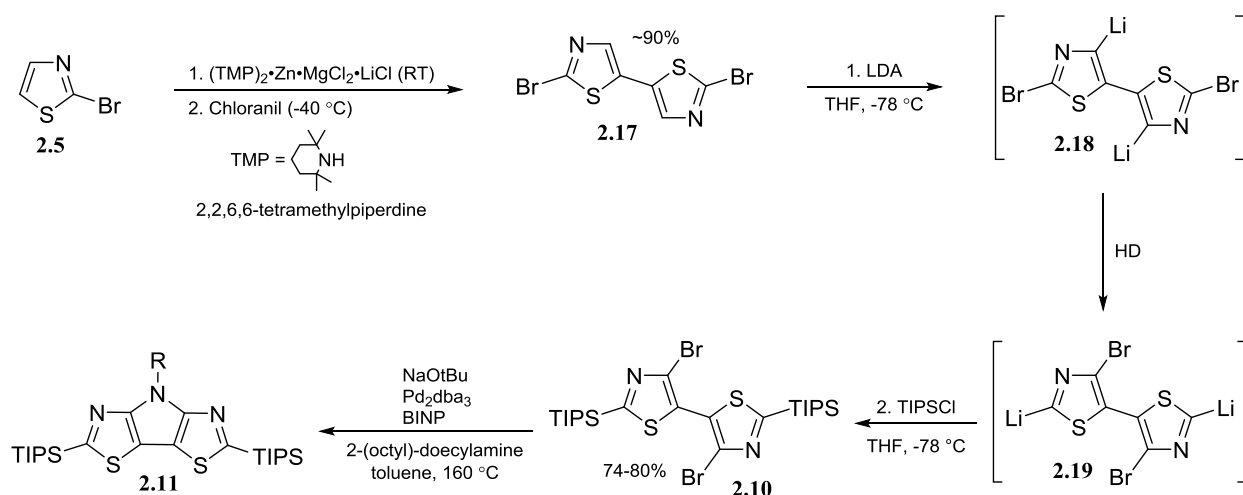


Figure 2.7. Use of $(\text{TMP})_2\text{Zn}\cdot 2\text{MgCl}_2\cdot \text{LiCl}$ in generation of 4,4'-dibromo-2,2'-bis(triisopropylsilyl)-5,5'-bithiazole

Knochel showed when this base was used in conjunction with the cheaper **2.5**, the resulting diarylzinc compound affords 2,2'-dibromo-5,5'-bithazole (**2.17**) when oxidized with chloranil at -40 °C in yields around 90%.^{20,21}

Although the aforementioned synthetic methods produce the desired precursor (**2.10**) to N-functionalized PBTz monomeric units in good overall yields, a desire to reduce the overall number of steps found in the Marder method (Figure 2.4) and to replace the costly **2.5** as the starting material in both schemes was the genesis for this part of our project. 2,4-Dibromothiazole (**2.21**) was an attractive option to replace **2.5** in that it already had a bromine in the desired 4-position eliminating both reagents and steps from the reported schemes. Unfortunately the cost of **2.21** far exceeds that of **2.5**. A cheaper alternative to buying the **2.21** was to synthesis the material ourselves and after a review of the literature, thiazolidinedione (**2.20**) was chosen as our starting point.

2.4. Results and discussions

Several groups have reported that when **2.20** was mixed with phosphorus(V) oxybromide (POBr₃) and heated at reflux under solvent-free conditions, **2.21** was produced (Figure 2.8). The yields varied significantly in the literature depending on the amounts of the very costly PBrO₃ used, ranging from 99% when 7.6 equivalents was used to as low 40% when 3.0 equivalents were added.^{22,23} When we attempted this reaction using the smaller equivalency yields of only 61% were obtained. Due to the high cost of POBr₃ and the large quantities needed this scheme was never seriously considered as an alternative route. In fact after figuring the cost of the reagents needed and expected yields it would be cheaper just to buy **2.21** than to produce it in this manner.

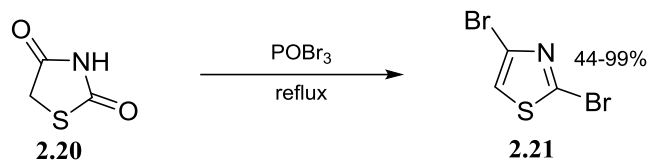


Figure 2.8. Use of POBr_3 for the generation of 2,4-dibromothiazole

A similar reaction was found using the cheaper brominating agent PBr_5 . Rasmussen and coworkers reported a conversion of a dione (**2.20**) into a dibrominated (**2.21**) species. This was accomplished when a solution of tetrabutylammonium bromide (Bu_4NBr), Na_2CO_3 and PBr_5 were heated at reflux in xylenes until a color change from deep red to light yellow was observed. After which the dione was added and refluxing was continued overnight (Figure 2.9).²⁴ The initially observed color change was contributed to the behavior of molecular PBr_5 in a non-coordinating solvent.²⁵ It has been shown that PBr_5 disassociates into bromine and PBr_3 in benzene and so it was assumed to do so in xylenes. Heating of the solution resulted in an equilibrium shift from Br_2 , red in color, back to the PBr_5 , which was a yellow solid before being dissolved.²⁴ Additionally PBr_5 could be generated through a reaction of PBr_3 with Br_2 in petroleum ether in yields of 70-80%, further reducing the cost of the overall reaction.²⁶

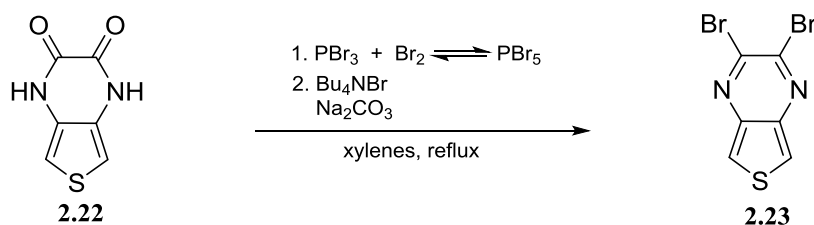
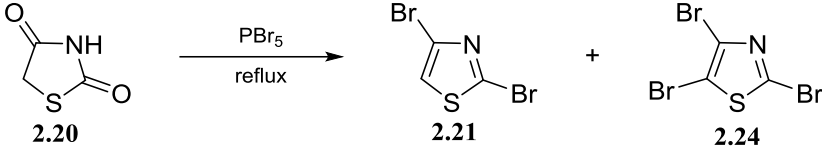


Figure 2.9. Equilibrium shift of PBr_5 and use of brominating agent

Using **2.20** and PBr_5 as the brominating agent the procedure reported by Rasmussen and coworkers was attempted. The desired **2.21** was not observed as a product so toluene was tried as

a solvent and the experiment was repeated. Again there was no observed formation of the product at which point we moved to a solvent-free reaction condition as originally reported with POBr_3 .^{22,23} This change proved successful in the generation of **2.21** and 2,4,5-tribromothiazole (**2.24**) as an additional product. A series of trials were then conducted in an attempt to optimize the reaction conditions with selected results reported in Table 2.2. It was determined that a reaction time of 3 h at a temperature of 120 °C with a two to one equivalent of PBr_5 to starting material produced the greatest amount of **2.21** in yields of 21%, but all the trials conducted still contained the unwanted **2.24**.

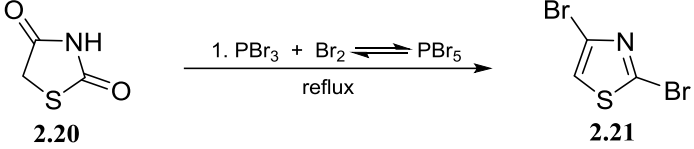
Table 2.2. Optimization of PBr_5 reaction conditions

						
2,4-Thiazolidinedione	PBr_5	Temp	Solvent	Time	Dibrominated Species	Tribrominated Species
1 equiv	7 equiv	120 °C	neat	4 h	0%	7%
1 equiv	3 equiv	120 °C	neat	3 h	0%	9%
1 equiv	2 equiv	120 °C	neat	5 h	13%	23%
1 equiv	2 equiv	120 °C	neat	3 h	21%	16%
1 equiv	1 equiv	100 °C	neat	2 h	10%	8%
1 equiv	1 equiv	100 °C	neat	1 h	1%	3%
1 equiv	2 equiv	Reflux	xylene	12 h	0%	0%

One observation during these trials was that upon heating of the reaction mixture it turned red indicating the presence of Br_2 . It was hypothesized that the presence of this bromine was responsible for the generation of the unwanted **2.24**. Borrowing from work previously reported from the Rasmussen group an adjustment was made in our reaction procedure.²⁴ PBr_5 was first

heated at reflux until the disappearance of the reddish color was observed and then the starting material was added. This resulted in the complete elimination of **2.24** and only **2.21** was formed. The reaction conditions were then optimized and are shown in Table 2.3. Based on the results, reaction times of 25 min at temperatures of 140 °C with a two to one equivalent of PBr₅ to starting material produced the highest yield of **2.21** at 50%

Table 2.3. Further optimization of PBr₅ reaction conditions

						
2,4-Thiazolidinedione	PBr ₅	Temp	Solvent	Time	Dibrominated Species	Tribrominated Species
1 equiv.	2 equiv	110 °C	neat	40 min	21%	0%
1 equiv.	2 equiv	120 °C	neat	1 h	9%	0%
1 equiv.	2 equiv	120 °C	neat	30 min	25%	0%
1 equiv.	2 equiv	140 °C	neat	25 min	50%	0%

Although promising this reaction did suffer from a lack of scalability with the highest yields resulting when 5.0 mmol of starting material was used. A doubling of the scale resulted in yields of 10-15% even after several attempts in which the reaction times, temperatures and reaction vessels were altered. Soon after these trials were completed, Sampson and co-workers reported on another synthetic route to the production of **2.21**. Their new method was based on the published work of Mase and co-workers in which they converted 2-bromobenzo[*d*]thiazol-2-ol to 2-bromobenzo[*d*]thiazole with the use of P₂O₅ and Bu₄NBr refluxed in toluene.²⁷ Sampson's group applied this approach to generate **2.21** using **2.20** as the starting material. They reported a yield of 95% after 20 h of refluxing (Figure 2.10).¹¹

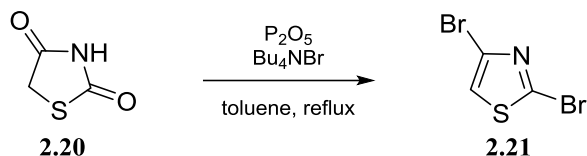


Figure 2.10. Preferred synthetic route to the production of 2,4-dibromothiazole

When compared to our method for the generation of **2.21** this newly published procedure had an improved yield in addition to the ability to increase the size of the reaction and is now the preferred method for the synthesis of **2.21**. Although, it should be noted we have never been able to reproduce the 95% yield reported by Sampson and coworkers, with our yields typically varying between 70-75%. Additionally we have detected the formation of **2.24** in addition to the **2.21** with use of longer reaction times and/or when a vigorous reflux is applied. With an efficient and scalable route to a cheap starting material in hand we focused our efforts on the generation of **2.10**. Three synthetic routes were explored.

The first proposed synthetic route was the addition of the TIPSCl as the protecting group on the 2-position and then a copper-assisted oxidative coupling to form **2.10** as shown in Figure 2.11. This was attempted through the slow addition of a solution of **2.21** to a solution of BuLi at -78 °C. Once the addition was complete the reaction mixture stirred for half an hour. TIPSCl was then added and the reaction was allowed to warm to room temperature overnight. After several attempts the highest yield achieved for the formation of 4-bromo-2-triisopropylsilyl thiazole (**2.25a**) was 25%. In addition 4-bromothiazole and unreacted TIPSCl was typically recovered from the reaction mixture, indicating a sluggish reaction between the bulky TIPSCl and the lithiated bromothiazole ring.

A series of experiments were then conducted in which the size of the silyl protecting group was varied (Figure 2.11). When the smaller TMSCl was employed the reaction preceded

smoothly giving a yield of 66% of 4-bromo-2-trimethylsilylthiazole (**2.25b**). As this is not a suitable compound for the generation of the PBTz molecule another silyl group, triethylchlorosilane (TESCl), was tested. It was hoped that the intermediate size of TESCl would allow for a good yield and yet be bulky enough to halt the silyl migration seen when TMS was employed as the protecting agent. After several attempts yields of only ~25% of 4-bromo-2-triethylsilylthiazole (**2.25c**) were obtained along with 4-bromothiazole and unreacted TESCl. With these results similar to those when TIPSCl was used as the protecting group, and this entire route was abandoned.

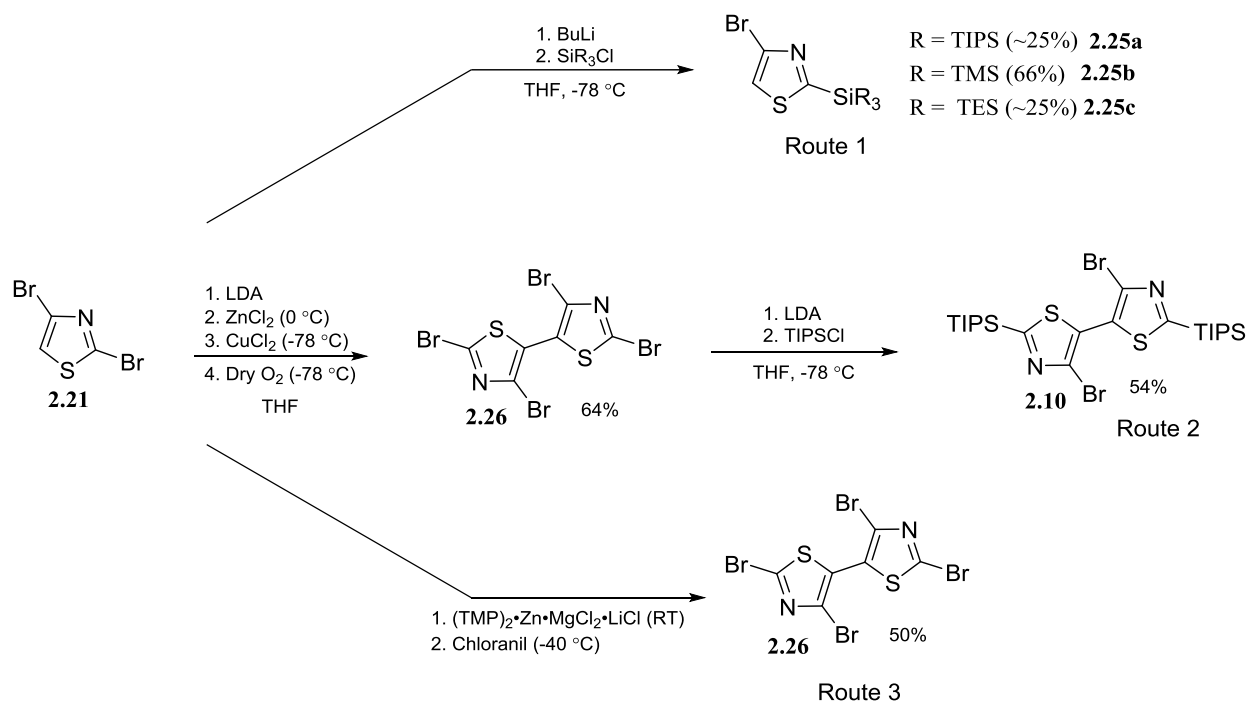


Figure 2.11. Synthetic routes for generation of 4,4'-dibromo-2,2'-bis(triisopropylsilyl)-5,5'-bithiazole

A second route was proposed due to the disappointing low yields encountered during the initial step with the first route. Figure 2.11 outlines an approach where **2.21** was to be directly homo-coupled obtaining 2,2',4,4'-tetrabromo-5,5'-bithiazole (**2.26**) to which TIPS would then be added as a protecting group. This was accomplished when a solution of **2.21** was added dropwise

to a solution of LDA at $-78\text{ }^{\circ}\text{C}$ and allowed to react for one hour. At which point an equivalent of ZnCl_2 was added and then 15 minutes later an additional equivalency of CuCl_2 was added to the reaction mixture. The reaction was stirred for 30 minutes and then dry air was bubbled into the solution. After warming to room temperature overnight the reaction was quenched with a solution of saturated NH_4Cl and then diluted with chloroform, heated, and finally filtered. The remaining residue was washed with hot chloroform and then hot acetone until the filtrate was clear. Purification, via column chromatography, produced **2.26** in yields of 54% with 25% of the starting material recovered but the purity of the product obtained was an issue. Only a small fraction (10-20%) of the overall yield is eluted as a clear solution before the solvent becomes a yellow-orange color. After removal of the clear solvent, a white-tan solid is formed whilst the other fraction leaves a solid with a yellow-orange color. Purification of the yellow solid through recrystallization has yet to be successful. Attempts to increase the yield and purity of the **2.26** through modifications of the reaction conditions have resulted in a positive outcome.

The modified procedure requires **2.21** to be dissolved in dry THF along with ZnCl_2 at room temperature. The cloudy mixture is then cooled to $-78\text{ }^{\circ}\text{C}$ before the LDA is added dropwise and then stirred until the mixture turns clear. At this point CuCl_2 is added in one portion and stirring is continued for another thirty minutes. Dry O_2 is then bubbled through the reaction mixture and it is allowed to warm to room temperature overnight. After the normal aqueous work-up and organic extraction the solution was concentrated in-vacuo to give a solid mixture of starting material and product. Methanol was used to wash the solid mixture removing the starting material (**2.21**). Another wash with hexanes removed additional impurities from the solid residue affording the desired compound (**2.26**). These modifications to original procedure resulted in a net increase of $\sim 10\%$ with the amount of recovered starting material staying the

same at around 25%. Additionally the overall appearance of the product changed from a solid with a yellow-orange color to one with a yellow-tan.

The last step of route two involved the double metal-halogen exchange of **2.26** through the use of two equivalencies of BuLi at -78 °C in THF. After which two equivalencies of TIPSCl were dripped into the reaction mixture and then warmed to room temperature overnight.

Compound **2.10** was generated in yields of 42% with 15% of the starting material recovered.

It is thought that the poor solubility of the starting material in nonpolar solvents is the chief reason for the moderate yields encountered. But it was noted during our attempts to recrystallize **2.26** that small amounts were soluble in THF when heated and that they would stay in solution upon cooling. A series of trials were then conducted with a 0.01 M solution of **2.26** which was heated at a gentle reflux until all the starting material was dissolved. It was then determined that at temperatures above -40 °C the mixture would stay in solution. Attempts to carry out the reaction at these elevated temperatures did not result in the generation of the desired product and we were not able to recover any of the starting material.

Additional attempts to increase the yield of **2.10** resulted in success. Using a more dilute reaction mixture resulted in a ~10% increase of both the yield of the product and the amount of starting material recovered from the crude reaction mixture. Although route two generated the better yield of the first two proposed schemes it was hoped we could boost the overall yield and purity of the tetrabromobisthiazole (**2.26**) generated.

A third route shown in Figure 2.11 which uses a bulkier base developed by Knochel and co-workers for the direct transmetalation of arenes and heterocycles was employed.^{21,22} The initial step was done at room temperature when a freshly titrated solution of (TMP)₂Zn-2MgCl₂•LiCl was added dropwise to a solution of **2.21** and stirred for an hour. The resulting

mixture was then cooled to -40 °C and chloranil was added in small portions. After which the reaction was placed in an ice bath and stirred for another five hours and then quenched with a saturated solution of NH₄Cl. The reaction produced **2.26** in 50% yield and we were able to recover 48% of the starting material. However this reaction scheme did suffer from the same purity issues encountered with the copper-assisted oxidative coupling and the overall yields were lower.

2.5. Conclusion

Using a modified procedure found in the literature,¹¹ a new and cheaper starting material **2.21** was utilized in the generation of the precursor **2.10** for the creation of thiazole analogues of DTPs. Several different synthetic schemes were explored (Figure 2.11). The low yields encountered in route one of the generation of **2.25a** made this path undesirable. Route two produced moderate yields of **2.26** (64%) with a 25% recovery of the starting material but issues with purity lead us to the investigation of an additional path. Route three resulted in comparable yields to the second route with even higher amounts of recovered starting material but difficulties in purifying **2.26** remained. With the additional expense and steps needed to generate and standardize (TMP)₂Zn•2MgCl₂•LiCl the second route was determined to be the most effective for overall yields, cost and time. The final step of generating **2.10** saw only moderate yields of 54% but happily 25% of the starting material is recoverable from the reaction mixture.

2.6. Experimental

If not specified, the following conditions were used in the synthesis, purification and characterization of the compounds listed in this section. Chemicals were reagent grade and used without further purification. Solvents were dried via distillation over sodium-benzophenone. Glassware was oven-dried then assembled hot and cooled under a dry nitrogen stream. Transfers

of liquids were carried out using standard syringe techniques and the reactions were performed under a dry nitrogen stream using air-free techniques. Silica gel (240-400 mesh) in conjunction with standard column chromatography methods were employed for chromatographic separations. Melting points were reported to a resolution of 0.1 °C using a digital thermocouple. The ^1H and ^{13}C NMR were performed with a 400 MHz spectrometer. NMR data collected was referenced to the chloroform signal and peak multiplicity is reported as follows: s = singlet, d = doublet, t = triplet, q = quartet, p = pentet, tt = triplet of triplets, m = multiplet and br = broad. HRMS data was collected using a Bruker-Daltonics BIOTOF HRMS. Previously reported procedures were used to generate the following compounds PBr_5 ²⁶, and $(\text{TMP})_2\text{Zn}\cdot 2\text{MgCl}_2\cdot \text{LiCl}$.²¹

2.6.1. Synthesis of 2,4-dibromothiazole (2.21) using PBr_5 as brominating agent

To a two-neck, round bottom flask with a condenser was added PBr_5 (4.30 g, 10.0 mmol) and heated to a temperature of 140 °C until the solution became clear. Then 1,3-thiazole-2,4-dione (0.59 g, 5.0 mmol) was then added in one portion and heated at reflux for 25 minutes. The round bottom was then cooled to room temperature and then water was added slowly to the reaction mixture. Solid Na_2CO_3 was added in small portions until the solution was basic. The aqueous solution was then extracted with hexanes. The organic layers were collected washed with brine, dried over MgSO_4 , filtered and then concentrated. The crude product was purified via column chromatography with hexanes producing 0.61 g of a white solid (50%). mp = 81.3 - 82.1 °C; ^1H NMR: 7.21 (s, 1H); ^{13}C HMR: δ 136.6, 124.6, 121.1. ^1H , ^{13}C and melting point values agree well with previously reported values.^{11,22,24}

2.6.2. Synthesis of 2,4-dibromothiazole (2.21) with P_2O_5 , Bu_4NBr and toluene

The following procedure was modified from one found in the literature.¹¹ A mixture of 1,3-thiazole-2,4-dione (3.51 g, 30 mmol), P_2O_5 (19.58 g, 138 mmol), and Bu_4NBr (22.25 g, 69

mmol) was dissolved in 60.0 mL of toluene then gently refluxed for 20 hours. The toluene was then removed in vacuo and 50 mL of distilled water was added to the chemical mixture in addition to solid Na_2CO_3 was added in small portions until the solution turned basic. The aqueous layer was then extracted with hexanes. The combined organic layers were then washed with a saturated solution of NaHCO_3 , water and finally brine. The organic layer was then dried over MgSO_4 , filtered and concentrated. The crude product was then recrystallized in hexanes to afford pure product 5.47 g (75%) of a white solid. mp = 81.3 - 82.1 °C; ^1H NMR: δ 7.21 (s, 1H); ^{13}C HMR: δ 136.6, 124.6, 121.1. ^1H , ^{13}C and melting point values agree well with previously reported values.^{11,22,24}

2.6.3. Synthesis of 2,4,5-tribromothiazole (2.24)

To a two-neck, round bottom flask with a condenser was added PBr_5 (4.30 g, 10.0 mmol) and thiazolidinedione (0.59 g, 5.0 mmol) which was then heated at reflux for 3 h at 120 °C. The flask was then cooled to room temperature and water was added slowly to the reaction mixture. Solid Na_2CO_3 was added in small portions until the solution was basic. The aqueous solution was then extracted with hexanes. The organic layers were collected, washed with brine, dried over MgSO_4 , filtered and then concentrated. The crude product was purified via column chromatography with hexanes producing 0.26 g of a white solid (16%). mp = 28.7 - 30.1 °C; ^{13}C HMR: δ 136.0, 127.8, 109.5

2.6.4. Synthesis of 4-bromo-2-(triisopropylsilyl)thiazole (2.25a)

To a round bottom flask was added 10.0 mL of THF and 0.84 mL of 2.5 M (2.0 mmol) BuLi in hexanes and cooled in a dry ice-acetone bath. To which a solution of 2,4-dibromothiazole (0.46 g, 2 mmol) in 10.0 mL of THF was added drop-wise. The reaction mixture was allowed to stir for 45 minutes then (0.38 mL, 2.1 mmol) of TIPSCl was added

slowly. The reaction was allowed to warm to room temperature overnight and then quenched with a saturated solution of NaHCO₃. The organic layer was extracted with diethyl ether and the combined organic layers were dried over MgSO₄, filtered and concentrated. The crude product was purified via column chromatography with diethyl ether: hexanes (1%) producing 0.16 g of a tan solid (25%). mp = 109.7-110.9 °C; ¹H NMR: δ 1.11 (d, *J* = 7.4 Hz, 18H), 1.43 sept, *J* = 7.4 Hz, 3H), 1.39 (s, 1H); ¹³C HMR: δ 172.0, 128.0, 119.5, 18.04, 11.56. ¹H, ¹³C and melting point values agree well with previously reported values.¹²

2.6.5. Synthesis of 2,2',4,4'-tetrabromo-5,5'-bithiazole (2.26) - route two

Diisopropylamine (0.72 mL, 5.5 mmol) was added to 10.0 mL of THF and cooled to 0 °C at which point BuLi (2.0 mL, 5.0 mmol) was added dropwise. The resulting mixture was allowed to stir for 30 min. 2,4-Dibromo-1,3-thiazole (1.21 g, 5.0 mmol) was dissolved in 40.0 mL of dry THF then ZnCl₂ (0.74 g, 5.5 mmol) was added in one portion to the reaction mixture which was then cooled to -78 °C. The solution of LDA was added drop-wise to the suspension of starting material and ZnCl₂ which was then stirred until it became clear at which point CuCl₂ (0.73 g, 5.5 mmol) was added in one portion. Thirty minutes later minutes dry O₂ was bubbled through the solution for 2 min and the reaction was allowed to warm to room temperature overnight. A solution of saturated NH₄Cl was used to quench the reaction and the aqueous layer extracted with chloroform. The combined organic extractions were concentrated in-vacuo to give a solid mixture of starting material and product. Methanol was used to wash the solid mixture removing the starting material. 2,4-Dibromothiazole was then purified by the previously described technique. Another wash with hexanes removed additional impurities from the solid residue affording the desired compound in yields of 64%. mp = 224.1 - 225.6 °C; ¹³C HMR: δ 138.01, 126.5, 125.4.

2.6.6. Synthesis of 2,2',4,4'-tetrabromo-5,5'-bithiazole (2.26) - route three

In a round-bottom flask 2,4-dibromo-1,3-thiazole (1.21 g, 5.0 mmol) was dissolved in 45 mL of dry THF and at RT bis(2,2,6,6-tetramethylpiperidine)•Zn•MgCl₂•LiCl complex (4.5 mL of 0.6 M solution in THF) was added drop-wise and allowed to react for 60 min. The reaction mixture was then cooled to -40.0 °C. Chloranil (0.74 g, 3.0 mmol) was added in a couple small portions. Once completed the reaction was placed in an ice bath and stirred for another 5 h and then quenched with a saturated solution of NH₄Cl. The mixture was then diluted with chloroform, heated, and filtered. The remaining residue was washed with hot chloroform and then hot acetone until the filtrate became clear. The combined organic layers were dried over MgSO₄, filtered and concentrated. Removal of the remaining starting material was accomplished by washing the crude product in hexanes and concentrating the filtrate. 2,4-Dibromothiazole was then purified by the previously described technique, 0.58 g recovered (48%). The remaining residue was purified via column chromatography with chloroform: hexanes (50%) producing 0.60 g of a yellow solid of the title compound (50%). mp = 224.1 - 225.6 °C; ¹³C HMR: δ 138.01, 126.5, 125.4.

2.6.7. Synthesis of 4,4'-dibromo-2,2'-bis(triisopropylsilyl)-5,5'-bithiazole (2.10)

To a round bottom flask was added 2,2',4,4'-tetrabromo-5,5'-dibromothiazole (1.49 g, 3.0 mmol) in 300.0 mL THF and cooled in an dry ice-acetone bath. BuLi (2.6 mL, 6.5 mmol) was added drop-wise and the reaction was stirred for a half hour. Then TIPSCl (1.16 mL, 6.5 mmol) was added drop-wise and the reaction was allowed to warm to room temperature overnight. Saturated NaHCO₃ was added and the organic layer was extracted with ethyl acetate. The combined organic layers were dried over MgSO₄, filtered and concentrated. The crude product was purified via column chromatography with chloroform:hexanes (30%) producing

0.84 g of a white solid which is the title compound (54%). mp = 109.7 - 110.9 °C; ¹H NMR: δ 1.18 (d, *J* = 7.4 Hz, 6H), 1.47 sept, *J* = 7.4 Hz, 36H); ¹³C HMR: δ 172.5, 130.3, 125.0, 18.44, 11.56. ¹H, ¹³C and melting point values agree well with previously reported values.⁷

2.7. References

1. Skotheim, T. A., Reynolds, J. R., Eds. *Handbook of Conducting Polymers*, 3rd ed.; CRC Press: Boca Raton, FL, 2007.
2. Perepichka, I. F., Perepichka, D. F., Eds. *Handbook of Thiophene-based Materials*; John Wiley & Sons: Hoboken, 2009.
3. Rasmussen, S. C.; Ogawa, K.; Rothstein, S. D. In *Handbook of Organic Electronics and Photonics*; Nalwa, H. S., Ed.; American Scientific Publishers: Stevenson Ranch, CA, 2008; Vol. 1, Chapter 1.
4. Ogawa, K.; Rasmussen, S. C. *J. Org. Chem.* **2003**, *68*, 2921-2928.
5. Evenson, S. J.; Rasmussen S. C. *Org. Lett.* **2010**, *12(18)*, 4054-4057.
6. Evanson, S. J.; Rasmussen S. C. *Prog. Polym. Sci.* **2013**, *38(12)*, 1773-1804.
7. Getmanenko, Y. A.; Risko, A.; Tongwa, P.; Kim, E.; Li, H.; Sandhu, B.; Timofeeva, T.; Bredas, J.; Marder, S. R. *J. Org. Chem.* **2011**, *76*, 2660-2671.
8. Getmanenko, Y. A.; Sing, S.; Sandhu, B.; Wang, C.Y.; Li, H.; Timofeeva, T.; Kippelen, B.; Marder, S.R. *J. Mater. Chem. C* **2014**, *2*, 124-131.
9. Chemburkar, S. R.; Bauer, J.; Deming, K.; Spiwek, H.; Patel, J.; Morris, J.; Henry, R.; Spanton, S.; Dziki, W.; Porter, W.; Quick, J.; Baure, P.; Donaubaue, J.; Narayanan, B. A.; Soldani, M.; Riley, D.;McFarland, K. *Org. Process Res. Dev.* **2004**, *4*, 413-417.
10. Yu, A. N.; Zhang, A.D. *Food Chem.* **2010**, 1060-1065.
11. Grubb, A. M.; Schmidt, M. J.; Seed, A. J.; Sampson, P. *Synthesis* **2012**, *44*, 1026-1029.

12. Stangeland, E. L.; Sammakia, T. *J. Org. Chem.* **2004**, *69*, 2381-2385.
13. Shen, K.; Fu, Y.; Li, J. N.; Liu, L.; Guo, Q.X. *Tetrahedron* **2007**, *63*, 1568-1576.
14. Getmanenko, Y.A.; Tongwa, P.; Timofeeva, T. V.; Marder S.R. *Org. Lett.* **2010**, *12*, 2136-2139.
15. Shen, K.; Li, J. N.; Liu, L.; Guo, Q.X. *Tetrahedron* **2007**, *63*, 1568-1576.
16. Schnurch, M.; Spina, M.; Khan, A. F.; Mihovilovic, M. D.; Stanetty, P. *Chem. Soc. Rev.* **2007**, *36*, 1046-1057.
17. Stanetty, P.; Schnurch, M.; Mereiter, K.; Mihovilovic, M. D. *J. Org. Chem.* **2005**, *70*, 567-574.
18. Zambon, A.; Borsato, G.; Brussolo, S.; Frascella, P.; Lucchini, V. *Tetrahedron Lett.* **2008**, *49*, 66-69.
19. Kelly, R. T.; Lang, F. *Tetrahedron Lett.* **1995**, *36*, 9293-9296.
20. Closoki, G. C.; Rohbogner, C. J.; Knochel P. *Angew. Chem. Int. Ed.* **2007**, *46*, 7681-7684.
21. Wunderlich, S. H.; Knochel, P. *Angew. Chem. Int. Ed.* **2007**, *46*, 7685-7699.
22. Stanetty, P.; Schnurch, M.; Mihovilovic, M. D. *J. Org. Chem.* **2006**, *71*, 3754-3761.
23. Le Flohic, A.; Meyer, C.; Cossy, J. *Tetrahedron* **2006**, *62*, 9017-9037.
24. Wen, Li.; Nietfeld, J. P.; Amb, C. M.; Rasmussen, S. C. *J. Org. Chem.* **2008**, *73*, 8529-8536.
25. Harris, G. S.; Payne, D. S. *J. Org. Chem.* **1956**, 4617-4621.
26. Kaslow, C. E.; Marsh, M. M. *J. Org. Chem.* **1947**, *12*, 456
27. Kato, Y.; Okada, S.; Tomimoto, K.; Mase, T. *Tetrahedron Lett.* **2001**, *42*, 4849-4851.

CHAPTER 3. SYNTHESIS AND CHARACTERIZATION OF FUNCTIONALIZED, FUSED-RING PYRROLO[3,2-*d*:4,5-*d'*]BISTHIAZOLES AND COMPARISON TO THE *N*-ALKYL- AND *N*-ACYL-DITHIENO[3,2-*b*:2',3'-*d*]PYRROLES

3.1. Introduction

The allure of semiconducting materials with low production costs, mechanical flexibility and the ease of processing displayed by conventional polymers is driving the research into conjugated polymers. Furthermore the ability to adjust a conjugated polymer's optical and electrical properties at the molecular level through the design of the monomeric units holds the promise of a wide range of materials for use in organic light emitting diodes (OLEDs) organic photovoltaic devices (OPVs) field effect transistors (FETs) and electrochromic devices.¹⁻³ One of the synthetic techniques employed in generating conjugated polymers is the annulation of repeating units creating a fused ring aromatic system along the polymer's backbone. Numerous examples of conjugated polymers found in the literature created using this method include *N*-alkyl-, aryl-, and *N*-acyl-dithieno[3,2-*b*:2',3'-*d*]pyrroles (DTPs).^{4,5}

Zanirato and co-workers were the first to report the synthesis of the unfunctionalized parent DTP (**3.5**) starting from 2,3-dibromothiophene (**3.1**) as outline in Figure 3.1.⁶ To improve the solubility of the parent compound Zotti and coworkers later developed chemistry allowing for the introduction of substituents at the bridging pyrrole nitrogen creating functionalized DTPs (**3.6**) but in low overall yields of ~19%.⁷ Due to the number of steps and low overall yield in the production of *N*-functionalized DTPs an alternative synthetic route was desirable.

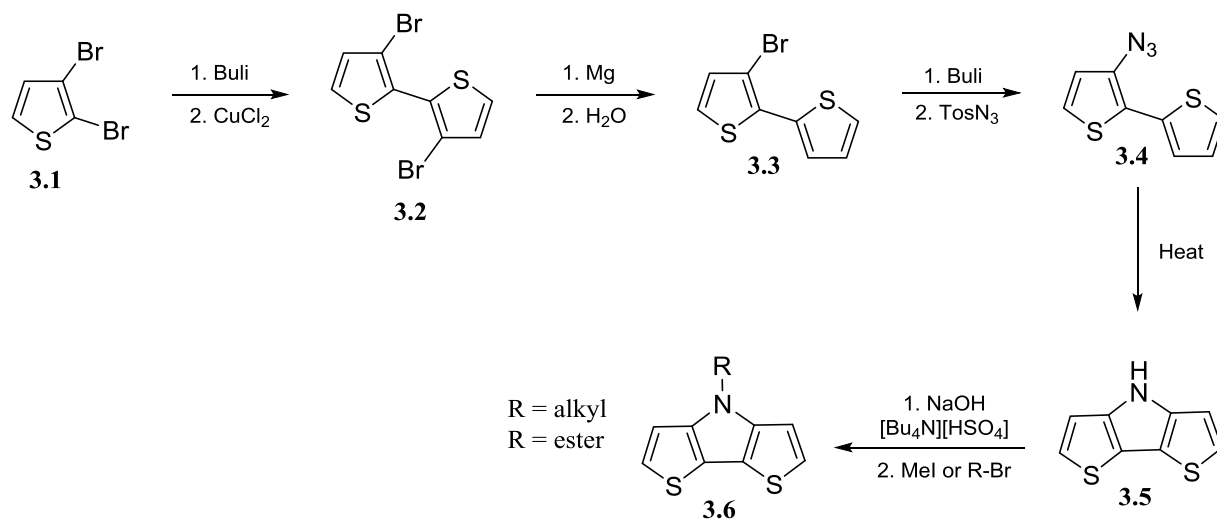


Figure 3.1. Previous synthetic route to N-functionalized DTPs

In 2003 Ogawa and Rasmussen reported a method employing a Buchwald-Hartwig amination of 3-bromothiophene (**3.7**) to produce a mixture of secondary aminothiophene (**3.8**) and tertiary bis(3-thienyl)amine (**3.9**).⁸ After separation **3.8a** could then be reacted with additional starting material resulting in improved yields for the production of **3.9**. The next step involved a double bromination followed by an annulation through a copper-mediated Ullman coupling resulting in **3.6** with a convenient one-pot reaction. This new method reduced the number of synthetic steps and increased the over yield to >40%.⁸

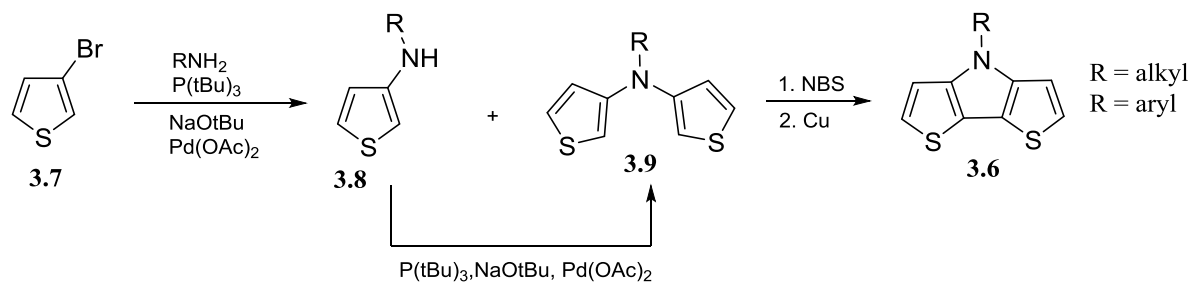


Figure 3.2. Tertiary bis(3-thienyl)amine route to N-functionalized DTPs

Around the time Rasmussen was developing his new synthetic route an alternative method using palladium-catalyzed chemistry was published by Nozaki and co-workers. Their

work was focused on the double N-arylation of primary amines in the production of carbazoles, but they were also able to show that it was possible to generate *N*-phenylDTP in a one-step reaction from 3,3'-dibromo-2,2'-bithiophene (**3.2**) in yields of 35%, as outlined in Figure 3.3.⁹ As this was not the main focus of their research the reaction conditions were never fully optimized. A couple years later Koeckelberghs and coworkers reported a modified procedure based on the chemistry developed by Nozaki for the generation of DTPs with greatly improved yields of ~75%.¹⁰

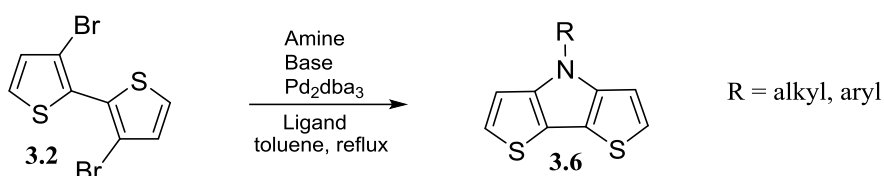


Figure 3.3. Improved method for synthesis of N-functionalized DTPs

Both Koeckelberghs and Zanirato synthetic schemes requires **3.2** as the precursor to DTPs. Zanirato synthesis borrowed a method developed by Gronowitz and co-workers that called for the use of costly **3.1** to generate **3.2** in a one-pot reaction as is shown in Figure 3.1.¹¹ Koeckelberghs elected to use the more cost effective 2-bromothiophene (**3.10**) as the starting material which was first homo-coupled and then brominated in the 5,5'- and 3,3'- positions. Finally the tetra-brominated molecule was selectively debrominated at the 5,5'- positions to achieve compound **3.2** (Figure 3.4).^{10,12} Each method described above suffered due to either the laborious number of steps required or the relatively high cost of the starting material.

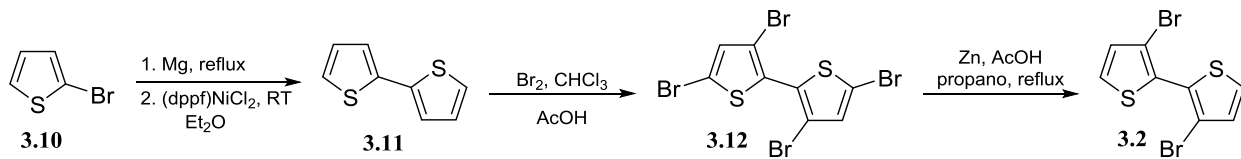


Figure 3.4. Alternative routes to the generation of 3,3'-dibromo-2,2'-bithiophene (**3.2**)

In 2010 Rasmussen and Evenson reported a modified reaction which is outlined in Figure 3.5 that uses the relatively cost-effective 3-bromothiophene (**3.7**) as the starting material.¹³ LDA was used to selectively deprotonate at the 2-position generating a lithiated intermediate which was then transmetalation by first reacting with ZnCl₂ and then CuCl₂. Oxidative homo-coupling is then assisted by the use of dry O₂ to produce compound **3.2** in yields of 85-90%.⁵ Around the same time Rasmussen's new route was being developed Patri and co-workers reported a similar synthetic scheme that only employed the use of LDA and CuCl₂. But without the modifications used by Rasmussen in the oxidative coupling step their reported yields were only 73%.¹⁴

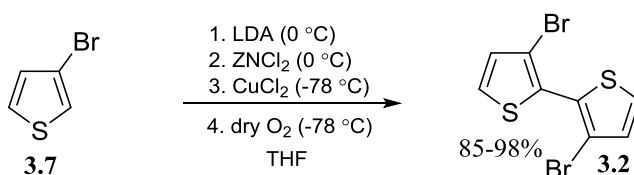


Figure 3.5. Preferred method for the generation of 3,3'-dibromo-2,2'-bithiophene (**3.2**)

These improved synthetic routes to **3.2** have been responsible for the noticeable uptake the use of DTPs in small molecule and polymeric materials and the application of these various devices. However materials made from DTPs suffer poor oxidative stability due to the high energy level of the polymer's HOMO.⁵ Attempts at modifying the HOMO and LUMO levels of these materials have employed the modification of the monomeric unit by changing the nature of the solubilizing side chains. Rasmussen and Evenson have reported the creation of N-functionalized DTP that incorporate an electron-withdrawing acyl group at the pyrrole nitrogen, which they called second generation DTPs. The chemistry used in the annulation of the pyrrole ring was derived from methods developed by Bachwald in which a copper-catalyzed reaction was used to form tandem C-N bonds in the production of dithieno[2,3-*b*:3'2'-*d*]pyrroles (Figure 3.6).¹⁵

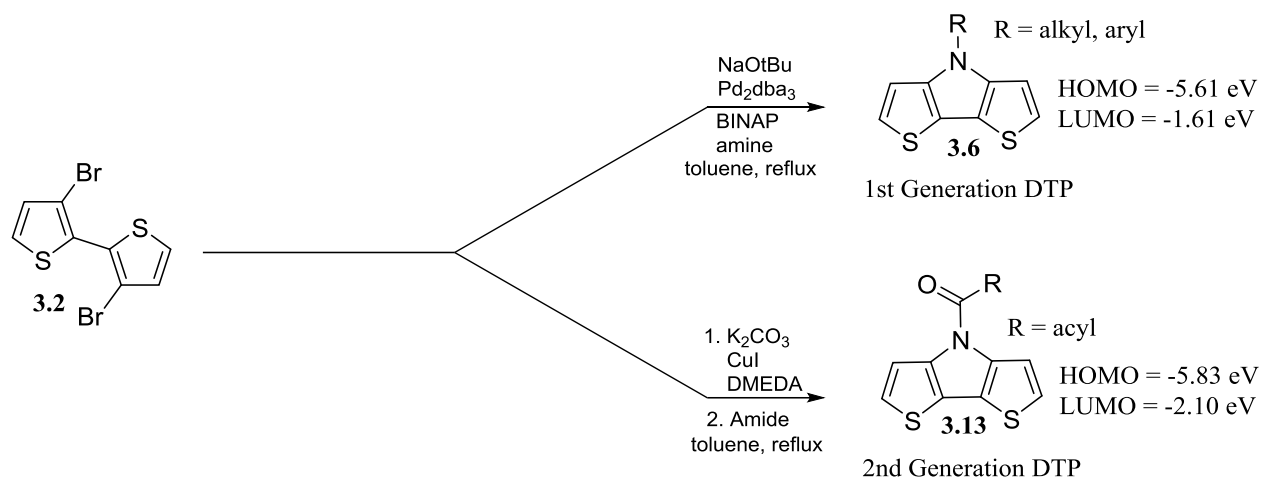
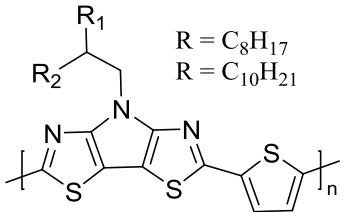
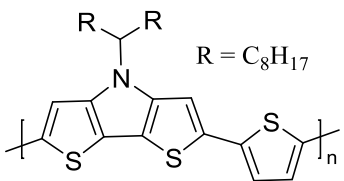


Figure 3.6. Generation and comparisons of first and second generation DTPs⁵

Another way of modifying the polymer's HOMO and LUMO is to generate analogues of DTP molecules which differ in their flanking aromatic units. This approach gives the same fused-ring, planar, and easily-substituted monomeric repeat units, but allows for modification of optical and electrical properties based on the choice of aromatic rings. The replacement of thiophene with a more electron-deficient heterocycle should result in materials with stabilized HOMO energy levels.

A few groups have reported the creation of such DTP analogues using thiazoles. Although the literature is sparse with examples of polymeric systems which incorporate fused-ring pyrrolo[3,2-*d*:4,5-*d'*]bisthiazoles (PBTz) it is possible to make direct comparison to copolymers of DTP.^{17,16} As expected, the addition of the electron-deficient thiazoles results in polymers that exhibit stabilized HOMO levels when compared to their DTP analogues as outlined in Table 3.1.

Table 3.1. A comparison of thiazole and thiophene annulated conjugated polymers

				
	HOMO	LUMO	Band Gap(E_g)	λ_{max} (film)
polyPBTz-T	-5.30 eV	-3.67 eV	1.63 eV	620 nm
polyDTP-T	-4.89 eV	-2.56 eV	1.90 eV	609 nm

3.2. Reported synthesis of thiazole analogues of DTP

The first reported synthesis and characterization of a series of copolymers that incorporated thiazole analogues of DTP were by Heeney and coworkers in 2010.¹⁷ The annulation of 4,4'-dibromo-2,2'-bis(triisopropylsilyl)-5,5'-bithiazole (**3.14**) was accomplished through a modified Buchwald-Hartwig amination. The reaction uses toluene in a sealed reaction vessel and temperatures of 160 °C to generate 2,6-bis(triisopropylsilyl)-4-(2-octyldodecyl)-4*H*-pyrrolo[3,2-*d*:4,5-*d'*]bisthiazole (**3.15**) in yields of 68%.

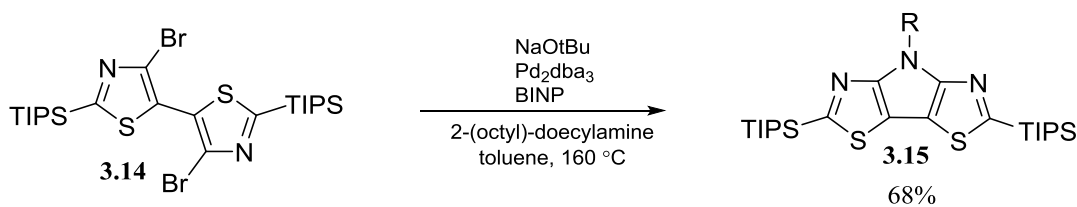


Figure 3.7. First reported synthesis *N*-alkyl functionalized PBTz

In 2010, Marder and co-workers also reported the synthesis and characterization of a tricyclic molecule that included flanking thiazoles but with mono- and dicarbonyl bridges.¹⁸ These were produced through a double lithiation of **3.14** via BuLi at -70 °C and trapping with different electrophiles. 2,6-Bis(triisopropylsilyl)cyclopenta[2,1-*b*:3,4-*b'*]bisthiazole-4-one (**3.16a**) was formed through the use of *N,N*-dimethylcarbonyl chloride. The α -dicarbonyl

bridged molecule was generated through the addition of *N,N*-dimethylpiperazine-2,3-dione producing 2,7-bis(triisopropylsilyl)benzo[2,1-*b*:3,4-*b'*]bisthiazole-4,5-dione (**3.16b**). The reported yields were 38% and 37% respectively (Figure 3.8).¹⁸

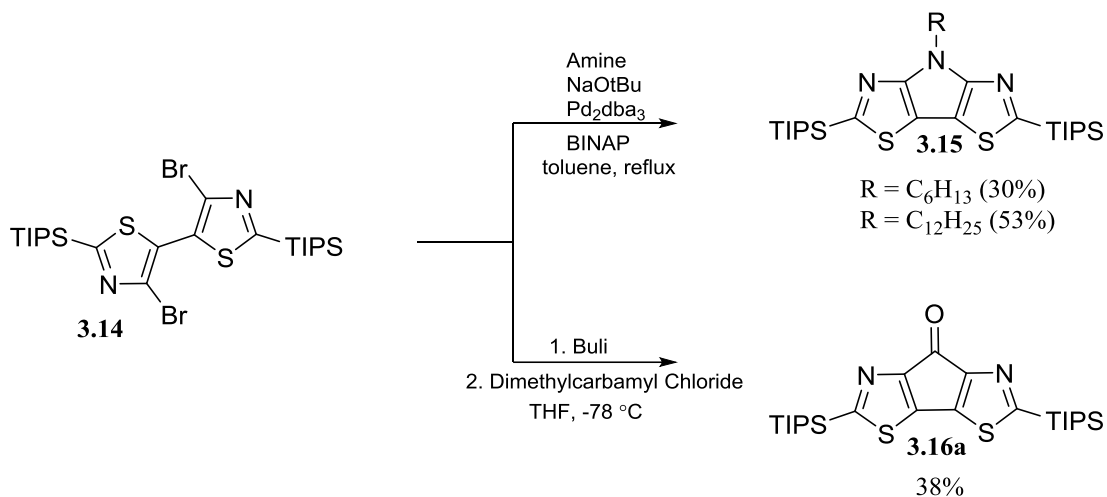


Figure 3.8. Alternative synthesis of PBTz and related analogues

In 2014 Marder also reported on the annulation of a pyrrole ring from **3.14** via a Buchwald-Hartwig amination which was adapted from the literature.¹⁹ The reaction conditions called for using 1,3,5-trimethylbenzene as the solvent which allowed for heating at reflux under normal atmospheric pressure. Two PBTz variants were discussed, one with an *N*-hexyl side chain and the other an *N*-dodecyl. The reported yield of the *N*-alkyl functionalized PBTz were 63% and 76% respectively (Figure 3.8).¹⁹

The last step in all the above reported synthesis is the removal of the silyl protecting group (Figure 3.9).^{17,19} This is accomplished through the addition of tetrabutylammonium fluoride (TBAF) at room temperature. After the reaction has gone to completion it was treated with water forming a protonated tricyclic thiazole molecule (**3.17**). Without any further purification a double bromination is performed through the addition of NBS in DMF at room temperature to produce the dibrominated PBTz molecule (**3.18**) as outlined in Figure 3.9.

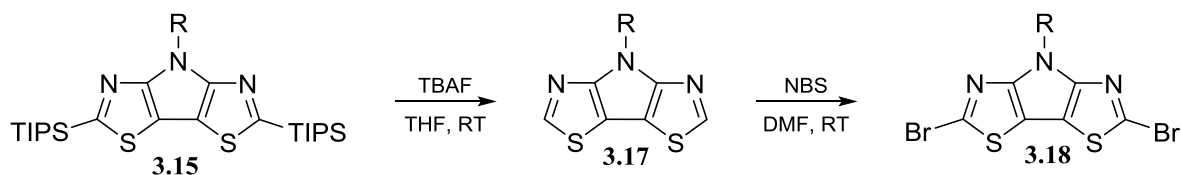


Figure 3.9. Removal of the TIPS protecting group and addition of bromines

The goal of this part of the project was to create thiazole analogues of both the first and second generation DTP molecules. Although both Marder and Heeney have reported on the synthesis of *N*-alkyl functionalized PBTz molecules, their schemes either required the use of high pressure and temperature reaction conditions or expensive solvents.^{17,19} Starting with **3.14** our proposed synthetic routes in the generation of both target molecules are based on the work previously reported by Rasmussen and Evanson⁵ and are outlined in Figure 3.10.

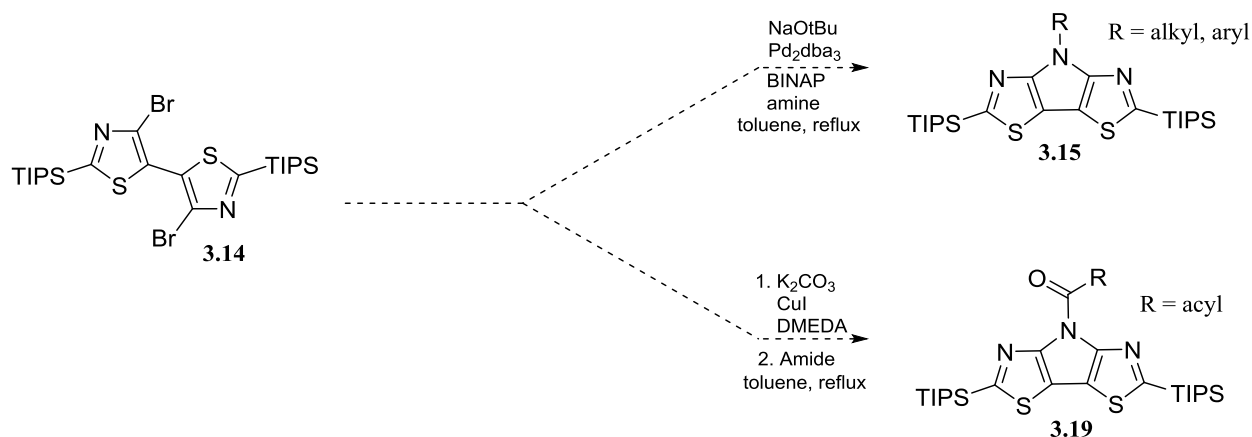


Figure 3.10. Proposed synthetic scheme for generation of thiazole analogues of first and second generation of DTP molecules

3.3. Results and discussion

3.3.1. Generation of *N*-alkylPBTz

The generation of an alkyl-functionalized PBTz monomeric unit was attempted via Buchwald-Hartwig amination using dry toluene as the solvent with heating to reflux under normal atmospheric pressure. This resulted in the generation of **3.15** in low yields of ~5% after

24 hours. The reaction conditions were then modified by replacing toluene with xylenes as the solvent and after 24 hours of refluxing **3.15** was produced in a good yield of 74% (Figure 3.12). This modification afforded improved yields with the use of readily available reagents reducing the over-all costs associated with this reaction.

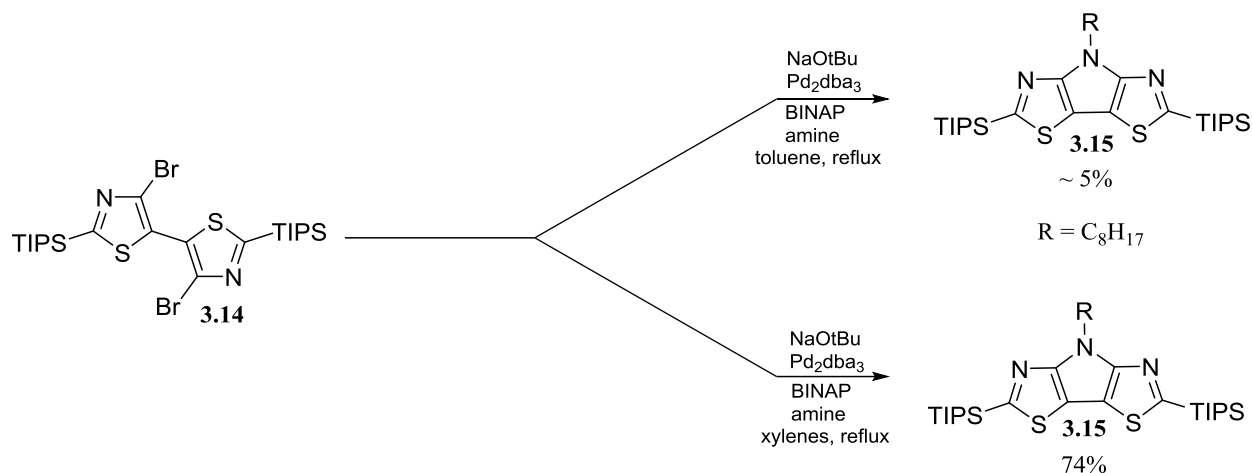


Figure 3.11. Generation of *N*-alkylPBTz

Removal of the TIPS protecting group was accomplished through the addition of two equivalents of TBAF to **3.15**. The mixture was then monitored by TLC until the starting material was gone and then it was treated with water forming 4-octyl-4*H*-pyrrolo[3,2-*d*:4,5-*d'*]bisthiazole (**3.17**). The reaction proceeded smoothly with a near quantitative yield of the desired product (Figure 3.12).

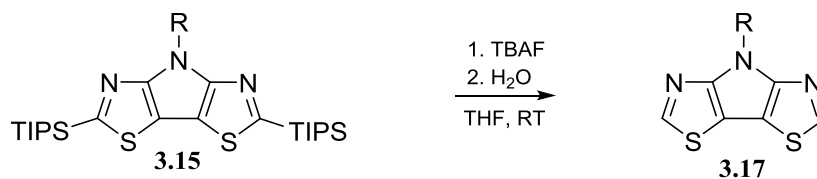


Figure 3.12. Removal of TIPS protecting group

3.3.2. Generation of *N*-acylPBTz

Attempts to generate the *N*-acylPBTz analogue using the scheme developed by Rasmussen and coworkers failed to meet with success (Figure 3.6).⁵ A series of trials were then conducted, based on the previous work of Buchwald and coworkers, in which the solvent and base were varied and the results are reported in Table 3.2.¹⁵ Most trials resulted in the recovery of some material but sadly not in the formation of the target molecule. Additionally the main by-product produced depended largely on the solvent not the base. When xylene was used small amounts (5-12%) of the mono-brominated starting material were formed. Reactions conducted in toluene resulted in mostly the recovery of starting material except when Cs₂CO₃ was used as the base and mono-brominated starting material was formed in 10% yields.

Table 3.2. Summary of reaction conditions for generation of *N*-acylPBTz

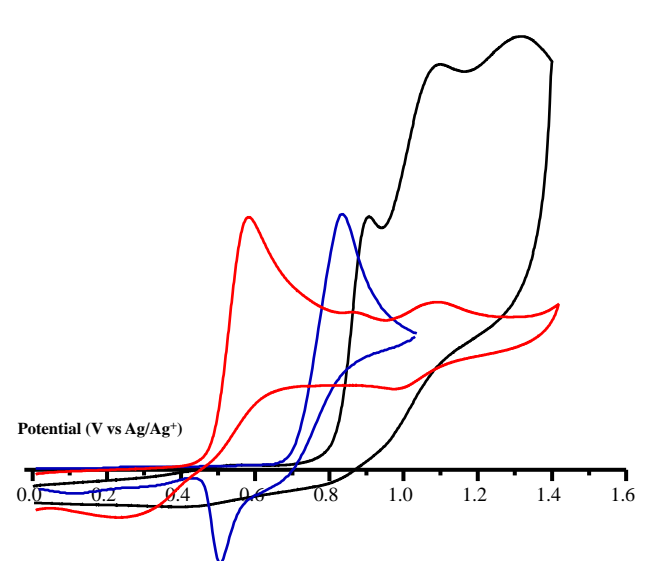
Solvent	Base	Catalyst	Ligand	Percent Yield		
				A	B	C
xylene	K ₂ CO ₃	CuI	DMEDA	13	~5	0
xylene	K ₃ PO ₄	CuI	DMEDA	44	12	0
xylene	Cs ₂ CO ₃	CuI	DMEDA	50	12	0
toluene	K ₂ CO ₃	CuI	DMEDA	0	0	0
toluene	K ₃ PO ₄	CuI	DMEDA	38	0	0
toluene	Cs ₂ CO ₃	CuI	DMEDA	40	10	0
xylene	Na ^t OBu	Pd ₂ dba ₃	BINAP	41	0	0

DMEDA =	
---------	--

3.3.3. Electrochemistry of monomeric PBTz units

Cyclic voltammetry was performed on the *N*-octylPBTz and for comparison the electrochemical data for the *N*-octyl and *N*-octanoylDTPs monomers are listed in Table 3.3. The *N*-octylPBTz showed a well-defined and irreversible oxidation peak which is suggestive of the formation a radical cation due to the loss of an electron from the π -system. A second and third broad oxidation peaks are also observed each with increasing intensity. These peaks could be the result of the oxidation of coupled products in-lieu of additional PBTz oxidations. As expected the *N*-octylPBTz oxidative onset was shifted towards positive potential when compared to *N*-octanoyl and *N*-octylDTP; the approximate shifts being around 130 mV and 350 mV, respectively. The calculated HOMO energy level for *N*-octylPBTz is -5.9 eV and is stabilized when compared to both DTP analogues, which is not surprising due to the electron-deficient nature of thiazoles compared to thiophenes. *N*-OctanoylDTP exhibited the smallest difference in HOMO levels (0.2 eV) which again is not surprising due the electron-withdrawing effect of the acyl group.⁵

Table 3.3. Electrochemical properties and cyclic voltammograms of *N*-octylPBTz, *N*-octylDTP and *N*-acylDTP

	Monomer ^b	$E_{\text{ox}}^{\text{onset}}$ (V)	E_{pa} (V)	E_{HOMO} (eV) ^a
	<i>N</i> -octylPBTz	0.82	0.91	-5.9
	<i>N</i> -octanoylDTP ^c	0.69	0.78	-5.7
	<i>N</i> -octylDTP ^c	0.51	0.56	-5.6
^a E_{HOMO} values were determined in reference to ferrocene (5.1 vs vacuum). ²⁰ ^b In CH ₃ CN. ^c Ref 4				

3.3.4. Electropolymerized homopolymers of PBTz

The first electropolymerization of *N*-alkylDTPs were reported by Zotti and coworkers in 1992.⁷ In 2010, Rasmussen and coworkers reported the successful electropolymerization of a series of *N*-acylDTP polymers.^{4,5,21} In order to further study the effects of replacing the thiophenes with the electron-deficient thiazoles, homopolymers of the DTP analogues would need to be produced. It was shown that electropolymerized films could be grown effectively from *N*-octylPBTz on ITO plates by cycling from a positive to negative potentials (Figure 3.13). The formation of new and broader oxidation peaks at a lower potential is indicative of chain growth during the polymerization process.

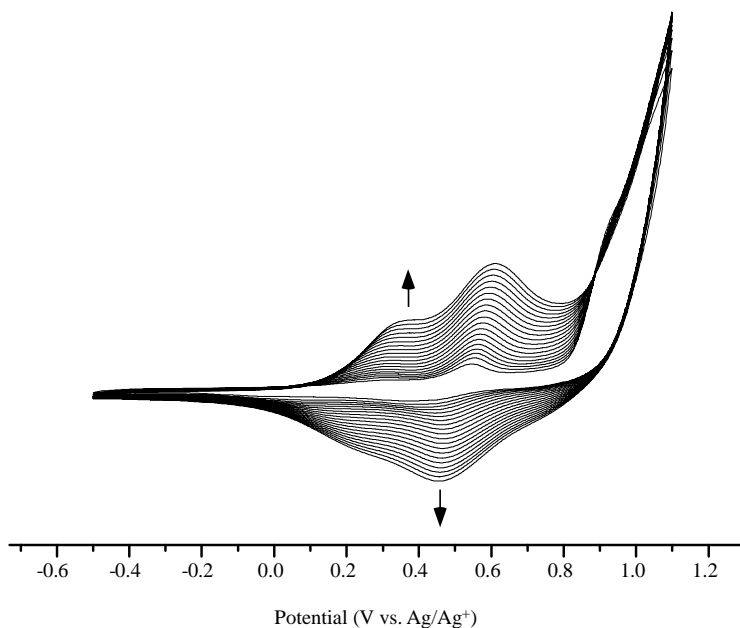
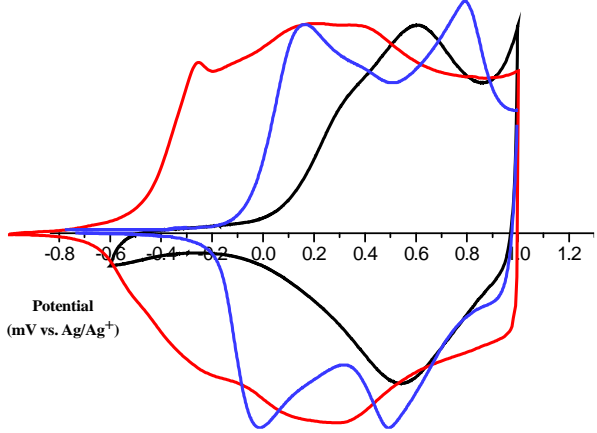


Figure 3.13. Cycling of the CV to show polymerization of poly(*N*-octylPBTz)

Cyclic voltammograms of poly(*N*-octylPBTz), poly(*N*-octylDTP) and poly(*N*-octanoylDTP) are shown in Table 3.4. Poly(*N*-octylPBTz) shows a positive shift in its oxidative onset when compared to the films of both the acyl and alkylDTP homopolymers; the

approximate shifts being around 300 mV and 700 mV respectively.²¹ This follows the general trend seen for the monomeric unit of the *N*-octylPBTz indicating a stabilization of the HOMO level of the resulting polymer. Additionally the profiles of the represented CVs are quite different. A sudden initial oxidation starting under zero volts is observed for *N*-alkylDTP homopolymers followed by a very broad response. This is suggestive of multiple waves which are overlapping with each other and could be indicative of variations in the chain lengths found in the polymer's film.²² Homopolymers of *N*-acylDTP exhibit two oxidations both of which are shifted towards positive potential and two well defined redox waves.

Table 3.4. Oxidation potentials and cyclic voltammograms of electropolymerized films of poly(*N*-octylPBTz), poly(*N*-decylDTP) and poly(*N*-acylDTP)

	Homopolymer ^a	$E_{\text{ox}}^{\text{onset}}$ (V)	E_{pa} (V)	E_{HOMO} (eV) ^d
	poly(<i>N</i> -octylPBTz)	0.17	0.60	-5.2
poly(<i>N</i> -octanoylDTP) ^b	-0.12	0.20	-4.9	
poly(<i>N</i> -octylDTP) ^b	-0.55	-0.28	-4.5	

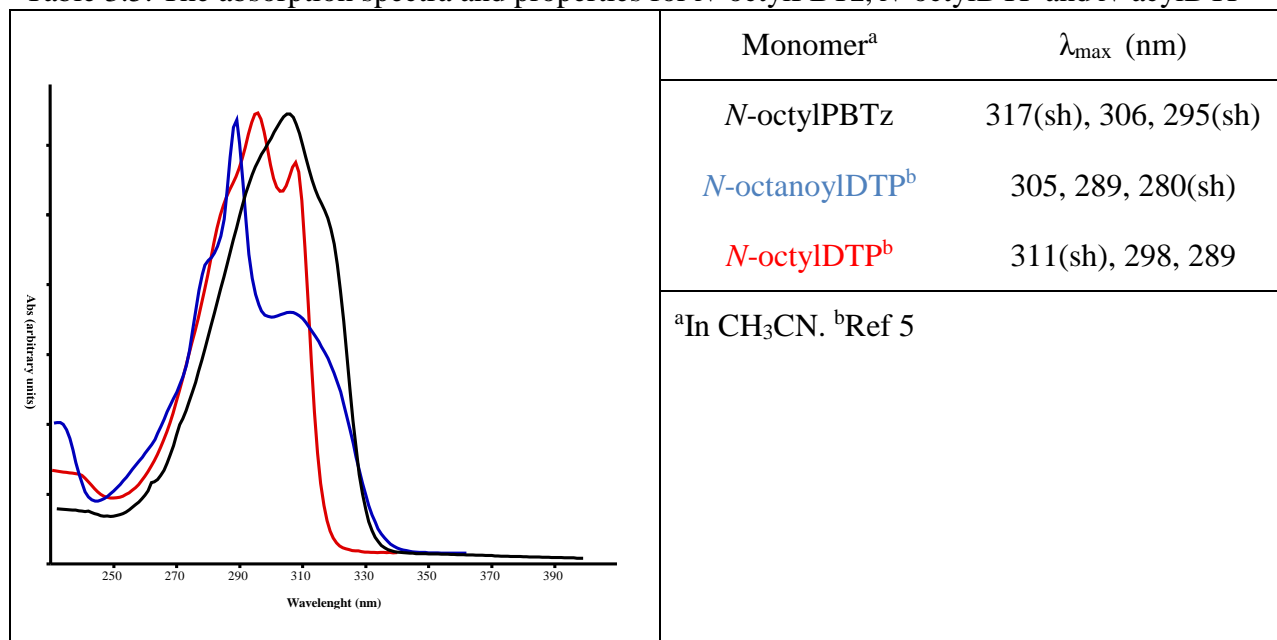
^aElectropolymerized onto an ITO plate. Potentials vs Ag/Ag⁺ in 0.1 M TBAPF₆.
^bRef 5.

3.3.5. UV-vis spectroscopy of PBTz monomers

Absorption spectra for *N*-octylPBTz, *N*-octylDTP and *N*-octanoylDTP are listed in Table 3.5. The spectra for both *N*-octanoylDTP and *N*-octylDTP are representative of most reported monomers. *N*-alkylDTPs show two transitions at approximately 310 nm and 300 nm with a high energy shoulder at 289 nm which have been attributed to various vibrational components of the same electronic transition.⁸ *N*-AcylDTPs tend to have a sharp peak around 298 nm and a wider

lower energy peak around 310 nm in addition to a shoulder at 280 nm. In contrast to the *N*-alkylDTPs it seems that the peaks are caused by two separate electronic transitions. The highest energy transition associated with π - π^* transition and the lower energy transition energy peak showing characteristics of a charge transfer.⁵ *N*-OctylPBTz has one broad high energy transition at 306 nm with two high energy shoulders appearing at 317 nm and 296 nm. These peaks can be attributed to a π - π^* transition because the energetic difference between them is consistent with the breathing mode of thiazoles and are most likely vibrational components of the same electronic transition.

Table 3.5. The absorption spectra and properties for *N*-octylPBTz, *N*-octylDTP and *N*-acylDTP

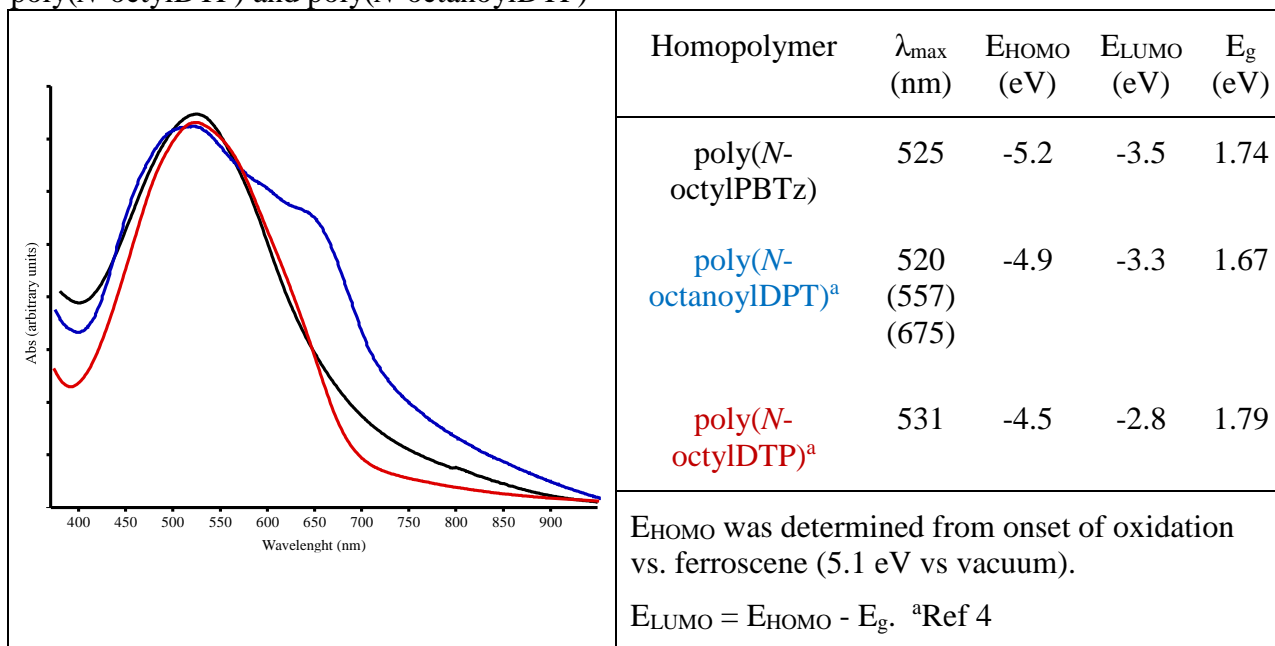


3.3.6. UV-vis spectroscopy of PBTz homopolymers

Thin films of poly(*N*-octylPBTz) were electropolymerized on ITO. The absorption spectra for the *N*-octyl and *N*-octanoylDTPs electropolymerized homopolymers are shown in Table 3.6 in addition to the poly(*N*-octylPBTz) along with the optical band gaps and the HOMO/LUMO energy levels. A prominent low energy shoulder seen in the spectra for poly(*N*-

octanoylDTP) is consistent with the spectra for the monomeric unit.⁵ This is responsible for a red-shift of its absorption onset of around 40 nm and 50 nm when compared to the films made from *N*-octylPBTz and *N*-octylDTP, respectively. Due to this the resulting band gap for poly(*N*-octanoylDTP) shows a reduction of 0.1 eV in comparison to both poly(*N*-octylPBTz) and poly(*N*-octylDTP).

Table 3.6. Solid state absorption spectra of electropolymerized films of poly(*N*-octylPBTz), poly(*N*-octylDTP) and poly(*N*-octanoylDTP)



Replacing the thiophenes with the more electron deficient thiazoles had the desired effect of stabilizing the HOMO level of generated polymeric films. The most dramatic change was observed between the films of *N*-octylPBTz and *N*-octylDTP with a reduction of 0.7 eV for the HOMO. The change is less dramatic for the poly(*N*-octanoylDTP) with the HOMO being stabilized by 0.3 eV. These results are not surprising because of the electron-withdrawing nature of the acyl functional group versus that of the alkyl chain.

3.3.7. Spectroelectrochemistry

Changes in the absorption profiles at various potentials were observed by performing oxidative spectral electrochemistry on poly(*N*-octylPBTz) which are listed in Figure 3.14. An absorption band was observed in the neutral state at 525 nm after incremental oxidation the initial peak fades and is replaced with another at around 1210 nm. The new broader peak extended into the IR swamping the low energy region of the neutral polymer which is indicative of a p-doped state.^{23,24}

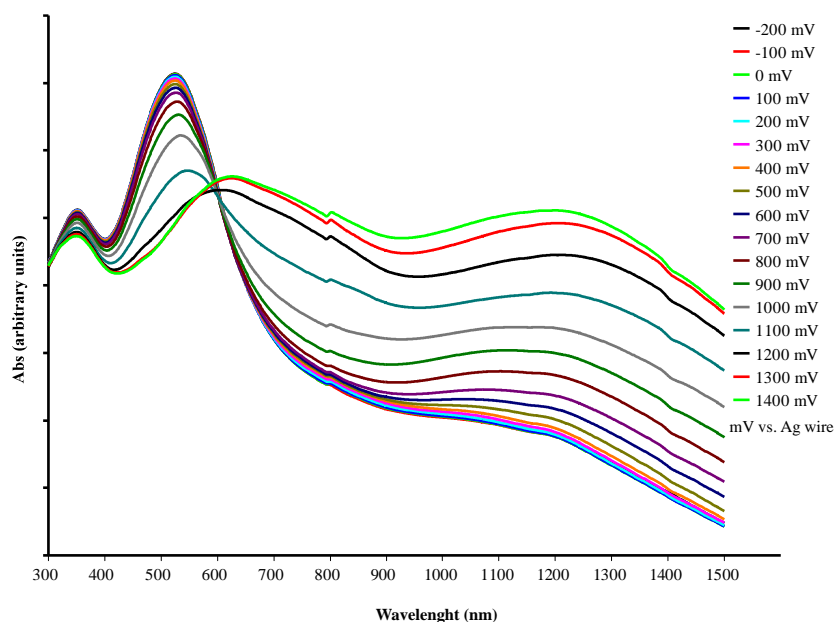


Figure 3.14. Spectroelectrochemistry of poly(*N*-octylPBTz)

3.4. Conclusion

All attempts to produce *N*-octanoylPBTz resulted in the recovery of starting material and unwanted by-products. *N*-octylPBTz was generated using a modified procedure found in the literature in yields of 74%.⁵ The optical and electrical properties of the alkyl functionalized PBTz were collected and compared to both *N*-octylDTP and *N*-octanoylDTP. Cyclic voltammetry was performed on a solution of the *N*-octylPBTz and it showed a well-defined and irreversible

oxidation peak which is suggestive of the formation a radical cation due to the loss of an electron from the π -system. As expected the *N*-octylPBTz oxidative onset was shifted towards positive potential when compared to both *N*-octanoylDTP and *N*-octylDTP. The approximate shifts being around 130 mV and 350 mV, respectively, this is not surprising due to the electron deficient nature of thiazoles compared to thiophenes. Electropolymerization was used to grow homopolymers of *N*-octylPBTz on to plates of glass coated with ITO. Poly(*N*-octylPBTz) shows a positive shift in its oxidative onset when compared to electropolymerized films of both the acyl and alkyl DTP homopolymers; \sim 300 mV and \sim 700 mV respectively (Table 3.4).

UV-vis spectroscopy was also performed on a solution of *N*-octylPBTz which showed a broad high energy transition at 306 nm with two high energy shoulders appearing at 317 nm and 296 nm. These peaks can be attributed to a π - π^* transition because the energetic difference between them is consistent with the breathing mode of thiazoles and are most likely vibrational components of the same electronic transition. Thin films of poly(*N*-octylPBTz) were electropolymerized on ITO and compared to homopolymers of the *N*-octylDTP and *N*-octanoylDTP grown in the same manner. The thiophenes based systems showed a stabilization of the HOMO level of when compared to the other polymers. The most dramatic change was observed between the films of *N*-octylPBTz and *N*-octylDTP with a reduction of 0.7 eV for the HOMO and a less dramatic change is observed for the poly(*N*-octanoylDTP) with the HOMO being stabilized by 0.3 eV. The spectra profile for both the poly(*N*-octylDTP) and poly(*N*-octylPBTz) are very similar resulting in nearly identical band gaps of \sim 1.7 eV. Due to the prominent low energy shoulder typically exhibited by *N*-acylDTP causes an earlier absorption onset which results in a lowered band gap of 1.67 eV.

3.5. Experimental

If not specified the following conditions were used in the synthesis, purification and characterization of the compounds listed in this section. Chemicals were reagent grade and used without further purification. Solvents were dried via distillation over sodium-benzophenone. Glassware was oven-dried then assembled hot and cooled under a dry nitrogen stream. Transfers of liquids were carried out using standard syringe techniques and the reactions were performed under a dry nitrogen stream using air-free techniques. Silica gel (240-400 mesh) in conjunction with standard column chromatography methods were employed for chromatographic separations. Melting points were reported to a resolution of 0.1 °C using a digital thermocouple. The ¹H and ¹³C NMR were performed with a 400 MHz spectrometer. NMR data collected was referenced to the chloroform signal and peak multiplicity is reported as follows: s = singlet, d = doublet, t = triplet, q = quartet, p = pentet, tt = triplet of triplets, m = multiplet and br = broad. HRMS data was collected using a Bruker-Daltronics BIOTOF HRMS. Previously reported procedures were used to generate the following compounds 4,4'-dibromo-2,2'-bis(triisopropylsilyl)-5,5'-bithiazole as detailed in Chapter 2.

3.5.1. Synthesis of 2,6-bis(triisopropylsilyl)-4-octyl-4*H*-pyrrolo[2,3-*d*:5,4'-*d'*]bisthiazole (3.15)

To a 100 mL three neck round bottom flask the following chemicals were added: 4,4'-dibromo-2,2'-bis(triisopropylsilyl)-5,5'-bithiazole (0.32 g, 0.5 mmol), Pd₂(dba)₃ (.015g, 0.01 mmol), BINAP (0.031 g, 0.1 mmol), NaO^tBu (0.12 g, 0.12 mmol), octylamine (0.10 mL, 0.55 mmol) and 25.0 mL dry xylenes. The following mixture was refluxed for 24 hour before being cooled to room temperature then treated with water. The organic phase was separated with diethyl ether which were combined and dried over MgSO₄ and volatile solvents were removed

via rotary evaporation. The resulting material was purified using column chromatography with hexanes: diethyl ether (95:5) producing 0.22g of a yellow oil as the title compound (73%). ^1H NMR: δ 4.61 (t, $J = 6.8$ Hz), 2.05 (p, $J = 6.9$ Hz, 2H), 4.48 (sept, $J = 7.6$ Hz, 6H), 1.24 (m, 46H); ^{13}C HMR: δ 166.4, 158.5, 106.7, 45.33, 31.81, 29.80, 29.10, 26.76, 22.65, 18.57, 14.07, 11.78.

3.5.2. Synthesis of 4-octyl-4*H*-pyrrolo[2,3-*d*:5,4']bisthiazole (3.17)

To a 25.0 mL 3-neck round-bottom flask was added the following: 2,6-bis(triisopropylsilyl)-4-octyl-4*H*-pyrrolo[2,3-*d*:5,4'-*d'*]bisthiazole (0.15g, 0.25 mmol), TBAF (0.30 mL of 1.0M solution in THF, 0.30 mmol) and 5.0 mL dry THF. The reaction mixture was stirred and monitored by TLC until the starting material dissapered (~1 to 2 h). The reaction was treated with water and the organic phase was separated using diethyl ether. The organic layers were combined and dried over MgSO_4 and the solvents were removed by rotary evaporation. ^1H NMR: δ 8.60 (s, 2H), 4.57 (t, $J = 7.2$ Hz, 2H), 2.02 (p, $J = 7.5$ Hz, 2H), 1.35 (m, 4H), 1.25 (m, 6H), 0.85 (t, $J = 6.7$ Hz, 3H); ^{13}C HMR: δ 154.86, 149.21, 104.11, 45.79, 31.94, 29.92, 29.34, 27.00, 22.80, 14.26, 12.95.

3.5.3. Electrochemistry and electropolymerizations

A Bioanalytical Systems BAS 100B/W electrochemical analyzer was used to perform all electrochemical techniques. Electro-polymerizations were performed using a three-electrode cell consisting of a Pt-disc working electrode, Pt wire auxillary electrode, and a Ag/Ag^+ reference electrode. Acetonitrile (MeCN) that was distilled over CaH_2 under an inert atmosphere was used to prepare dilute monomer solutions. A 0.1 M solution of tetrabutylammonium hexafluorophosphate (TBAPF_6) was used as the supporting electrolyte. Argon was used to deoxygenate the solutions for at least 20 min prior to each scan and blanketed with argon during polymerizations. 0.05 mm alumina was used to polish the Pt disc working electrode and washed

well with MeOH and dry MeCN prior to film formation. The polymers were grown by cycling from -0.5 V to 1.1 V for ninety segments. Clean MeCN was used to wash the polymer-coated electrode which was then placed in a fresh electrolyte solution. Cyclic voltammetry (CV) was then performed in the cell described above at a sweep rate of 100 mV/s. E_{HOMO} values were determined in reference to ferrocene (5.1 vs vacuum) and the E_{LUMO} was determined from the following equation: $E_{\text{LUMO}} = E_{\text{HOMO}} - \text{optical band gap}$.

3.5.4. UV-vis-NIR spectroscopy

All absorption spectroscopy was performed on a Carry 500 dual-beam UV-vis-NIR spectrophotometer. MeCN was used as the spectroscopy solvent and was dried via distillation over CaH_2 under an inert atmosphere prior to use. All samples were prepared using either a dilute solution of the monomer in MeCN or a thin polymer film on ITO coated glass slides. ITO was substituted for the Pt disc working electrode in generating the electrochemically polymerized films. After formation of the film the polymer-coated electrode was held at a reducing potential to ensure dedoping then removed and cleaned with fresh MeCN. A blank ITO-coated glass slide was then used as a reference before the spectroscopy was performed. The optical band gaps were determined from the onset of the lowest energy absorption by extrapolation of the steepest slope to the intersection with the wavelength axis.

3.5. References

1. Skotheim, T. A., Reynolds, J. R., Eds. *Handbook of Conducting Polymers*, 3rd ed.; CRC Press: Boca Raton, FL, 2007.
2. Perepichka, I. F., Perepichka, D. F., Eds. *Handbook of Thiophene-based Materials*; John Wiley & Sons: Hoboken, 2009.

3. Rasmussen, S. C.; Ogawa, K.; Rothstein, S. D. In *Handbook of Organic Electronics and Photonics*; Nalwa, H. S., Ed.; American Scientific Publishers: Stevenson Ranch, CA, 2008; Vol. 1, Chapter 1.
4. Rasmussen, S. C.; Evenson, S. J. *Prog. Polym. Sci.* **2013**, *38*, 1773–180.
5. Evenson, S. J.; Rasmussen S. C. *Org. Lett.* **2010**, *12*, 4054-4057.
6. Zanirato, P.; Spagnolo, P.; Zanardi, G. *J. Chem. Soc., Perkin Trans. 1*, **1983**, 2551-2554.
7. Berlin, A.; Pagani, G.; Zotti, G.; Schiavon, G. *Makromol. Chem.* **1992**, *193*, 399-409.
8. Ogawa, K.; Rasmussen, S. C. *J. Org. Chem.* **2003**, *68*, 2921-2928.
9. Nozaki, K.; Takahashi, K.; Nakano, K.; Hiyama, T.; Tang, H. Z.; Fujiki, M.; Yamaguchi, S.; Tamao, K. *Angew. Chem. Int. Ed.* **2003**, *42*, 2051-2053.
10. Koeckelberghs, G.; De Cremer, L.; Vanormelingen, W.; Dehaen, W.; Verbiest, T.; Persoons A.; Samyn, C. *Tetrahedron* **2005**, *61*, 687-691.
11. Gronowitz, S. *Acta Chem. Scand.* **1961**, *15*, 1393-1395.
12. Khor, E.; Ng, S. C.; Li, H. C.; Chai, S. *Heterocycles* **1991**, *32*, 1805-1810.
13. Kabir, S. M. H.; Miura, M.; Sasaki, S.; Harada, G.; Kuwatani, Y.; Yoshida, M.; Iyoda, M. *Heterocycles* **2000**, *52*, 761-774.
14. Mishra, S. P.; Palai, A. K.; Srivastava, R.; Kamalasanan, M. N.; Patri, M. *J. Polym. Sci., Part A: Polym. Chem.* **2009**, *47*, 6514-6525.
15. Martín, R.; Larsen, C. H.; Cuenca, A.; Buchwald, S. L. *Org. Lett.* **2007**, *9*, 3379-3382.
16. Price, S. C.; Sturt, A. C.; You, W. *Macromolecules*, **2010**, *43*, 797-804.
17. Al-Hashimi, M.; Labram, G. J.; Watkins, S.; Motevalli, M.; Anthopoulos, T. D.; Heeney, M. *Org. Lett.* **2010**, *12*, 5478–5481

18. Getmanenko, Y. A.; Risko, A.; Tongwa, P.; Kim, E.; Li, H.; Sandhu, B.; Timofeeva, T.; Bredas, J.; Marder, S. R. *J. Org. Chem.* **2011**, *76*, 2660–2671.
19. Getmanenko, Y. A. ; Sing, S.; Sandhu, B; Wang, C. Y.; Li, H.; Timofeeva, T.; Kippelen, B.; Marder, S. R. *J. Mater. Chem. C* **2014**, *2*, 124-131.
20. Koeckelberghs, G.; De Cremer, L.; Vanormelingen, W.; Dehaen, W.; Verbiest, T.; Persoons, A.; Samyn, C. *Tetrahedron* **2005**, *61*, 687.
21. Evanson, S. Ph.D. Dissertation, North Dakota State University: Fargo, ND, 2010.
- 22 . Ogawa, K.; Rasmussen, S. C. *Macromolecules* **2006**, *39*, 1771-1778.
23. Steckler, T. T.; Zhang, X.; Hwang, J.; Honeyager, R.; Ohira, S.; Zhang, X. H.; Grant, A.; Ellinger, S.; Odom, S. A.; Sweat, D.; Tanner, D. B.; Rinzler, A. G.; Barlow, S.; Bredas, J. L.; Kippelen, B.; Marder, S. R.; Reynolds, J. R. *J. Am. Chem. Soc.* **2008**, *131*, 2824-2826.
24. DuBois, C. J.; Abboud, K. A.; Reynolds, J. R. *J. Phys. Chem. B* **2004**, *108*, 8550-8557.

CHAPTER 4. SYNTHESIS AND CHARACTERIZATION OF N-FUNCTIONALIZED FUSED-RING DIFURO[3,2-*b*:2',3'-*d*]PYRROLES AND COMPARISON TO THE N-ALKYL- AND N-ACYL-DITHIENO[3,2-*b*:2',3'-*d*]PYRROLES

4.1. Introduction

The use of polythiophenes is prolific in the field of conjugated polymers because of its electrical and optical properties but it does suffer from some limitations chiefly a general lack of solubility.¹ Furans traditionally have received little attention as a viable alternative to thiophenes due to a belief that oligomers and polymers built would be unstable because of the electron rich nature of the resulting materials.² In recent years, Bendikov and coworkers have published a series of papers in which they have constructed and characterized a series of linear alpha-linked furans with up to sixteen units and then compared them to their thiophene analogues (Figure 4.1). They found that furan-based oligomers exhibited good environmental stability in addition to enhanced solubility, planarity, solid state packing, and fluorescence when compared to their thiophene analogues.³⁻⁷ Additionally, furans derivatives can be considered a green material, as some furans can be produced on an industrial scale from biomass and making them a possible source of renewable materials.⁸

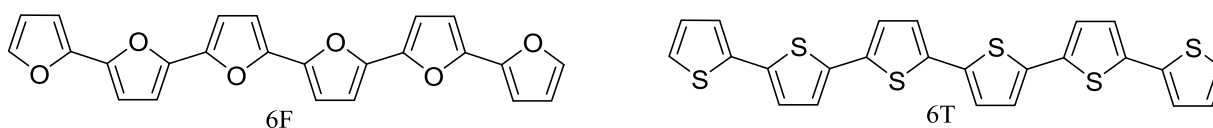


Figure 4.1. Heximeric furan- and thiophene- based oligomers

The solubility and solid-state packing of furan-based oligomers either surpasses or closely matches those of its thiophene analogues. A direct comparison of the solubility, in chloroform, between oligomers consisting of 6 units of both furan (6F) and thiophene (6T), gives values of 0.7 mg mL⁻¹ and 0.05 mg mL⁻¹, respectively.⁷ The charge-transport properties of

material are strongly influenced by the packing or molecular organization of the conjugated polymer in the solid state.¹ As such when X-ray crystal structures of 6F and 6T are compared, both exhibit similar herringbone packing motifs but the molecular density of 6F is 17% higher indicating stronger intermolecular attractions and a good argument for the better charge-transport properties seen in 6F.⁷

As mentioned previously the planarity of conjugated materials directly affects the resulting electrical and optical properties by determining the overall conjugation of the system. The energy required to twist the inter-annular bonds found in 6F and 6T to an angle of 36° has been calculated to be 12.5 kcal/mol and 2.3 kcal/mol respectively, meaning furan analogues tend to adapt more rigid backbones.⁷ A contributing factor to this increased planarity is the differences in the size of the heteroatoms involved with the smaller oxygen atom reducing the amount of β -hydrogen steric interactions in the furan-based materials (Figure 4.2).

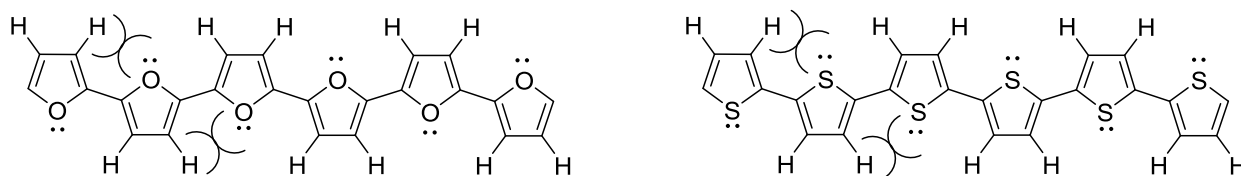


Figure 4.2. Steric interactions between heteroatoms and beta-hydrogens

The rigid π -conjugated backbone of furan-based materials is also evident in their observed photophysical properties. Increased fluorescence quantum yields have been reported for shorter oligomers, 78% in 3F compared to 6.6% in 3T, with strong fluorescence still exhibited for longer oligofurans.^{9,10} Additionally smaller Stokes Shift are seen for furan oligomers around 0.25 eV for 3F-9F as compared to around 0.40 eV for 3T-9T. The increased planarity of the furan systems decreases the out-of-plane vibrations exhibited by the oligomers thus reduces the non-radiative decay pathways through interannular torsional vibrations. Also the

absence of the heavier sulfur atom in the furan analogue decreases intersystem crossing resulting in higher quantum efficiencies.⁹

Bendikov and coworkers have reported on the incorporation of oligofurans into OFETS and found that their mobilities were similar to thiophene counterparts. In addition the output curves for the furan-based devices exhibited good ohmic contact with the electrodes and the higher HOMO energy values displayed lowered contact resistance.^{4,11} Several groups have also reported solar cells made with copolymers that contain furan oligomers.^{7,12} Frechet and coworkers built a device employing an oligofuran/diketopyrrole copolymer with efficiencies up to 3.8%.⁷

As previously mentioned one of the benefits of thiophene-based systems is their synthetic utility.¹ Rasmussen and coworkers have reported extensively on the generation and characterization of dithieno[3,2-*b*:2',3'-*d*]pyrroles (DTPs) and their ability to alter the monomer's optical and electrical properties through the use of different side chains.¹³ The goal of this part of my project is to create furan analogues of both the first and second generation of DTPs. Recent reports in the literature have shown that furan-based conjugated materials already exhibit many of the properties displayed by DTPs and it is not unreasonable to assume the furan analogues would be comparable or even surpass them in their performance.^{3-9,12} Using the reported methods for the generation of *N*-alkyl- and *N*-acyl-DTPs, which were discussed in great detail in previous chapters, the synthesis of the furan analogues, difuro[3,2-*b*:2',3'-*d*]pyrroles (DFPs), will be attempted.¹³ The proposed synthetic routes are listed in Figure 4.3.

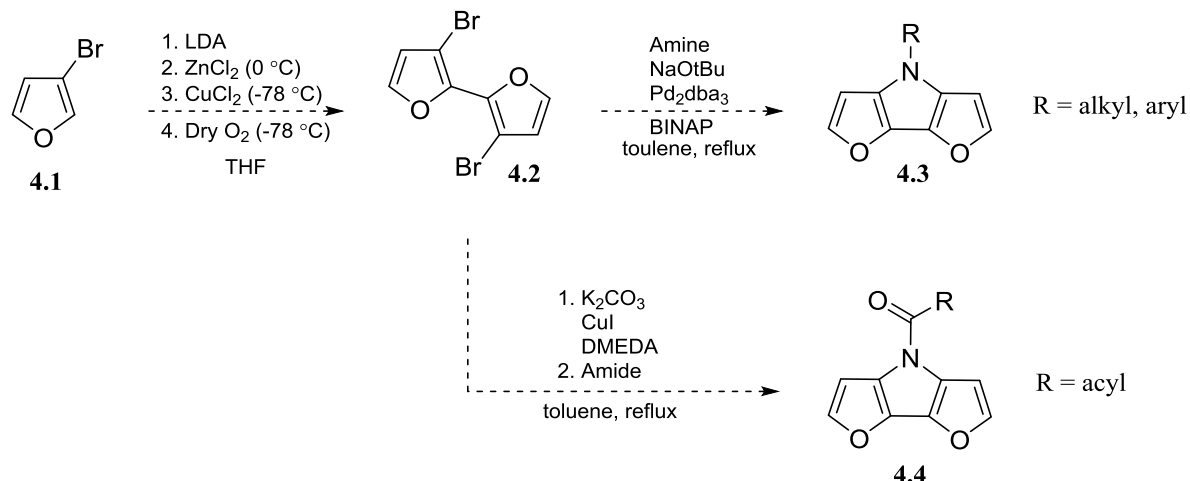


Figure 4.3. Proposed synthetic scheme for generation of difuro[3,2-*b*:2',3'-*d*]pyrroles (DFPs)

4.2. Results and discussion

4.2.1. Synthesis of 3,3'-dibromo-2,2'-bifuran

At the time this project was started there was not a reported synthesis of 3,3'-dibromo-2,2'-bifuran (4.2) in the literature. Using the already reported methods for generating 3,3'-dibromo-2,2'-bithiophene as our starting point, we repeated the reaction conditions using 3-bromofuran (4.1) as our starting material (Figure 4.4). Lithium diisopropylamide (LDA) is used to selectively deprotonate at the alpha-position of the furan ring, generating a lithiated intermediate. Next a transmetalation occurs by first adding ZnCl₂ and then CuCl₂. Initially dry O₂ was bubbled through the reaction mixture in hopes of assisting the homo-coupling but low yields (15-30%) of 4.2 were observed. This was not altogether surprising due to the well documented ability of furans to photooxidize in the presence of light and oxygen.⁶ When the experiment was repeated without the addition of the dry O₂ our yields jumped to 60-68%. In early 2014 Bendikov and coworkers also reported on the generation of 4.2 but without the use of ZnCl₂ their reported yields were about 10% less than ours.³

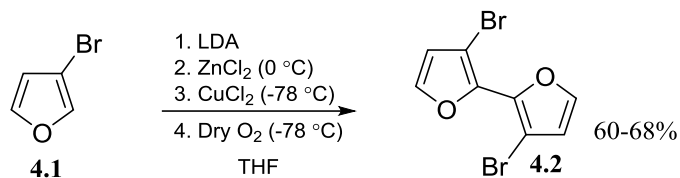


Figure 4.4. Generation of 3,3'-dibromo-2,2'-bifuran

4.2.2. Synthesis of *N*-alkylDFPs

At the time of writing this dissertation the author is unaware of any reports in the literature of any furan analogues of DTPs. We initially attempted to generate *N*-octylDFP using Buchwald-Hartwig amination via tris(dibenzylideneacetone)-dipalladium(0) (Pd₂(dba)₃) as the catalyst and 2,2'-bis(diphenylphosphino)-1,1'-binaphthyl (BINAP) as the ligand with dry toluene as the solvent. Several reaction conditions were tried with reaction times ranging from 12-48 hours. All the trials resulted in only the recovery of starting material (Figure 4.5).

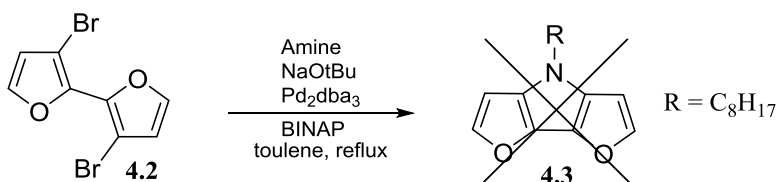


Figure 4.5. Attempted synthesis of *N*-octylDFP

A series of experiments were then conducted in which we attempted a monoamination of the parent compound 3-bromofuran (**4.1**) using Buchwald amination conditions. The results are listed in Table 4.1. Octylamine was first tested with two different ligands BINAP and tri(tert-butyl)phosphine (P^tBu₃). We were unable to produce the monoaminated furan product. 4-Hexylaniline was then selected as the amine and the reactions were rerun using the same two ligands. Again we were unable to produce the desired monoaminated furan product (**4.5**).

Table 4.1. Attempted monoamination of 3-bromofuran

Solvent	Amine	Ligand	Catalyst	Percent Yield
toluene	octylamine	BINAP	Pd ₂ dba ₃	0 %
toluene	octylamine	P ^t Bu ₃	Pd ₂ dba ₃	0 %
toluene	4-hexylaniline	BINAP	Pd ₂ dba ₃	0 %
toluene	4-hexylaniline	P ^t Bu ₃	Pd ₂ dba ₃	0 %

After the disappointing results encountered a review of the literature was undertaken to better understand the proposed reaction (Figure 4.6). A series of papers in the early 2000s were published in which the palladium-catalyzed aminations of different five-membered heterocyclic halides were studied.^{14,15,16}

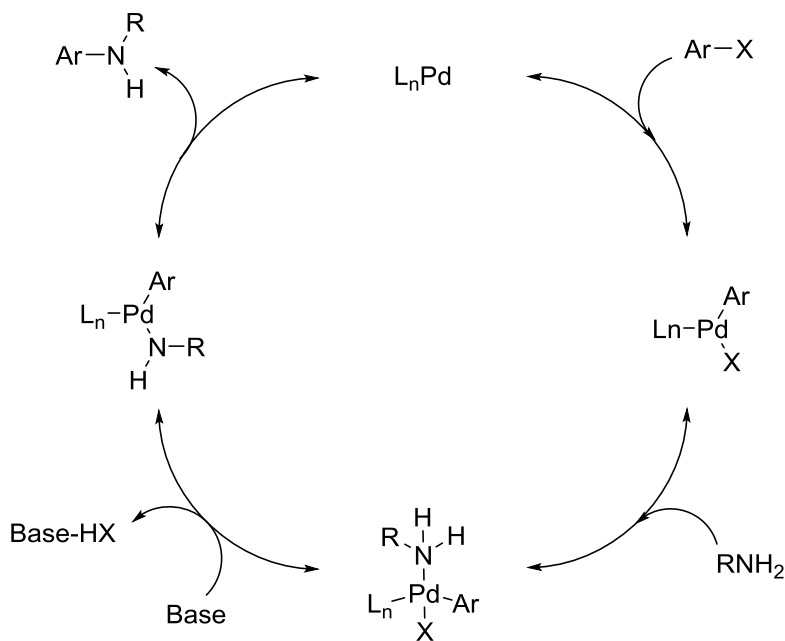


Figure 4.6. Proposed catalytic cycle for Buchwald-Hartwig amination

In general they found that 3-bromothiophene was the most versatile giving higher yields and reacting with a broader range of amines. Using aniline as the amine, 3-bromothiophene produced good yields of 88% but surprisingly 2-bromothiophene and both bromo-isomers of furan (2- and 3-bromo) were completely unreactive.¹⁶ In fact they found that reactions with bromofurans with primary and secondary alkylamines showed no formation of the desired product. They attribute some of these results to the catalyst being poisoned by the presence of the alkylamines.¹⁶ However, the use of diphenylamine and N-methylaniline both resulted in successful formation of the desired products. Overall, the previously reported results agreed well with ours and strongly indicate a different synthetic approach is needed in the generation of *N*-alkylDTPs.

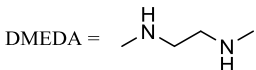
4.2.3. Synthesis of *N*-acylDTPs

Attempts to generate the *N*-acylDTP analogue using the scheme developed by Rasmussen and coworkers failed to meet with success (Figure 4.3).¹³ A series of trials were conducted, based on the previous work of Buchwald and coworkers, in which the solvent and base were varied and the results are reported in Table 4.2.¹⁷ Most trials resulted in the recovery of some material but sadly not in the formation of the target molecule. The by-products produced in these reactions was a monoaminated difuran compound (**4.6**) and a black insoluble solid. The choice of solvent and base did determine the amount of **4.6** produced with both potassium and cesium carbonate giving yields of 44% and 30%, respectively, in toluene but only potassium carbonate producing **4.6** in 7% yields with dioxane. These results indicate at least one full catalytic cycle being completed and an additional cycle starting but for unknown reason it stalls resulting in only the formation of **4.6**. A search of the literature was conducted to help us better understand the mechanism for the catalytic cycle of this reaction. What we learned is that this process is not well

understood and there are currently multiple mechanisms proposed with no clear consensus on which is the actual catalytic cycle.^{18,19}

Table 4.2. Attempted generation of *N*-acylDFPs

Solvent		Base	Catalyst	Ligand	Percent yield		
					A	B	C
toluene		K ₂ CO ₃	CuI	DMEDA	35	44	0
toluene		K ₃ PO ₄	CuI	DMEDA	80	0	0
toluene		Cs ₂ CO ₃	CuI	DMEDA	28	30	0
dioxane		K ₂ CO ₃	CuI	DMEDA	14	7	0
dioxane		K ₃ PO ₄	CuI	DMEDA	75	0	0
dioxane		Cs ₂ CO ₃	CuI	DMEDA	20	0	0

 DMEDA = <chem>CNCCN</chem>

4.3. Conclusions

We were able to successfully generate 3,3'-dibromo-2,2'-bifuran (**4.2**) in good yields of 60-68% using a modified procedure found in the literature.⁶ Unfortunately all attempts at using **4.2** to generate either the acyl or alkyl analogues of DFP did not meet with success. Under Buchwald-Hartwig reaction conditions only starting materials were recovered when we attempted the annulation of **4.2** or the amination of the parent compound 3-bromofuran (**4.1**). Buchwald and coworkers also encountered similar results when attempting similar amination of halofurans

which is a good indicator a different synthetic approach for the generation of *N*-alkylDFPs is probably needed.^{14,15,16}

Our attempts to create an *N*-acylDFP meet with negative results as well. When toluene was used with potassium carbonate or cesium carbonate as the base a monoaminated bisfuran(**4.6**) was the only product formed. This suggests that **4.2** undergoes one full catalytic cycle and an additional catalytic cycle starts but for reasons unknown it never goes to completion. Similar results were obtained when dioxane and potassium carbonate were used as the solvent and base system.

4.4. Experimental

If not specified the following conditions were used in the synthesis, purification and characterization of the compounds listed in this section. Chemicals were reagent grade and used without further purification. Solvents were dried via distillation over sodium-benzophenone. Glassware was oven-dried then assembled hot and cooled under a dry nitrogen stream. Transfers of liquids were carried out using standard syringe techniques and the reactions were performed under a dry nitrogen stream using air-free techniques. Silica gel (240-400 mesh) in conjunction with standard column chromatography methods were employed for chromatographic separations. Melting points were reported to a resolution of 0.1 °C using a digital thermocouple. The ¹H and ¹³C NMR were performed with a 400 MHz spectrometer. NMR data collected was referenced to the chloroform signal and peak multiplicity is reported as follows: s = singlet, d = doublet, t = triplet, q = quartet, p = pentet, tt = triplet of triplets, m = multiplet and br = broad. HRMS data was collected using a Bruker-Daltronics BIOTOF HRMS.

4.4.1. Synthesis of 3,3'-dibromo-2,2'-bifuran (4.2)

The following procedure was modified from one found in the literature.³ A solution of LDA was prepared by adding 4.4 mL of BuLi (2.5 M in hexanes) to a 100.0 mL solution diisopropylamide (1.54 mL, 11.0 mmol) in THF at 0.0 °C. The mixture was stirred for a half hour before being cooled in a dry ice-acetone bath after which 0.88 mL (10.0 mmol) of 3-bromofuran was added dropwise. After an additional 2 hours 1.50 g of ZnCl₂ (11.0 mmol) was added in portion and 15 minutes later 1.49 g of CuCl₂ (11.0 mmol) was added again in one portion. At which point the reaction was allowed to warm to room temperature overnight. The reaction was then quenched with a saturated solution of NH₄Cl and the aqueous layer was extracted with chloroform. The organic layers were combined and dried over MgSO₄ and then evaporated. The crude material was then purified using column chromatography using hexanes. A white solid (1.46 g) was collected for a yield of 68.0%. mp = 84.3-85.5 °C; ¹H NMR: δ 7.47 (d, *J* = 2.0 Hz, 2H), 6.55 (d, *J* = 2.0 Hz, 2H); ¹³C HMR: δ 143.38, 141.74, 115.76, 99.25.

4.4.2. Attempted Synthesis of *N*-octyldifuro[3,2-*b*:2',3'-*d*]pyrroles (4.3)

To a 100 mL three-neck round-bottom flask the following chemicals were added: 3,3'-dibromo-2,2'-bisfuran (0.15g, 0.5 mmol), Pd₂(dba)₃ (0.015g, 0.01 mmol), BINAP (0.031 g, 0.1 mmol), NaO^tBu (0.12 g, 0.12 mmol), octylamine (0.10 mL, 0.55 mmol) and 25.0 mL dry solvent. The following mixture was refluxed for 24 hour before being cooled to room temperature then treated with water. The organic phase was separated with diethyl ether which were combined and dried over MgSO₄ and volatile solvents were removed via rotary evaporation.

4.4.3. Attempted synthesis of *N*-octanoyldifuro[3,2-*b*:2',3'-*d*]pyrroles (4.4)

To a 50mL three-neck round-bottom flask was added the base (3.0 mmol), DMEDA (0.0176g, 0.2 mmol), CuI (0.02g, 0.1 mmol) and 10.0mL of dry solvent and then the mixture was stirred for 30 min. Octanamide (0.16g, 1.1mmol) and 3,3'-dibromo-2,2'-bisfuran (0.30g, 1.0 mmol) were then each added in a single portions and the reaction was heated to a gentle reflux for 24 h. The reaction was then cooled to room temperature, quenched with water and extracted with diethyl ether. The combined organic layers were dried over MgSO₄, filtered, concentrated via rotary evaporation, and purified by silica gel chromatography. The starting material (4.2) was eluded using hexanes (20-80% recovery) and 30% ethyl acetate/hexanes was used to elude 3-octanoylamino-2,2'-bifuran (4.6) yield 7-44%. mp = 61.7 - 62.6 °C; ¹H NMR: δ 7.96 (br s, 1H), 7.47 (dd, *J* = 1.8, 0.8 Hz, 1H), 7.31 (d, *J* = 1.8 Hz, 1H), 7.27 (d, *J* = 1.9 Hz, 1H), 6.53 (dd, *J* = 3.42, 1.59 Hz, 1H), 6.51 (dd, *J* = 3.42, 0.85 Hz, 1H), 2.40 (t, *J* = 7.48 Hz, 2H), 1.74 (p, *J* = 7.72 Hz, 2H), 1.29 (m, 8H), 0.882 (t, *J* = 6.88, 3H); ¹³C HMR: δ 170.73, 147.01, 141.09, 132.41, 111.62, 107.96, 104.08, 37.41, 31.67, 29.18, 29.04, 25.51, 14.07.

4.5. References

1. Perepichka, I. F., Perepichka, D. F., Eds. *Handbook of Thiophene-based Materials*; John Wiley & Sons: Hoboken, 2009.
2. Distefano, G.; Jones, D.; Guerra, M.; Favaretto, L.; Modelli, A.; Mengoli, G. *J. Phys. Chem.* **1991**, *95*, 9746.
3. Gidron, O.; Bendikov, M. *Angew. Chem. Int. Ed.* **2014**, *53*, 2546-2555.
4. Gidron, O.; Varsano, N.; Shimon, L.J.W.; Leitun, G.; Bendikov, M. *Chem. Commun.*, **2013**, *49*, 6256.

5. Jin, X.; Sheberla, D.; Shimon, L.J.W.; Bendikov, M. *J. Am. Chem. Soc.* **2014**, *136*, 2592-2601.
6. Bunz, U.H.f. *Angew. Chem. Int. Ed.* **2010**, *49*, 5037-5040.
7. Gidron, O.; Diskin-Posner, Y.; Bendikov, M. *J. Am. Chem. Soc.* **2010**, *132*, 2148-2150.
8. Okada, K.; Tachikawa, K. A. *J. Appl. Polym. Sci.* **1999**, *74*, 3342-3350.
9. Seixas de Melo, j.; Elisei, F.; Gartner, C.; Alosis, G.G.; Becker, R.S. *J. Phys. Chem. A* **2000**, *104*, 6907.
10. Becker, R. S.; Seixas de Melo, j.; Mancanita, A.L.; Elisei, F.; *J. Phys. Chem.* **1996**, *100*, 18683-18695.
11. Giridon, O.; Dadvand, A.; Shenynin, Y.; Bendikov, M.; Perepichka, D. F. *Chem. Commun.* **2011**, *47*, 1976-1978.
12. J. M.; Wienk, M. M.; de Leeuw, D. M.; Janssen, R. A. *J. Mater. Chem.* **2011**, *21*, 1600-1606.
13. Evenson, S. J.; Rasmussen S. C. *Org. Letters* **2010**, *12(18)*, 4054-4057.
14. Wolfe, J. P.; Buchwald, S. L. *J. Org. Chem.* **2000**, *65*, 1144-1157.
15. Hooper, M. W.; Hartwig, J. F. *Organometallics* **2003**, *22*, 3394-3403.
16. Wolfe, J. P.; Utsunimiya, M.; Buchwald, S.L. *J. Org. Chem.* **2003**, *68*, 2861-2873.
17. Price, S. C.; Staurt, A. C.; You, W. *Macromolecules*, **2010**, *43*, 797-804.
18. Sambiago, C.; Marsden, S. P.; Blacker, A. J.; McGowan, P. C. *Chem. Soc. Rev.*, **2014**, *42*, 3525.
19. Sperotto, E.; van Klink, G. P. M.; van Koten, G.; de Vries, J. G. *Dalton Trans.*, **2010**, *39*, 10338-10351.

CHAPTER 5. SYNTHESIS OF *N*-(4-OCTYLBENZOYL)DITHIENO[3,2-*b*:2',3'-*d*]PYRROLE AND POLY(*N*-OCTYLDITHIENO[3,2-*b*:2',3'-*d*]PYRROLE-CO-*N*-OCTANOYLDITHIENO[3,2-*b*:2',3'-*d*]PYRROLE)

5.1. Introduction

The enhanced electronic and optical properties of conjugated polymers (CPs) in addition to their advantageous mechanical attributes have drawn considerable attention to studying their synthesis and properties. As a result CPs have been utilized in a variety of different applications including organic photovoltaic devices (OPVs), organic light-emitting diodes (OLEDs), field effect transistors (FETs), electrochromic devices and sensors.¹⁻³ The desirable properties of CPs are dominated by the material's band gap (E_g), which is governed by the amount of conjugation, or π -orbital overlap, along the polymer's backbone. To be practical for electronic devices CPs must be soluble in common organic solvents. This often means that functional groups must be added to enhance their processability. The inclusion of side chains disrupts the backbone planarity via steric interactions decreasing the amount of electron delocalization along the polymer's backbone. In order to minimize this effect the regiochemistry of the asymmetric polymers must be controlled and accordingly considerable effort has been expended on this endeavor.² One way to avoid these problems caused by asymmetry is to generate *N*-functionalized symmetric monomeric units such as dithieno[3,2-*b*:2',3'-*d*]pyrroles (DTPs).⁴ An added benefit of these annulated thiophene units is a greater degree of electron delocalization caused by their enhanced planar nature. This is evident when you compare band gaps of poly(3-hexylthiophene) (P3HT), ~2.0 eV, and its fused-ring analogue DTP, 1.7 eV. (Figure 5.1).^{2,4} Additional tuning of the optical and electrical properties of DTPs can be attained through the choice of side chains. As outline in Chapter 3 the incorporating an electron-withdrawing acyl

group at the pyrrole nitrogen effectively lowered the observed band gap in comparison to the *N*-alkylDTP analogues.⁵

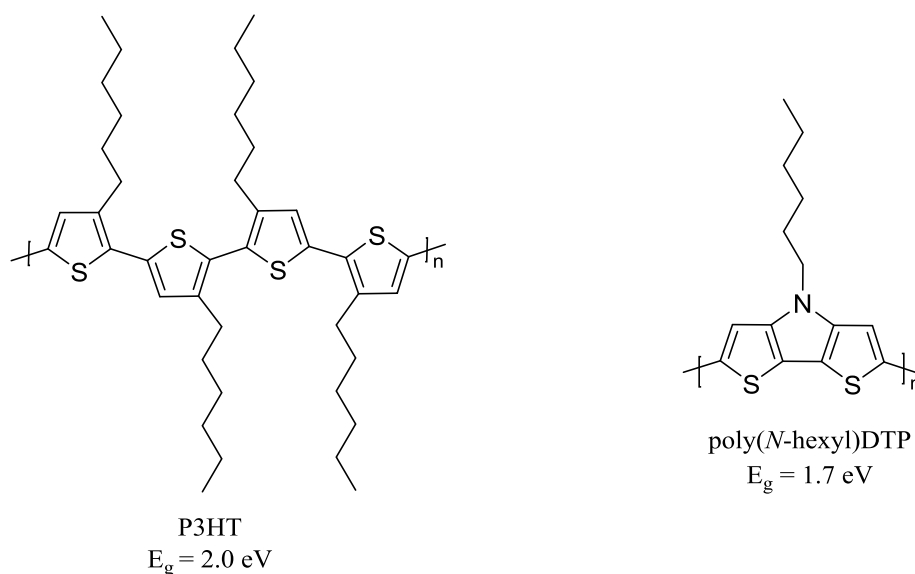


Figure 5.1. Comparison of band gaps of fused ring *N*-functionalized DTP to parent polythiophene

The majority of oligomeric materials made with DTP exhibit stronger fluorescence than their oligothiophene parents.^{4,6-8} This is attributed to the planar nature of the fused ringed DTP which among other things decreases low frequency, non-radiative deactivation through interannular torsional vibrations. The choice of the *N*-functionalized group will also affect the fluorescence of DTPs. When alkyl side chains are used a decrease in the observed quantum yield is observed. A direct relationship is observed between the length of the chain and fluorescence which is attributed to the increased high frequency modes associated with the methylene units. The use of *N*-phenyl solubilizing groups show the highest fluoresces because of their lack of high frequency modes.^{4,6-8}

Second generation DTPs with the *N*-acyl functionalized moiety shows an even greater fluorescence.⁵ The carbonyl group is thought to increase the effective conjugation of the

oligomer reducing non-radiative decay and results in materials that can have doubled the observed quantum yields.⁶ Our objectives were to synthesis an *N*-alkylbenzoylDTP with enhanced solubility through the addition of an alky side chain on the phenyl ring and to generate a copolymer of the first and second generation DTPs to study the optical and electrical effects of the resulting polymer.

5.2. Results and discussion

5.2.1. Synthesis of *N*-(4-octylbenzoyl)DTP

Our overall plan was to use the Ullman-type chemistry developed by Rasmussen and coworkers for the synthesis of the second generation DTPs (Figure 5.2).⁵ We choose 4-octylbenzamide as our amide but it was determined that the amide was not commercial available. A review of the literature was then conducted to determine the best way in which to synthesize the desired molecule.

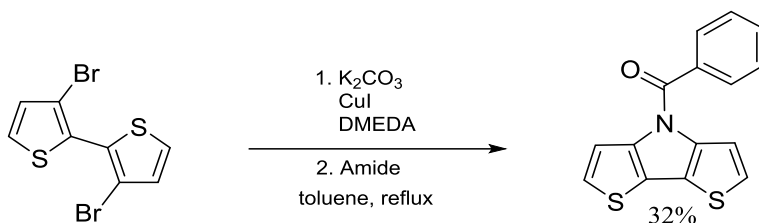


Figure 5.2. Synthetic route for *N*-acyl-phenylDTPs

A visiting undergraduate working in our lab for the summer was originally tasked with the synthesis of the amide. Based on the work of Zarea and coworkers she attempted the conversion of 4-octylbenzoic acid (**5.1**) into 4-octylbenzamide (**5.2**) using solvent free conditions with a silica gel-supported ammonium salt which is outlined in Figure 5.3 (Method A).⁹ The silica gel-supported ammonium salts were prepared by mixing 20.0 mmol of ammonium chloride with 5.0 g of silica gel and 5.0 mL of water which was thoroughly mixed and then allowed to

evaporate overnight to dryness. Triethylamine (TEA) was added to a well-grounded mixture of 4-octylbenzoic acid, silica-supported ammonium salt and 4-toluenesulfonyl chloride (TsCl) and stirred vigorously for 3-5 minutes (Figure 5.3). This reaction was tried several times resulting in yields ranging from 15-25% with recovery of starting material as well (30-40%).

In an effort to increase the yield of this reaction the conditions were modified and are shown in Figure 5.3 (Method B). We decided to remove the silica-supported ammonium salt and rerun the reaction with a solvent, acetonitrile (MeCN). After 1-2 h of stirring the desired product (**5.2**) was obtained in yields as high as 58.0% but unreacted starting material remained in the mixture. This was problematic because the product and starting materials eluded almost together during purification and multiple columns were needed to obtain pure product.

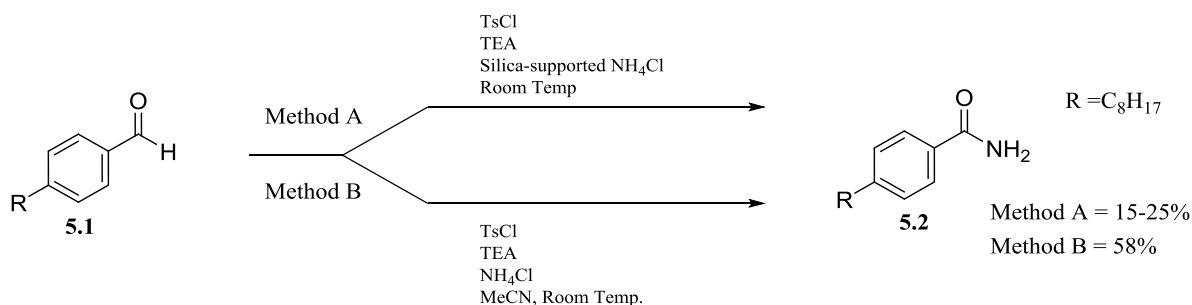


Figure 5.3. Early synthetic route to 4-octylbenzamide (Method A and B)

In an attempt to improve the yield and find a simpler purification process the literature was reexamined. Wang and coworkers, in 2013, reported on the synthesis of a series of amides starting from benzoic acids.¹⁰ 4-Octylbenzoic acid (**5.1**) was slowly added to a solution of thionyl chloride (SOCl₂) in dichloromethane (DCM) to which a few drops of dimethylformamide (DMF) is added. The resulting mixture is then gently refluxed at 60.0 °C for one hour. The excess SOCl₂ is removed from the reaction mixture in vacuo and the resulting acid chloride is used in the next step without further purification. Ether was added to the acid chloride along with TEA and

stirred to which dry NH₃ gas was bubbled through the reaction mixture at room temperature. The new synthetic scheme is shown in Figure 5.4. After purification via column chromatography the desired amide (**5.2**) was produced in yields of ~60.0%. Although the reported yields of this new reaction are not that much greater than the previously describe in method B the purification is much simpler making it the reaction of choice for the generation of the amide.

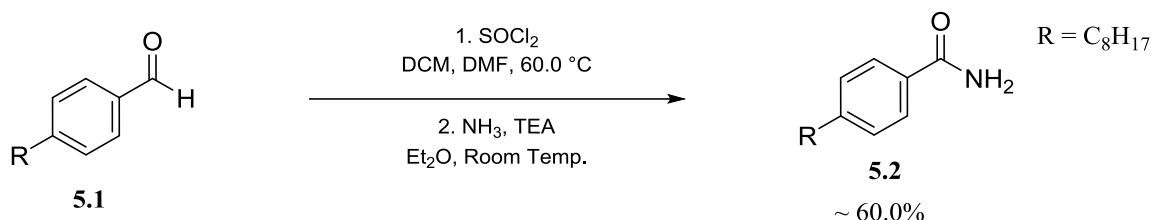
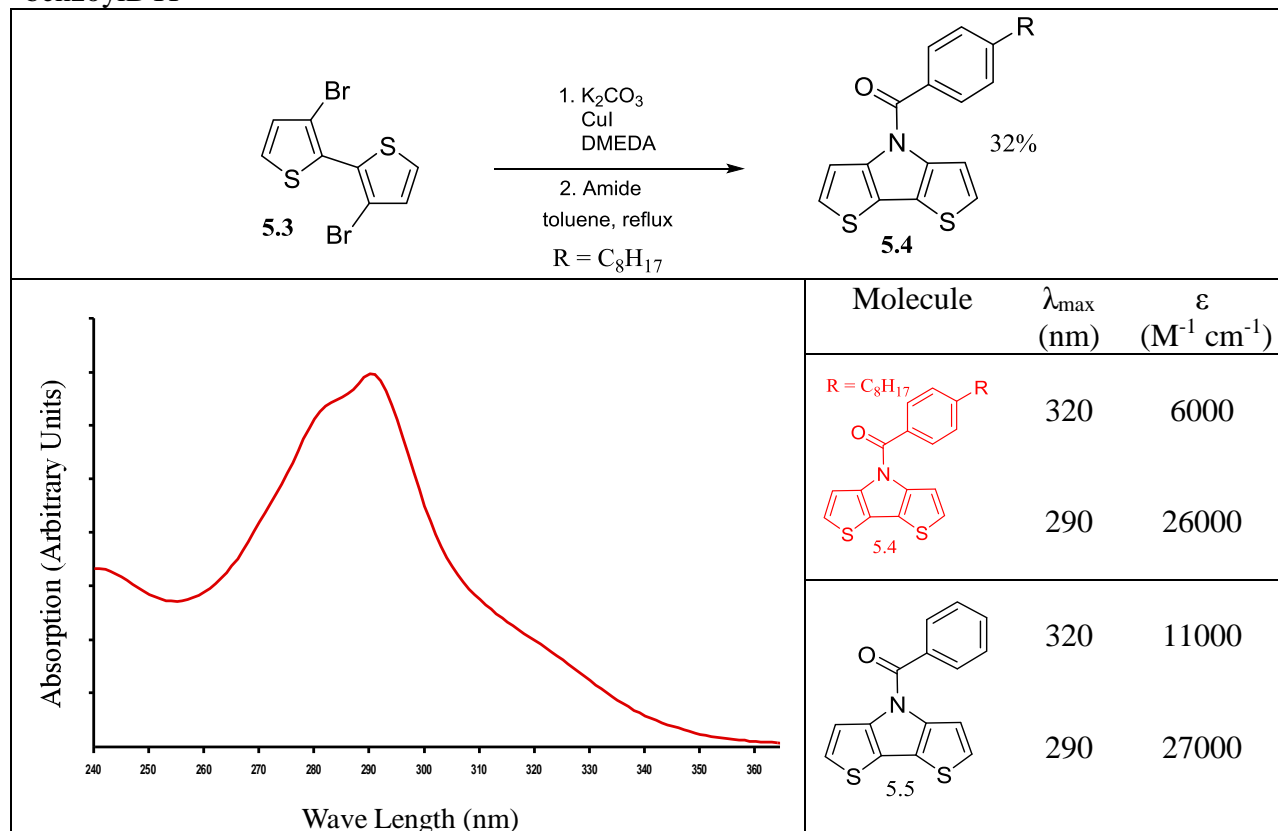


Figure 5.4. Preferred method for generation of 4-octylbenzamide

With the desired amide in hand we used Rasmussen and coworkers reported methods for the generation of *N*-acylDTPs using 3,3'-dibromo-2,2'-bithiophene (**5.3**) as shown in Table 5.1.⁵ The reaction produced *N*-(4-octylbenzoyl)dithieno[3,2-*b*:2',3'-*d*]pyrrole (**5.4**) in yields of 32%. As expected the UV-vis of this compound had a very similar profile of the reported *N*-benzoylDTP (**5.5**) by Rasmussen and coworkers.⁵ In table 5.1 we have shown the UV-vis spectra of **5.4** and will treat it as being representative of both *N*-benzoylDTPs (**5.4** and **5.5**). Each compound has a sharp peak at 290 nm consistent with a π - π^* transition and a lower energy transition at 320 nm with a broad nature indicative of a charge transfer (CT). The only difference in the two spectra is the intensity and shape of the CT peaks. The alkyl-functionalized benzoylDTP (**5.4**) peak's absorbance is lower and less defined than the unfunctionalized benzoylDTP (**5.5**) which is evident in the lower extinction coefficient, 6000 M⁻¹ cm⁻¹ vs. 11000 M⁻¹ cm⁻¹, respectively.

Table 5.1. Summary of optical data^a for *N*-(4-octylbenzoyl)DTP with a comparison to *N*-benzoylDTP



5.2.2. Synthesis of copolymer of 1st and 2nd generation DTP

The copolymer (**5.10**) of both *N*-octylDTP (**5.6**) and *N*-octanoylDTP (**5.8**) was accomplished through the use of a Stille cross-coupling reaction. Both the first and second generation *N*-functionized DTPs were synthesized from 3,3'-dibromo-2,2'-bithiophene (**5.3**) as previously reported.⁵ The *N*-octylDTP distannyl (**5.7**) intermediate were created through the use of tetramethylethylenediamine (TMEDA), BuLi and trimethyltin chloride at 0.0 °C in quantitative yields.¹¹ TMEDA acts as a ligand de-aggregating the BuLi making it a stronger base and avoids the use of the more reactive ^tBuLi. Removal of the some of the inorganic by-products was accomplished by running the crude reaction mixture through a plug of silica which has been

treated with triethylamine (Et_3N). Rotatory evaporation of the eluted products removes volatile organics and the residual tin species are removed by pumping on the oil overnight (Figure 5.5).

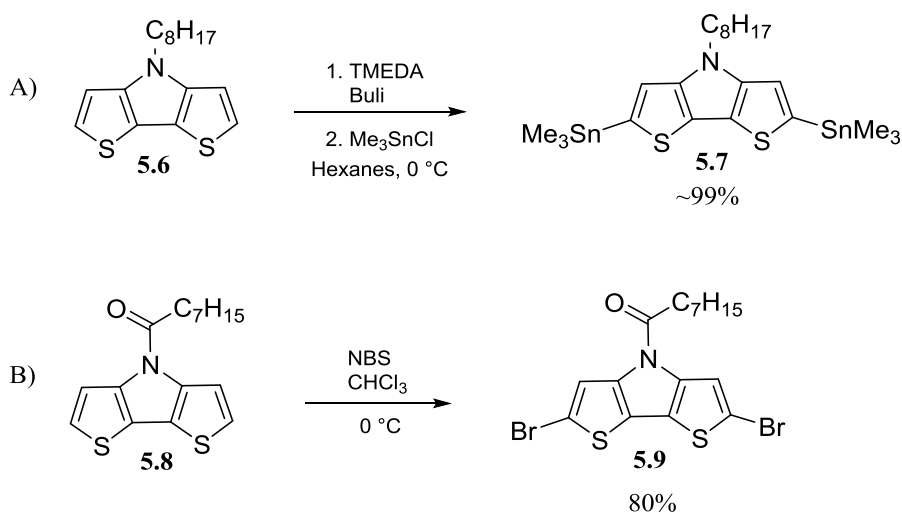


Figure 5.5. Generation of: A) distannane of *N*-octylIDTP B) and dibromide of *N*-octanoylIDTP

A dibromide was synthesized of the *N*-octanoylIDTP. The addition of the acyl carbonyl opens up that position to nucleophilic attack and excludes the use of BuLi. Fortunately *N*-acylIDTPs can be easily brominated with the use of *N*-bromosuccinimide (NBS) in chloroform as shown in Figure 5.5.¹¹ The resulting compound (**5.9**) is quite stable and easily purified through recrystallization in hexanes. A $\text{Pd}_2\text{dba}_3/\text{P}(o\text{-toly})_3$ catalytic-ligand system was used to polymerize the comonomers in dry and degassed toluene (Figure 5.6). After gently refluxing for 96 h the reaction was cooled to room temperature and methanol was added. The resulting mixture was then filtered and the remaining residue was washed with boiling chloroform. A Soxhlet extraction using acetone, hexane and finally chloroform was performed on the resulting polymer.

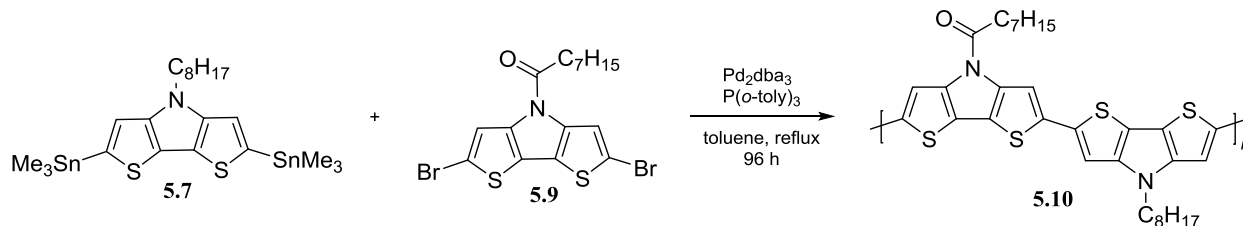
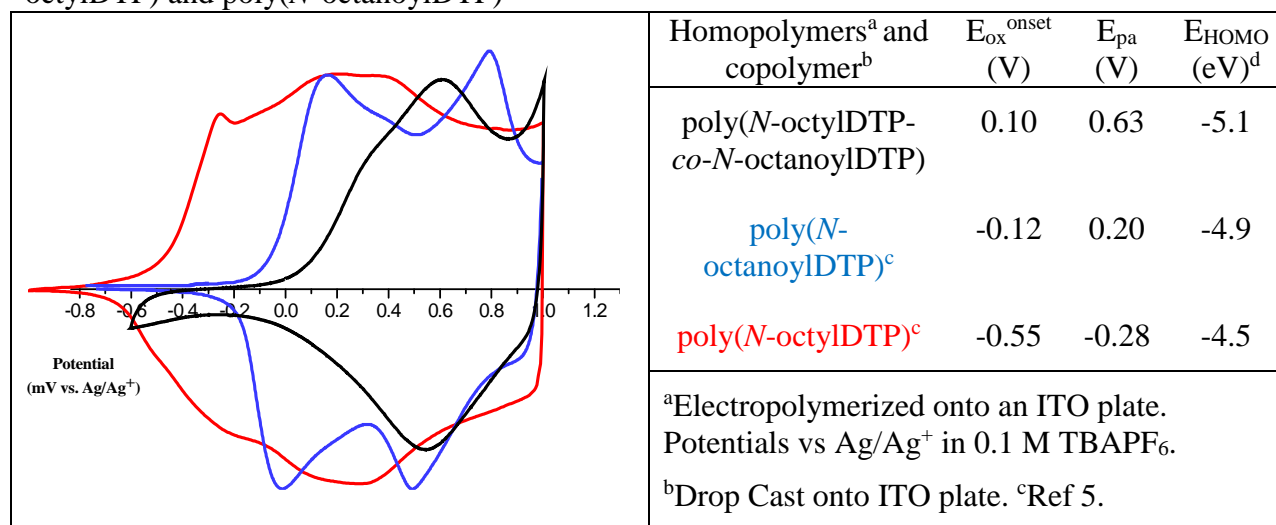


Figure 5.6. Stille cross-coupling of 1st and 2nd generation DTPs

5.2.3. Electrochemistry of poly(*N*-octylDTP-*co*-*N*-octanoylDTP)

A thin film of the poly(*N*-octylDTP-*co*-*N*-octanoylDTP) (**5.10**) was made on an ITO plate using drop casting. Cyclic voltammetry was then performed on the film and for comparison the values for the electro-polymerized homopolymers are listed in Table 5.2.

Table 5.2. Cyclic voltammograms of films of poly(*N*-octylDTP-*co*-*N*-octanoylDTP), poly(*N*-octylDTP) and poly(*N*-octanoylDTP)

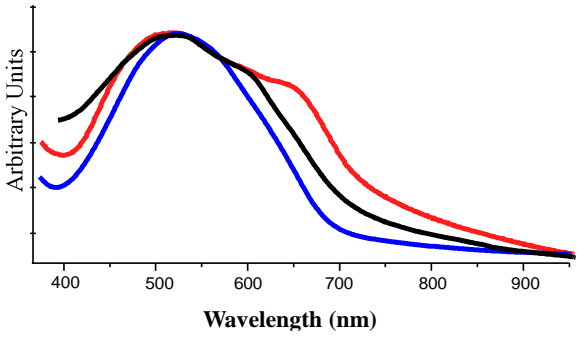


The copolymer showed a positive shift in its oxidative onset in relation to the homopolymers of approximately 1500 mV for poly(*N*-octylDTP) and 1100 mV for poly(*N*-octanoylDTP) resulting in a HOMO energy level of -5.1 eV. This delayed oxidative onset is due to the tendency of chemical formed polymers to have lower molecular weights than films made by electropolymerization.

5.2.4. UV-vis spectroscopy of poly(*N*-octylDTP-*co*-*N*-octanoylDTP)

The absorption spectra for the drop-cast poly(*N*-octylDTP-*co*-*N*-octanoylDTP) in addition to the electropolymerized homopolymers of *N*-octylDTP and *N*-octanoylDTPs are shown in Table 5.3 along with their optical band gaps and the HOMO/LUMO energy levels. The profile for the copolymer has the appearance of a hybrid between both homopolymers exhibiting a similar low energy shoulder as the *N*-acylDTP polymer, although less pronounced.⁵ This is responsible for a red-shift of the absorption onset of the copolymer when compared to the *N*-alkylDTP homo polymer of around 10.0 mV and a blue shift of around 40.0 mV for the acyl based polymer. Due to this the resulting band gap for poly(*N*-octanoylDTP) shows a reduction of ~0.1 eV in comparison to both the poly(*N*-octylDTP) and copolymer.

Table 5.3. Solid state absorption spectra of films poly(*N*-octylDTP-*co*-*N*-octanoylDTP), poly(*N*-octylDTP) and poly(*N*-octanoylDTP)

	Homopolymers ^a & copolymer	λ_{\max} (nm)	E_{HOMO} (eV)	E_{LUMO} (eV)	E_g (eV)
		poly(<i>N</i> -octylDTP- <i>co</i> - <i>N</i> -octanoylDTP)	526	-5.1	-3.4
	poly(<i>N</i> -octanoylDTP) ^a	520 (557) (675)	-4.9	-3.3	1.66
	poly(<i>N</i> -octylDTP) ^a	531	-4.5	-2.8	1.78

E_{HOMO} was determined from onset of oxidation vs. ferrocene (5.1 eV vs vacuum).
 $E_{\text{LUMO}} = E_{\text{HOMO}} - E_g$. ^aRef 5

5.3. Conclusion

We were able to synthesis an *N*-benzoylDTP through the conversion of a substituted benzoic acid to an amide. The choice of the commercially unavailable 4-octylbenzamide for use

in the production of the *N*-benzoylDTP resulted in multiple synthetic routes being explored for its synthesis. Methods A and B used 4-octylbenzoic acid as the starting material, 4-toluene-sulfonyl chloride (TsCl) and an ammonium salt either neat (Method A) or in solution (Method B) both routes lead to low or moderate yields of the product in addition to a difficulty purification.⁹ In an attempt to improve the yield of the reaction and purification process a new procedure adapted from the literature using thionyl chloride (SOCl₂) and ammonia gas.¹⁰ This new procedure produced 4-octylbenzamide in yields of 60.0% with and a much simpler purification. With amide in hand *N*-(4-octylbenzoyl)dithieno[3,2-*b*:2',3'-*d*]pyrrole was synthesized in yields of 32.0% using the procedures reported by Rasmussen and coworkers for the production of *N*-acyDTPs.⁵ A UV-vis spectra of the *N*-(4-octylbenzoyl)dithieno[3,2-*b*:2',3'-*d*]pyrrole showed a π - π^* transition at 290 nm, and a lower energy transition at 320 nm with a broad nature indicative of a charge transfer (CT). A comparison of *N*-phenylamineDTP showed that both spectra were very similar with only the intensity and shape of the CT peaks differing.

A copolymer of *N*-octylDTP and *N*-octanoylDTP was produced via a Stille cross-coupling of 2,6-bis(trimethylstannyl)-*N*-octyldithieno[3,2-*b*:2',3'-*d*]pyrrole and 2,6-dibromo-*N*-octanoyldithieno[3,2-*b*:2',3'-*d*]pyrrole.¹¹ The resulting poly(*N*-octylDTP-*co*-*N*-octanoylDTP) was purple in appearance. A thin film of the poly(*N*-octylDTP-*co*-*N*-octanoylDTP) was made on an ITO plate using drop-casting and cyclic voltammetry was then performed. When compared to electropolymerized films of the homopolymers a positive shift in its oxidative onset of approximately 1500 mV for poly(*N*-octylDTP) and 1100 mV for poly(*N*-octanoylDTP) was observed resulting in a HOMO energy level of -5.1 eV. Polymers formed via electropolymerization tend to have higher molecular weights than those made chemically resulting in the delayed oxidative onset observed for the copolymer.

The UV-vis spectra for the copolymer is a hybrid between both homopolymers including a less pronounced low energy shoulder typical of poly(*N*-acylDTPs). This shoulder is responsible for a red-shift of the absorption onset when compared to the poly(*N*-octylDTP) (~0.01 eV) and a blue shift of ~0.04 eV for the poly(*N*-octanoylDTP). Due to the similar profiles the optical band gap for the copolymer is approximately equivalent to the *N*-alkylDTP polymer and both differ around 0.1 eV from the *N*-acyl analogue.

5.4. Experimental

If not specified the following conditions were used in the synthesis, purification and characterization of the compounds listed in this section. Chemicals were reagent grade and used without further purification. Solvents were dried via distillation over sodium-benzophenone. Glassware was oven-dried then assembled hot and cooled under a dry nitrogen stream. Transfers of liquids were carried out using standard syringe techniques and the reactions were performed under a dry nitrogen stream using air-free techniques. Silica gel (240-400 mesh) in conjunction with standard column chromatography methods were employed for chromatographic separations. Melting points were reported to a resolution of 0.1 °C using a digital thermocouple. The ¹H and ¹³C NMR were performed with a 400 MHz spectrometer. NMR data collected was referenced to the chloroform signal and peak multiplicity is reported as follows: s = singlet, d = doublet, t = triplet, q = quartet, p = pentet, tt = triplet of triplets, m = multiplet and br = broad. HRMS data was collected using a Bruker-Daltronics BIOTOF HRMS. Previously reported procedures were used to synthesize the following compound: 3,3'-dibromo-2,2'-bithiophene⁵, *N*-octyldithieno[3,2-*b*:2',3'-*d*]pyrrole,¹² 2,6-bis(trimethylstannyl)-*N*-octyldithieno[3,2-*b*:2',3'-*d*]pyrrole,¹¹ 2,6-dibromo-*N*-octanoyldithieno[3,2-*b*:2',3'-*d*]pyrrole¹¹, *N*-octanoyldithieno[3,2-*b*:2',3'-*d*]pyrrole.⁵

5.4.1. Synthesis of 4-octylbenzamide (5.2) method A

The silica gel-supported ammonium salts were prepared by mixing 20.0 mmol of ammonium chloride with 5.0 g of silica gel and 5.0 mL of water which was thoroughly mixed and then allowed to evaporate overnight to dryness. A well-ground mixture of 4-octylbenzoic acid (0.24 g, 1.0 mmol), silica-supported ammonium salt (2 equivalents) and 4-toluenesulfonyl chloride (TsCl) (0.19 g, 1.0 mmol) was added to a test tube. To which 0.40 g (4.0 mmol) of triethylamine (TEA) was combined and the resulting mixture was stirred vigorously for 3-5 minutes. Ethyl acetate was then poured into the test tube and the suspension was filtered. The filtrate was then washed with a 2.0 N solution of HCl. Extraction of the aqueous layer was done with ethyl acetate which were combined and dried over MgSO₄ before the solvent was removed via rotary evaporation. The resulting crude material was purified via column chromatography with hexanes resulting in 0.06 g (25%) of a white solid. mp = 130.6 - 131.7 °C; ¹H NMR: δ 7.74 (d, *J* = 8.3 Hz, 2H), 7.21 (d, *J* = 8.3, 2H), 6.00 (s, 1H), 5.58 (s, 1H), 2.65 (t, *J* = 7.8 Hz, 2H), 1.62 (p, *J* = 7.6 Hz, 2H), 1.26 (m, 10H), 0.88 (t, *J* = 6.7 Hz, 3H); ¹³C HMR: δ 169.21, 147.56, 130.62, 128.67, 127.39, 35.86, 31.85, 31.18, 29.41, 29.22, 22.65, 14.09.

5.4.2. Synthesis of 4-octylbenzamide (5.2) method B

A mixture of 4-octylbenzoic acid (0.24 g, 1.0 mmol), ammonium chloride (0.11 g, 2.0 mmol) and 4-toluenesulfonyl chloride (TsCl) (0.19 g, 1.0 mmol) was placed in a round bottom flask. Acetonitrile (10.0 mL) was added and the solution stirred for 15.0 min before 0.40 g (4.0 mmol) of triethylamine (TEA) was added in one portion. The reaction mixture was stirred for another 60 min before being diluted with water. The aqueous layer was extracted with ethyl acetate which were combined and dried over MgSO₄ before the solvent was removed via rotary

evaporation. The resulting crude material was purified via column chromatography with hexanes then a hexanes:ethyl acetate (1:1) resulting in 0.13 g (57%) of a white solid.

5.4.3. Preferred method for synthesis of 4-octylbenzamide (5.2)

In a 100.0 mL 3-neck round bottom flask (RBF) equipped with a condenser, addition funnel and thermometer add thionyl chloride (SOCl₂) (0.33 mL, 4.5 mmol). In addition funnel add 4-octylbenzoic acid (0.58 g, 2.5 mmol), 5.0 mL dry DCM and a drop of dry DMF. Slowly add contents of addition funnel to RBF and then reflux in a water bath at 60.0 °C for three h. In vacuo remove excess SOCl₂ and then add 5.0 mL dry diethyl ether (Et₂O) and triethylamine (Et₃N) (0.42 mL, 3.0 mmol) at room temperature. Then bubble dry ammonia gas through the Et₂O solution and let mix for 60 min before adding water. The aqueous layer was extracted with Et₂O which were combined and dried over MgSO₄ before the solvent was removed via rotary evaporation. The resulting crude material was purified via column chromatography with hexanes:Et₂O (4:6) before running straight Et₂O resulting in 0.36 g (62%) of a white solid.

5.4.4. *N*-(4-Octylbenzoyl)dithieno[3,2-*b*:2',3'-*d*]pyrrole (5.4)

To a 25.0 mL 3-neck round-bottom flask was added potassium carbonate (2.0 g, 15.0 mmol), copper(I) iodide (0.05g, 5% mmol), dimethylethylenediamine (DMEDA) (0.11 mL, 20% mmol) and 10.0 mL of dry toluene. The contents of the RBF were allowed to stir for 30 min before 3,3'-dibromo-2,2'-bithiazole (1.60 g, 5.0 mmol) and 4-octylbenzamide (1.28 g, 5.5 mmol) both were added in one portion. The resulting mixture was then gently refluxed for 24 h before being cooled to room temperature and quenched with a saturated solution of NH₄Cl. The aqueous layer was extracted with hexanes which were combined and dried over MgSO₄ before the solvent was removed via rotary evaporation. The resulting crude material was purified via column chromatography with hexanes affording 0.59 g of a white solid (32%). mp = 116.2 –

117.9 °C; ¹H NMR: δ 7.66 (d, *J* = 8.2 Hz, 2H), 7.34 (d, *J* = 8.2 Hz, 2H), 7.11 (d, *J* = 5.4 Hz, 2H), 6.98 (d, *J* = 4.8 Hz), 2.73 (t, *J* = 7.6 Hz, 2H), 1.69 (p, *J* = 7.1 Hz, 2H), 1.29 (m, H = 10), 0.89 (t, *J* = 7.1, 2H); ¹³C NMR: δ 167.07, 147.88, 143.04, 131.56, 128.90, 128.70, 123.94, 121.37, 116.39.

5.4.5. Poly(*N*-octyldithieno[3,2-*b*:2'3'-*d*]pyrrole-*co*-*N*-octanoyldithieno[3,2-*b*:2',3'-*d*]pyrrole) (5.10)

To a 60 mL schlenk tube was added 2,6-dibromo-*N*-octanoyldithieno[3,2-*b*:2',3'-*d*]pyrrole (0.10 g, 0.20 mmol), 2,6-bis(trimethylstannyl)-*N*-octyldithieno[3,2-*b*:2',3'-*d*]pyrrole (0.12 g, 0.20 mmol), Pd₂dba₃ (0.0036 g, 0.004 mmol), and P(*o*-tolyl)₃ (0.0048 g, 0.016 mmol). The schlenk tube was evacuated and backfilled with N₂ five times. Toluene (20 mL) was added and the reaction was heated to 90-95 °C for 4 days. The reaction was cooled to RT and precipitated in MeOH (500 mL). The crude polymer was purified via Soxhlet extraction with MeOH for 24 h, followed by acetone and then hexane. The soluble portion of the purified polymer was then isolated by washing with CHCl₃. The polymer was then concentrated via rotary evaporation to produce a purple solid.

5.5. References

1. Skotheim, T. A., Reynolds, J. R., Eds. *Handbook of Conducting Polymers*, 3rd ed.; CRC Press: Boca Raton, FL, 2007.
2. Perepichka, I. F., Perepichka, D. F., Eds. *Handbook of Thiophene-based Materials*; John Wiley & Sons: Hoboken, 2009.
3. Rasmussen, S. C.; Ogawa, K.; Rothstein, S. D. In *Handbook of Organic Electronics and Photonics*; Nalwa, H. S., Ed.; American Scientific Publishers: Stevenson Ranch, CA, 2008; Vol. 1, Chapter 1.
4. Rasmussen, S. C.; Evenson, S. J. *Prog. Polym. Sci.* **2013**, *38*, 1773– 180.
5. Evenson, S. J.; Rasmussen S. C. *Org. Letters* **2010**, *1*), 4054-4057.

6. Evenson, S. J.; Pappenfus, T. M.; Delgado, C. R.; Raske-Wohlers, K. R.; Navarrete, J. T.; Rasmussen, S. C. *Phys. Chem. Chem. Phys.*, **2012**, *14*, 6101-6111.
7. Radke, K. R.; Ogawa, K.; Rasmussen, S. C. *Org. Lett.* **2005**, *7*, 5253-5256.
8. Mo, H.; Radke, K. R.; Ogawa, K.; Heth, C. L.; Erpelding, B. T.; Rasmussen, S. C. *Phys. Chem. Chem. Phys.* **2010**, *12*, 14585-14595.
9. Khalafi-Nezhad, A.; Parhami, A.; Soltani-Rad, M.N.; Zarea, A. *Tetrahedron Lett.* **2005**, *46*, 6879-6882.
10. Tang, Q.; Xia, D.; Jin, X.; Zhang, Q.; Sun, X.q.; Wang, C. *J. Am. Chem. Soc.* **2013**, *135*, 4628-4631.
11. Evenson, S. J.; Mumm, M.; Konstantin, P. I.; Rasmussen, S. C. *Macromolecules* **2011**, *44*, 835-841.
12. Koeckelberghs, G.; De Cremer, L.; Vanormelingen, W.; Dehaen, W.; Verbiest, T.; Persoons, A.; Samyn, C. *Tetrahedron* **2005**, *61*, 687-691.

CHAPTER 6. SUMMARY AND FUTURE DIRECTIONS

6.1. Summary

Using a modified procedure found in the literature, a new and cheaper starting material, 2,4-dibromothiazole, was utilized in the generation 4,4'-dibromo-2,2'-bis(triisopropylsilyl)-5,5'-bithiazole, a precursor needed for the creation pyrrolo[3,2-*d*:4,5-*d'*]bisthiazoles (PBTz) a thiazole based analogue of dithieno[3,2-*b*:2',3'-*d*]pyrrole (DTP).¹ Various synthetic routes were tried and rejected due to either low yields, difficult in purification or the costs of the reagents needed. The preferred method produces the desired precursor as a yellow/tan solid in yields of 54% with 25% of the starting material being recoverable.

All attempts to produce *N*-octanoylPBTz resulted in the recovery of starting material and unwanted by-products. A modified procedure found in the literature was used to generate *N*-octylPBTz in yields of 74%.² Cyclic voltammetry of a solution of *N*-octylPBTz exhibited a well-defined and irreversible oxidation peak and as expected the *N*-octylPBTz oxidative onset was shifted towards more positive potential when compared to both *N*-octanoylDTP and *N*-octylDTP; ~130 mV and ~350 mV, respectively. These results were not a surprise due to the electron deficient nature of thiazoles compared to thiophenes. Homopolymers of *N*-octylPBTz were electropolymerized on to plates of glass coated with ITO. Poly(*N*-octylPBTz) shows a positive shift in its oxidative onset when compared to the films of both the poly(*N*-acylDTP) and poly(*N*-alkylDTP) electropolymerized homopolymers; approximately at 300 mV and 700 mV respectively.²

UV-vis spectroscopy was also performed on the solution of *N*-octylPBTz which showed a broad high energy transition at 306 nm with two high energy shoulders appearing at 317 nm and 296 nm. These peaks can be attributed to a π - π^* transition because the energetic difference

between them is consistent with the breathing mode of thiazoles and are most likely vibrational components of the same electronic transition. The thin films of poly(*N*-octylPBTz) showed a stabilization of the HOMO levels when compared to the other polymers. The most dramatic change was observed between the films of *N*-octylPBTz and *N*-octylDTP with a reduction of 0.7 eV for the HOMO and a less dramatic change is observed for the poly(*N*-octanoylDTP) with the HOMO being stabilized by 0.3 eV. Profiles for both the spectra for poly(*N*-octylDTP) and poly(*N*-octylPBTz) have similar shapes. *N*-acylDTP typically exhibit a prominent low energy shoulder and therefore has a red-shifted absorption onset a consequently a reduced band gap of 1.67 eV.

We were able to successfully generate 3,3'-dibromo-2,2'-bifuran in yields of 60-68% using a modified procedure found in the literature.³ Unfortunately all attempts to generate either the *N*-acyl- or *N*-alkyl-difuro[3,2-*b*:2',3'-*d*]pyrroles (DFPs) did not meet with success. Under Buchwald-Hartwig reaction conditions to generate the *N*-alkylDFP, only starting material and unwanted by-products were recovered. Buchwald and coworkers also encountered similar results with their attempts at the amination of halofurans indicating that a rethink of our synthetic approach for the generation of *N*-alkylDFPs is probably needed.^{4,5,6} Our attempts to create an *N*-acylDFP using Ullman-type reaction conditions also resulted in the recovery of unreacted starting material and under certain conditions the formation of a monoamide-bisfuran by-product.

The synthesis of *N*-benzoylDTP was accomplished through the conversion of a substituted benzoic acid to an amide using thionyl chloride (SOCl₂) and ammonia gas. This procedure produced 4-octylbenzamide in yields of 60.0%. *N*-(4-octylbenzoyl)dithieno[3,2-*b*:2',3'-*d*]pyrrole was synthesized in yields of 32.0% using the procedures reported by

Rasmussen and coworkers for the production of *N*-acylDTPs.² A UV-vis spectra showed a π - π^* transition at 290 nm, and a lower energy transition at 320 nm with a broad nature indicative of a charge transfer (CT). When compared to *N*-phenylamineDTP both had similar profiles and only differed in the intensity and shape of the CT peaks.

A Stille cross-coupling between 2,6-bis(trimethylstannyl)-*N*-octyldithieno[3,2-*b*:2',3'-*d*]pyrrole and 2,6-dibromo-*N*-octanoyldithieno[3,2-*b*:2',3'-*d*]pyrrole produced poly(*N*-octylDTP-*co-N*-octanoylDTP) as purple solid. Drop-casting onto an ITO coated glass plate created a thin film of the copolymer and optical and electrical data was collected. The resulting data was compared to electropolymerized films of the homopolymers. A positive shift in the oxidative onset of copolymers was observed; ~1500 mV for poly(*N*-octylDTP) and ~1100 mV for poly(*N*-octanoylDTP). This can be explained by the tendency of polymers formed via electropolymerization to have higher molecular weights than those made chemically resulting in the delayed oxidative onset.

The UV-vis spectra for the copolymer is a hybrid between both homopolymers including a less pronounced low energy shoulder typical of poly(*N*-acylDTPs). This shoulder is responsible for a red-shift of the absorption onset when compared to the poly(*N*-octylDTP) (~10.0 mV) and a blue shift of ~40.0 mV for the poly(*N*-octanoylDTP). Due to the similar profiles the optical band gap for the copolymer is roughly equivalent to the *N*-alkylDTP polymer (~1.7 eV) and both differ by around ~0.1 eV from the *N*-acyl analogue.

6.2. Future directions

Attempts to create an *N*-acylPBTz monomeric unit using both palladium catalyzed Buchwald-Hartwig conditions and copper-catalyzed Ullman-type cross-coupling failed. A series of trials in which the solvent and base using copper as the catalyst was performed but a screening

of ligands was not undertaken. Additional experiments using a variety of ligands might provide the desired compound. Happily we were successfully able to produce an *N*-alkylPBTz molecule using Buckwald-Hartwig conditions the next logical step is to create an *N*-arylPBTz analogue (**6.2**) and is outlined in Figure 6.1.

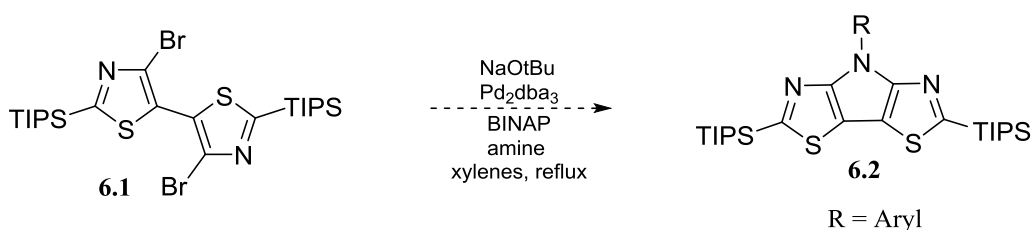


Figure 6.1. Proposed synthetic route to *N*-aryl functionalized PBTz

All efforts to synthesize the *N*-acylDFP and *N*-alkylDFP (**6.5**) furan analogues using both palladium catalyzed Buckwald-Hartwig conditions and copper-catalyzed Ullman type cross-coupling also failed. A series of trials in which the solvent and base using copper as the catalyst was performed but a screening of ligands was not undertaken. Additional experiments using a variety of ligands might provide the desired compound. Also using a catalyzed Ullman type cross-coupling with 3-bromofuran (**6.3**) to produce a tertiary bifurylamide (**6.4**) which is then annulated via another copper assisted cross-coupling has the potential to produce the desired *N*-acylDFP (Figure 6.2).

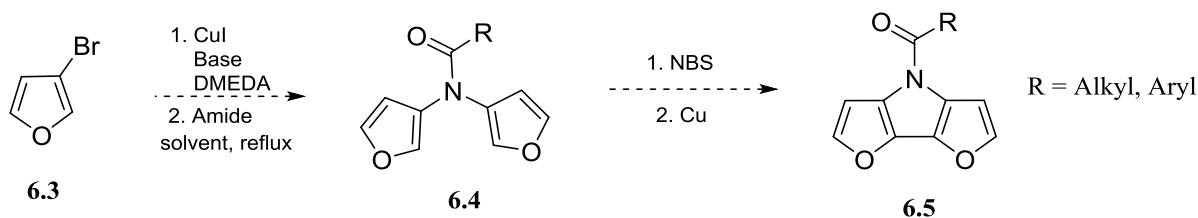


Figure 6.2. Proposed synthetic route to *N*-acylDFP

6.3. References

1. Grubb, A. M.; Schmidt, M. J.; Seed, A. J.; Sampson, P. *Synthesis*, **2012**, *44*, 1026-1029.
2. Evenson, S. J.; Rasmussen S. C. *Org. Letters* **2010**, *12*, 4054-4057.
3. Bunz, U. H. F. *Angew. Chem. Int. Ed.* **2010**, *49*, 5037-5040.
4. Wolfe, J. P.; Utsunimiya, M.; Buchwald, S. L. *J. Org. Chem.* **2003**, *68*, 2861-2873.
5. Price, S. C.; Staurt, A. C.; You, W. *Macromolecules*, **2010**, *43*, 797-804.
6. Hooper, M. W.; Hartwig, J. F. *Organometallics* **2003**, *22*, 3394-3403.